Univerzita Karlova v Praze

Přírodovědecká fakulta

Studijní program: Fyzikální chemie

Mgr. Ludmila Müllerová

Vliv interagující složky základního elektrolytu na elektroforetickou separaci

Influence of the interacting constituent of the background electrolyte
on electrophoretic separation

Dizertační práce

Školitel: Mgr. Pavel Dubský, Ph.D.

Praha, 2015

Předkládaná dizertační práce shrnuje výsledky získané během mého doktorského studia ve Skupině elektroforetických a chromatografických separačních metod (ECHMET) na Katedře fyzikální a makromolekulární chemie Přírodovědecké fakulty Univerzity Karlovy v Praze.

Práce byla financována v souvislosti s řešením projektů GA UK, čísla grantů 669412 a 510214, projektu GA ČR, číslo grantu 203-08-1428, a projektu CEEPUS CIII-RO-0010-08-1314.

Prohlášení:

Prohlašuji, že jsem závěrečnou práci zpracovala samostatně a že jsem uvedla všechny použité informační zdroje a literaturu. Tato práce ani její podstatná část nebyla předložena k získání jiného nebo stejného akademického titulu.

V Praze,

podpis

Poděkování


školiteli Pavle,
paní profesorko Evo,
mým milým
pane profesore Bobe,
mami,
všechny echmeťačky,
tati,
všichni echmeťáci,
Vlasto,
díky,
díky,
díky,
díky,
díky,
díky,
díky,
díky,
díky,
díky,
díky,
díky,
díky
moc!

Motto

„Jak říká náš Joe, cesty Páně jsou ještě neprozkoumaný…“

Enzo Barboni (překlad Jiří Lexa), Podivné dědictví

Klíčová slova

Kapilární elektroforéza, selektor, komplexační rovnováha, systémy se dvěma selektory, systémy s více selektory, efektivní mobilita, afinitní kapilární elektroforéza

Keywords

Capillary electrophoresis, selector, complexation equilibria, dual-selector systems, multi-selector systems, effective mobility, affinity capillary electrophoresis

Abstrakt

Kapilární elektroforéza je široce používanou separační metodou analytické chemie. Pokud je do základního elektrolytu přidána interagující látka, selektor, lze tuto metodu využít i pro separace enantiomerů nebo látek s velmi podobnými fyzikálně-chemickými vlastnostmi. V analytické praxi se často využívají také směsi selektorů, jednak záměrně připravené pro dosažení lepší separace, jednak proto, že komerčně dodávané derivatizované selektory mohou být ve skutečnosti směsmi látek lišícími se stupněm derivatizace a polohou substituentů. Matematický popis elektromigrace analytu v systémech s více selektory může usnadnit hledání optimálních separačních podmínek a zároveň poskytuje užitečný vhled do mechanismu separace v těchto z aplikačního hlediska velmi významných systémech.

V rámci této práce byl představen a experimentálně ověřen model elektromigrace analytu interagujícího se směsí dvou selektorů, který vychází z obecnějšího popisu systému s libovolným počtem selektorů. Tento model ukazuje, že směs, ve které se vzájemný poměr koncentrací selektorů nemění, lze pokládat za selektor jeden. V případě záměrné kombinace dvou selektorů lze pomocí tohoto popisu předpovědět, jak se budou separační schopnosti směsi měnit se změnou zastoupení obou selektorů, a zvolit nejvhodnější složení směsi i její celkovou koncentraci.

Dále byl představen model elektromigrace, který poprvé zahrnoval vedle interakce analytu s více selektory i možnost acidobazické disociace analytu. Model ukazuje, že závislost efektivní mobility na koncentraci selektoru, odvozená pro jedinou volnou formu analytu interagující s jediným selektorem, je obecně platná pro systémy se stechiometrií komplexace 1:1. Tento model také umožňuje na vzájemně provázané komplexační a acidobazické rovnováhy nahlížet odděleně a zvolit perspektivu vhodnou pro optimalizaci daného separačního systému. Závěry vyplývající z modelu byly experimentálně ověřeny na systému slabé jednosytné kyseliny jako analytu a dvou selektorů.

Pro určení komplexačních parametrů, se kterými pracují výše zmíněné elektromigrační modely, je klíčové stanovení správné efektivní mobility analytu. Z toho důvodu byla v rámci této práce navržena metoda umožňující měření efektivní mobility v systémech, kde může nabitý selektor interagovat s markerem elektroosmotického toku a tak výsledky měření znehodnotit. Dále byl navržen způsob, kterým lze určit správný migrační čas analytů podléhajících elektromigrační disperzi bez nutnosti nelineární regrese experimentálních dat.

Abstract

Capillary electrophoresis is a widely used separation method of analytical chemistry. Addition of a selector into the background electrolyte extends its applicability to separation of enantiomers or of compounds of similar physicochemical properties. In analytical practice, mixtures of selectors are also commonly used – either prepared intentionally to achieve better separation or because commercially available selectors may be mixtures of compounds differing in the degree of substitution and substituent positions. Mathematical description of these systems, which are highly relevant in analytical practice, can simplify search for optimal separation conditions. Also, it provides a useful insight into the separation mechanism.

In this work, a model of electromigration of an analyte interacting with a mixture of two selectors is proposed and experimentally verified. This model results from a more general description of systems with an arbitrary number of selectors. The model shows that a selector mixture can be treated as a single selector if the ratio of the respective selector concentrations is kept constant. When the mixture is prepared intentionally, this description predicts, how separation potential of the mixture changes with its composition. Thus it allows the optimal composition and total concentration of the selector mixture to be chosen.

Consequently, a generalized model of electromigration was proposed that for the first time considers analyte undergoing acid-base equilibria along with complexation with multiple selectors. The generalized model shows that the dependency of the effective mobility on the selector concentration, which was originally developed for the case of a single free form of an analyte interacting with a single selector, is generally applicable for systems with 1:1 complexation stoichiometry. The model also enables decoupling of the highly interconnected complexation and acid-base dissociation equilibria. Therefore, the most suitable perspective can be chosen for the particular system optimization. Assumptions resulting from the generalized model were experimentally verified on a system of a week monoprotic acid as an analyte and two selectors.

Determination of complexation parameters serving as input for the above mentioned models requires measurement of correct effective mobilities of analytes. Therefore, this work proposes a method enabling measurement of unbiased effective mobilities in system in which a charged selector may interact with a neutral marker of the electroosmotic flow. A procedure is also proposed for determination of correct migration time of analyte peaks deformed by the electromigration dispersion without the need of nonlinear regression.

Obsah

Seznam použitých zkratek a symbolů

A-β-CD	6-monodeoxy-6-monoamino-β-cyclodextrin
ACE	afinitní kapilární elektroforéza (*affinity capillary electrophoresis*)
BGE	základní elektrolyt (*background electrolyte*)
β-CD	nativní β-cyclodextrin
CD	cyclodextrin
CE	kapilární elektroforéza (*capillary electrophoresis*)
DM-β-CD	heptakis(2,6-di-O-methyl)-β-cyclodextrin
EMD	elektromigrační disperze
EMO	elektromigračního pořadí analytů (*electromigration order*)
EOF	elektroosmotický tok (*electroosmotic flow*)
HVL	Haarhoffovou – van der Lindeho (funkce)
Malt-β-CD	6-O-α-maltosyl-β-cyclodextrin
M_AM_S	(systém, model) s více volnými formami analytu a více selektory (*multi-free-analyte-form multi-selector*)
M_AS_S	(systém, model) s více volnými formami analytu a jedním selektorem (*multi-free-analyte-form single-selector*)
S_AM_S	(systém, model) s jednou volnou formou analytu a více selektory (*single-free-analyte-form multi-selector*)
S_AS_S	(systém, model) s jednou volnou formou analytu a jedním selektorem (*single-free-analyte-form single-selector*)
S-β-CD	nedefinovaně sulfatovaný β-cyclodextrin

a_0	parametr HVL funkce odpovídající ploše píku
a_1	parametr HVL funkce odpovídající poloze píku

a_2	parametr HVL funkce odpovídající symetrickému rozšíření píku
a_3	parametr HVL funkce odpovídající asymetrické deformaci píku
α	frakce maximální výšky píku
c_S	analytická koncentrace selektoru
c_{Sj}	analytická koncentrace *j*-tého selektoru
c_{tot}	celková koncentrace selektorů v systému (součet analytických koncentrací všech přítomných selektorů)
c_{tot}^{Tr}	celková koncentrace selektoru, při které dochází k záměně elektromigračního pořadí analytů
$\Delta\mu_{AB,eff}$	rozdíl efektivních mobilit separovaných enantiomerů A a B
$\Delta\mu_{AB,eff,j}$	rozdíl efektivních mobilit separovaných enantiomerů způsobený interakcí s *j*-tým selektorem
$f_q^{-1}(q)$	závislost parametru a_3 příslušné HVL funkce na asymetrii píku
$HVL(t)$	funkční hodnota HVL funkce v čase *t*
χ_{Ai}	molární zlomek *i*-té volné formy analytu vzhledem k celkovému množství volného analytu
χ_{Sj}	molární zlomek *j*-tého selektoru ve směsi selektorů
i	číslovací index pro volné formy analytu
j	číslovací index pro selektory
$K'_{a,HA}$	koncentračně definovaná acidobazická disociační konstanta analytu
$K'_{a,HAS}$	koncentračně definovaná acidobazická disociační konstanta komplexu analytu se selektorem
$K'_{a,HASj}$	koncentračně definovaná acidobazická disociační konstanta komplexu analytu s *j*-tým selektorem
K'_{AiSj}	koncentračně definovaná komplexační konstanta interakce *i*-té volné formy analytu s *j*-tým selektorem
K'^{M}_{AiS}	M-souhrnná komplexační konstanta interakce *i*-té volné formy analytu se směsí selektorů

K'_{AS}	koncentračně definovaná komplexační konstanta interakce analytu se selektorem
K'_{A^-S}	koncentračně definovaná komplexační konstanta interakce disociované formy analytu se selektorem
K'_{ASj}	koncentračně definovaná komplexační konstanta interakce analytu s *j*-tým selektorem
K'_{A^-Sj}	koncentračně definovaná komplexační konstanta interakce disociované formy analytu s *j*-tým selektorem
K'^{pH}_{ASj}	pH-souhrnná komplexační konstanta interakce analytu přítomného ve více volných formách s *j*-tým selektorem
K'^{M}_{AS}	souhrnná komplexační konstanta interakce analytu se směsí selektorů (M-souhrnná komplexační konstanta)
$K'^{M}_{A^-S}$	M-souhrnná komplexační konstanta interakce disociované formy analytu se směsí selektorů
$K'^{M_AM_S}_{AS}$	souhrnná komplexační konstanta interakce analytu přítomného v libovolném počtu volných forem se směsí selektorů (M_AM_S-souhrnná komplexační konstanta)
K'^{pH}_{AS}	komplexační konstanta interakce analytu přítomného ve více volných formách se selektorem (pH-souhrnná komplexační konstanta)
K_α	převodní parametr mezi asymetrií píku a šířkou píku v α-frakci jeho maximální výšky a parametrem a_1 příslušné HVL funkce
K'_{BSj}	koncentračně definovaná komplexační konstanta interakce analytu B s *j*-tým selektorem
K'_{HAS}	koncentračně definovaná komplexační konstanta interakce protonované formy analytu se selektorem
K'_{HASj}	koncentračně definovaná komplexační konstanta interakce protonované formy analytu s *j*-tým selektorem
K'^{M}_{HAS}	M-souhrnná komplexační konstanta interakce protonované formy analytu se směsí selektorů
K'^{M}_{S}	souhrnná komplexační konstanta interakce analytu A nebo B se směsí selektorů (M-souhrnná komplexační konstanta)
L	počet volných forem analytu v systému

L_α	převodní parametr mezi asymetrií píku a šířkou píku v α-frakci jeho maximální výšky a parametrem a_2 příslušné HVL funkce
μ_A	mobilita volné formy analytu
μ_{A^-}	mobilita volné disociované formy analytu
$\mu_{A,eff}$	efektivní mobilita analytu A
μ_{Ai}	mobilita *i*-té volné formy analytu
$\mu_A^{M_AM_S}$	souhrnná mobilita volného analytu přítomného v libovolném počtu volných forem (M_AM_S-souhrnná mobilita volného analytu)
μ_{AiSj}	mobilita komplexu *i*-té volné formy analytu s *j*-tým selektorem
μ_{AiS}^M	M-souhrnná mobilita komplexu *i*-té volné formy analytu se směsí selektorů
μ_A^{pH}	mobilita volného analytu při daném pH (pH-souhrnná mobilita volného analytu)
μ_{AS}	mobilita komplexu analytu se selektorem
μ_{A^-S}	mobilita komplexu disociované formy analytu se selektorem
μ_{ASj}	mobilita komplexu analytu s *j*-tým selektorem
μ_{ASj}^{pH}	pH-souhrnná mobilita komplexu analytu přítomného ve více volných formách s *j*-tým selektorem
μ_{AS}^M	souhrnná mobilita komplexu analytu se směsí selektorů (M-souhrnná mobilita komplexu)
$\mu_{AS}^{M_AM_S}$	souhrnná mobilita komplexu analytu přítomného v libovolném počtu volných forem se směsí selektorů (M_AM_S-souhrnná mobilita komplexu)
μ_{AS}^{pH}	souhrnná mobilita komplexu analytu přítomného ve více volných formách se selektorem (pH-souhrnná mobilita komplexu)
μ_B	mobilita volné formy analytu B
$\mu_{B,eff}$	efektivní mobilita analytu B
μ_{BS1}	mobilita komplexu analytu B s prvním selektorem
μ_{BS2}	mobilita komplexu analytu B se druhým selektorem
μ_f	mobilita volné formy chirálního analytu stejná pro oba enantiomery

μ_{HA}	mobilita volné protonované formy analytu
μ_{HAS}	mobilita komplexu protonované formy analytu se selektorem
$\mu_{S,j}$	mobilita komplexu chirálního analytu a *j*-tým selektorem stejná pro oba enantiomery
μ_S^M	souhrnná mobilita komplexu analytu A nebo B se směsí selektorů (M-souhrnná mobilita komplexu)
N	počet selektorů v systému
q	asymetrie píku
r	koeficient vyjadřující míru, s jakou první selektor přispívá k rozdílu mobilit enantiomerů v systému se dvěma selektory
s	koeficient vyjadřující míru, s jakou druhý selektor přispívá k rozdílu mobilit enantiomerů v systému se dvěma selektory
t	čas
t_M	čas odpovídající maximu píku
T_{USP}	faktor chvostování píku podle Amerického lékopisu (*U. S. Pharmacopeia tailing factor*)
$w_{0,05}$	šířka píku v 5 % jeho maximální výšky
$w_{0,5}$	šířka píku v polovině jeho maximální výšky
w_α	šířka píku v α-frakci jeho maximální výšky
w_β	šířka píku v β-frakci jeho maximální výšky
$w_{L0,05}$	levá pološirka píku v 5 % jeho maximální výšky
$w_{L\alpha}$	levá pološirka píku v α-frakci jeho maximální výšky
$w_{P\alpha}$	pravá pološirka píku v α-frakci jeho maximální výšky

1 Úvod

Kapilární elektroforéza (CE) je široce používanou separační metodou analytické chemie. Přídavek interagující látky (selektoru) do základního elektrolytu rozšiřuje pole využitelnosti CE například o separace neutrálních analytů, separace látek s velmi podobnými fyzikálně-chemickými vlastnostmi, a zejména o enantioselektivní separace. Velkou výhodou CE je možnost snadno měnit použitý selektor a jeho koncentraci. V analytické praxi se využívá široká škála chirálních selektorů: crown-ethery, makrocyklická antibiotika, proteiny, chirální micely, cyklofruktany a další [1, 2]. Nejčastěji používanými chirálními selektory v CE jsou cyklodextriny (CD) [1-7], cyklické oligosacharidy skládající se nejběžněji ze šesti (α-cyklodextrin), sedmi (β-cyklodextrin) nebo osmi (γ-cyklodextrin) glukopyranozových jednotek.

Současně s využíváním selektorů v CE se rozvíjel také matematický popis takových systémů. Důvodem k sestavování matematických modelů elektromigrace byla a je možnost předpovědět výsledek separace na základě fyzikálně-chemických parametrů systému, což může významně usnadnit hledání optimálních podmínek pro konkrétní separaci. Stejně důležité ale je, že modely umožňují lépe pochopit mechanismy, které k separaci vedou.

1.1 Popis elektromigrace v komplexujících systémech

Systémy s jednou formou volného analytu a jedním selektorem (S_AS_S systémy)

Pravděpodobně první matematický popis elektromigrace v komplexujícím systému byl představen už v roce 1969 [8, 9]. Nicméně jako nejstarší vztah popisující efektivní mobilitu[*] analytu podléhajícího komplexaci se selektorem, se většinou uvádí model publikovaný Wrenem a Rowem roku 1992 [10].

Pokud se analyt vyskytuje ve více formách, mezi kterými se ustavuje rychlá rovnováha (ve srovnání s elektroforetickou migrací), lze efektivní mobilitu tohoto analytu obecně

[*] Přesnějším výrazem by byla „elektroforetická mobilita“, protože termín „mobilita“ má obecnější význam. Jelikož se však tato dizertační práce zabývá pouze elektroforézou a nehrozí zmatení pojmů, bude přívlastek „elektroforetická“ vynechávána.

vyjádřit jako vážený průměr mobilit jeho jednotlivých forem, přičemž vahou je molární zlomek příslušné formy analytu vzhledem k jeho celkové (analytické) koncentraci. V případě popsaném v modelu Wrena a Rowa je jedinou takovou rovnováhou interakce analytu A se selektorem S charakterizovaná komplexační konstantou K'_{AS}:

$$\mathrm{A} + \mathrm{S} \rightleftharpoons \mathrm{AS} \qquad K'_{AS} = \frac{[\mathrm{AS}]}{[\mathrm{A}][\mathrm{S}]} \tag{1}$$

Konstanta K'_{AS} je definována pomocí rovnovážných koncentrací (nejedná se o termodynamickou konstantu, která by byla definována pomocí aktivit; K'_{AS} závisí nejen na teplotě, ale i na iontové síle). Analyt je tedy přítomen ve dvou formách: volné nekomplexované formě A s mobilitou μ_A a ve formě komplexu AS s mobilitou μ_{AS} a jeho efektivní mobilitu $\mu_{A,eff}$ lze vyjádřit vztahem:

$$\mu_{A,eff} = \frac{\mu_A + \mu_{AS} K'_{AS}[\mathrm{S}]}{1 + K'_{AS}[\mathrm{S}]} \tag{2}$$

Pro praktické užití je třeba zavést aproximaci, že rovnovážná koncentrace volného selektoru [S] je rovna analytické koncentraci selektoru c_S (zanedbá se úbytek volného selektoru způsobený interakcí s analytem):

$$[\mathrm{S}] = c_S \tag{3}$$

Dosazením podmínky (3) do rovnice (2) získáme závislost efektivní mobility analytu na koncentraci selektoru v základním elektrolytu (BGE, *background electrolyte*) publikovanou Wrenem a Rowem [10]:

$$\mu_{A,eff} = \frac{\mu_A + \mu_{AS} K'_{AS} c_S}{1 + K'_{AS} c_S} \tag{4}$$

Vztah (4) je platný pouze za následujících podmínek:

(i) Teplota je konstantní, což je obecně „kategorickým imperativem“ ve fyzikální chemii. S teplotou se mění jak rovnovážné konstanty, tak mobility všech částic v roztoku. Instrumentace pro CE umožňuje termostatovat většinu délky kapiláry, a proto lze tento požadavek zpravidla pokládat za splněný.

(ii) Iontová síla je konstantní. Komplexační konstanta K'_{AS} je definovaná pomocí koncentrací a je tedy platná pouze pro danou hodnotu iontové síly BGE. Mobility μ_A a μ_{AS} jsou rovněž závislé na iontové síle a za konstantní parametry v rovnici (4) je lze pokládat pouze pokud se při změně koncentrace selektoru iontová síla zachová konstantní. Tato podmínka je splněna v případě neutrálních selektorů, pokud nedochází k jejich významné interakci s některou složkou základního elektrolytu [11]. V případě nabitých selektorů je nutné zvýšení koncentrace selektoru kompenzovat snížením koncentrace složek základního elektrolytu [12, 13] nebo zavést do rovnice (4) příslušnou korekci [12].

(iii) Je možné zavést aproximaci (3) – úbytek volného selektoru způsobený komplexací s analytem je zanedbatelný. Tato podmínka je vždy splněna na okraji píku analytu. V případě, že uvnitř zóny analytu dochází v důsledku komplexace k významnému úbytku selektoru, není důsledkem posun píku jako celku, ale jeho deformace do trojúhelníkového tvaru [14, 15]. Proložení takového píku Haarhoff – van der Lindeho (HVL) funkcí [16, 17] poskytuje migrační čas odpovídající nekonečnému zředění analytu [18], při kterém je podmínka (3) automaticky splněna (*viz* též kapitolu 1.2).

(iv) Viskozita BGE je konstantní. Při vysokých koncentracích selektoru je mobilita analytu ovlivněna nejen komplexací, ale i změnou viskozity BGE. V literatuře je však popsáno několik způsobů, jak při matematickém zpracování tento efekt korigovat [12, 19, 20].

(v) Dochází pouze ke komplexaci o stechiometrii 1:1 (analyt : selektor). Tato stechiometrie samozřejmě není jediná možná, nicméně je všeobecně pokládána za nejrelevantnější, zejména pokud jde o interakci s cyklodextriny [21, 22].

Všechny matematické popisy elektromigrace v komplexujících systémech, o kterých bude tato dizertační práce dále pojednávat, vycházejí z modelu (4) a výše zmíněné podmínky platnosti se tím pádem vztahují i na ně.

Na základě rovnice (4) byla odvozena řada dalších modelů popisujících S_AS_S (*single-free-analyte-form single-selector*) systémy [19, 23-27]. Jejich cílem bylo pomocí efektivních

mobilit separovaných analytů vyjádřit parametry kvantifikující úspěšnost separace: rozdíl efektivních mobilit [10, 19], relativní rozdíl mobilit (rozdíl mobilit dělený jejich průměrem) [28], selektivitu (poměr mobilit) [28], rozlišení [23, 24] nebo počet teoretických pater [27]. Některé z modelů zavádějí další aproximaci, a sice že při chirální separaci je mobilita vzniklého komplexu μ_{AS} stejná pro oba enantiomery [10, 19, 23, 24]. Tento předpoklad lze pokládat za oprávněný v případě interakce s jediným definovaným selektorem, jelikož oba takové komplexy mají stejný náboj a podobnou strukturu. Přestože velká část S_AS_S modelů se zaměřovala na chirální separace, vztah (4) lze samozřejmě použít i pro optimalizaci nechirálních separací, při kterých se využívá komplexace se selektorem [26, 29].

Popis systémů s více formami volného analytu a jedním selektorem (M_AS_S systémy)

Nevýhodou modelu (4) (a S_AS_S modelů na něj navazujících) bylo, že braly v úvahu pouze jednu formu volného analytu. Látkami separovanými kapilární elektroforézou jsou ale často slabé kyseliny, báze nebo amfolyty podléhající elektrolytické disociaci. Obě přítomné formy (například disociovaná a protonovaná u slabé kyseliny) pak mohou interagovat se selektorem s různými komplexačními konstantami za vzniku komplexů o různých mobilitách. Tím pádem pH základního elektrolytu, kterým je řízen stupeň disociace analytu, může mít velký vliv na výsledek separace.

Popisem M_AS_S (*multi-free-analyte-form single-selector*) systémů se dlouhodobě zabývala skupina profesora Vigha [30-33]. Pro efektivní mobilitu slabé jednosytné kyseliny [30] byl odvozen následující vztah:

$$\mu_{A,eff} = \frac{\mu_{A^-} + K'_{A^-S}\mu_{A^-S}c_S + \frac{[\mathrm{H_3O^+}]}{K'_{a,HA}}(\mu_{HA} + K'_{HAS}\mu_{HAS}c_S)}{1 + K'_{A^-S}\mu_{A^-S}c_S + \frac{[\mathrm{H_3O^+}]}{K'_{a,HA}}(1 + K'_{HAS}c_S)} \tag{5}$$

kde μ_{A^-}, μ_{A^-S} a K'_{A^-S} jsou mobilita volného disociovaného analytu, mobilita jeho komplexu se selektorem a příslušná komplexační konstanta; μ_{HA}, μ_{HAS} a K'_{HAS} jsou mobilita volného protonovaného analytu, mobilita jeho komplexu se selektorem a příslušná komplexační

konstanta, $[H_3O^+]$ je koncentrace oxoniového kationtu v BGE a $K'_{a,HA}$ je disociační konstanta analytu definovaná pomocí koncentrací:

$$K'_{a,HA} = \frac{[H_3O^+][A^-]}{[HA]} \tag{6}$$

Obdobný vztah byl odvozen i pro slabé jednosytné báze [31]. Modely popisující M_AS_S systémy byly publikovány i dalšími skupinami [34-38].

Lelièvre *et al.* [34] ukázali, že při konstantním pH lze závislost efektivní mobility slabé jednosytné kyseliny na koncentraci selektoru popsat funkcí formálně shodnou se vztahem (4):

$$\mu_{A,eff} = \frac{\mu_A^{pH} + \mu_{AS}^{pH} K_{AS}^{'pH} c_S}{1 + K_{AS}^{'pH} c_S} \tag{7}$$

kde μ_A^{pH}, μ_{AS}^{pH} a $K_{AS}^{'pH}$ jsou mobilita volného analytu, mobilita komplexu a komplexační konstanta při daném pH:

$$\mu_A^{pH} = \frac{K'_{a,HA}\mu_{A^-} + [H_3O^+]\mu_{HA}}{K'_{a,HA} + [H_3O^+]} \tag{8}$$

$$\mu_{AS}^{pH} = \frac{K'_{a,HAS}\mu_{A^-S} + [H_3O^+]}{K'_{a,HAS} + [H_3O^+]} \tag{9}$$

$$K_{AS}^{'pH} = K'_{HAS}\frac{K'_{a,HAS} + [H_3O^+]}{K'_{a,HA} + [H_3O^+]} \tag{10}$$

$K'_{a,HAS}$ je (koncentračně definovaná) acidobazická disociační konstanta komplexu analytu se selektorem. Její hodnota je jednoznačně dána disociační konstantou analytu $K'_{a,HA}$ a komplexačními konstantami jeho disociované a nedisociované formy K'_{A^-S} a K'_{HAS}:

$$K'_{a,HAS} = K'_{a,HA} \frac{K'_{A^-S}}{K'_{HAS}} \quad (11)$$

Parametry μ_A^{pH}, μ_{AS}^{pH} a $K_{AS}^{\prime pH}$ byly později [37] vyjádřeny i pro dvojsytnou kyselinu. Tyto parametry jsou závislé na hodnotě pH (a iontové síle) BGE. Lelièvrův model (dále bude označován jako pH-souhrnný model) tedy umožňuje optimalizovat koncentraci selektoru v BGE, ale nikoli pH, které musí zůstat konstantní. Na druhou stranu model teoreticky potvrzuje, že optimalizační postupy vyvinuté pro S_AS_S systémy lze použít i v případě M_AS_S systémů, pokud se pH BGE nemění.

V případě chirálních separací je důležitou výjimkou z předešlého tvrzení předpoklad stejné mobility pro komplexy obou enantiomerů se selektorem: Jak je zjevné z rovnic (9) a (11), parametr μ_{AS}^{pH} nezávisí jen na mobilitách komplexů fyzicky přítomných v roztoku (o nichž lze předpokládat, že se příliš neliší pro oba enantiomery v daném disociovaném respektive protonovaném stavu), ale závisí i na hodnotách komplexačních konstant (o nichž lze naopak předpokládat, že se pro oba enantiomery liší – protože jinak by při stejné mobilitě komplexů interakce se selektorem nevedla k separaci). To odpovídá experimentálním výsledkům Moffadela *et al.* [37], kteří při popisu chirální separace pomocí pH-souhrnného modelu pozorovali, že pH-souhrnné mobility komplexů se pro dvojici enantiomerů lišily.

Systémy s jednou formou volného analytu a více selektory (S_AM_S systémy)

V analytické praxi se často používají směsi selektorů. Je to jednak proto, že komerčně vyráběné derivatizované cyklodextriny jsou ve skutečnosti mnohdy směsí selektorů lišících se jak stupněm substituce, tak polohou substituentů [39-41]. Někdy jsou ale směsi selektorů připravovány záměrně za účelem dosažení lepší separace [2, 5, 7, 42, 43]. Publikované teoretické popisy S_AM_S (*single-free-analyte-form multi-selector*) systémů v CE byly shrnuty v přehledovém článku, který je zařazen na konci této kapitoly (*Publikace I*).

První matematický model elektromigrace analytu v BGE se dvěma selektory byl publikován v roce 1994 [44] a byl přirozeným rozšířením modelu (4) o interakci s dalším selektorem:

$$\mu_{A,eff} = \frac{\mu_A + \mu_{AS1} K'_{AS1} c_{S1} + \mu_{AS2} K'_{AS2} c_{S2}}{1 + K'_{AS1} c_{S1} + K'_{AS2} c_{S2}} \quad (12)$$

kde c_{S1} a c_{S2} jsou koncentrace prvního a druhého selektoru, K'_{AS1} a K'_{AS2} jsou komplexační konstanty analytu s prvním a druhým selektorem a μ_{AS1} a μ_{AS2} jsou mobility komplexů analytu s prvním a druhým selektorem.

V následujících dvaceti letech byla publikována řada prací zabývajících se teoretickým popisem S_AM_S systémů (jsou podrobně rozebrány v *Publikaci I*). Velká část z nich vycházela z modelu (12) [44-51]. Tyto modely obsahují dvě nezávislé proměnné – koncentrace dvou selektorů v BGE. Hledání optimálních podmínek je tím pádem náročnější ve srovnání s S_AS_S modely. Například pro grafické znázornění závislosti optimalizovaného parametru (relativní rozdíl mobilit [47], selektivita [47], rozlišení [45]) je nutné vykreslit třídimenzionální graf, případně studovat závislost toliko na koncentraci jednoho selektoru při konstantní koncentraci selektoru druhého [45-48]. Proto autoři často využívali matematický popis S_AM_S systémů pouze ke kvalitativnímu vysvětlení pozorovaných experimentálních výsledků, jako například záměny migračního pořadí analytů [44, 46, 52-54]. Mezi pětapadesáti pracemi, ve kterých byl k separaci použit BGE obsahující dva cyklodextriny, jenom ve třech byly optimální koncentrace selektorů vybrány na základě výpočtů a pomocí elektromigračního modelu [45, 49, 50].

Alternativním přístupem používaným pro chirální separace pomocí dvou selektorů je vyjádřit rozdíl efektivních mobilit separovaných enantiomerů A a B, $\Delta\mu_{AB,eff}$, jako vážený průměr rozdílů efektivních mobilit generovaných interakcí s jedním a s druhým selektorem, $\Delta\mu_{AB,eff,1}$ a $\Delta\mu_{AB,eff,2}$ [50, 54, 55]:

$$\Delta\mu_{AB,eff} = r \cdot \Delta\mu_{AB,eff,1} + s \cdot \Delta\mu_{AB,eff,2} \quad (13)$$

Rozdíl mobilit generovaný *j*-tým selektorem, $\Delta\mu_{AB,eff,j}$, je odvozen z rovnice (4) se zavedením předpokladu, že mobilita komplexu je stejná pro oba enantiomery:

$$\Delta\mu_{AB,eff,j} = \frac{\left(\mu_{S,j} - \mu_f\right)\left(K'_{BSj} - K'_{ASj}\right) c_{Sj}}{1 + \left(K'_{BSj} + K'_{ASj}\right) c_{Sj} + K'_{BSj} K'_{ASj} c_{Sj}^2} \quad (14)$$

kde $\mu_f = \mu_A = \mu_B$ je mobilita volného analytu (stejná pro oba enantiomery), $\mu_{S,j} = \mu_{ASj} = \mu_{BSj}$ je mobilita komplexu analytu se sektorem, K'_{ASj} a K'_{BSj} jsou komplexační konstanty prvního a druhého enantiomeru se selektorem a c_{Sj} je koncentrace selektoru. Koeficienty r a s v rovnici (13) nejsou přesně specifikovány, ale při používání tohoto modelu se obecně předpokládá, že se jedná o kladná čísla závislá na parametrech komplexace a koncentracích obou selektorů. Vztah (13) tedy není možné použít pro výpočet optimálních koncentrací obou selektorů. Je ale v praxi hojně využíván ke kvalitativnímu posouzení, jaké selektory je vhodné zkombinovat, aby přidání obou selektorů do BGE přineslo lepší separaci ve srovnání se situací, kdy je přidán pouze jeden z nich [56-59]. Za předpokladu, že r a s jsou kladná čísla, musí být členy $\Delta\mu_{AB,eff,1}$ a $\Delta\mu_{AB,eff,2}$ buďto oba kladné, nebo oba záporné, aby kombinace selektorů separaci nezhoršovala. Z toho vyplývá, že pokud mají selektory opačný vliv na mobilitu enantiomerů (*mobility effect*) – komplexace s jedním selektorem pohyb enantiomerů zrychluje, komplexace se druhým zpomaluje, pak musí mít i opačný rozpoznávací vzorec (*recognition pattern*) – enantiomer, který interaguje silněji s jedním selektorem, interaguje se druhým slaběji. Naopak, pokud mají oba selektory souhlasný vliv na mobilitu enantiomerů – komplexace s oběma selektory pohyb enntiomerů buďto zrychluje, nebo zpomaluje, musí mít také souhlasný rozpoznávací vzorec – oba selektory komplexují silněji se stejným enantiomerem. Nicméně v pozdějších publikacích [43, 50] došli autoři modelu k závěru, že ve druhém z výše uvedených případů nebude sice smísení selektorů separaci výrazně zhoršovat, ale ani ji nezlepší a je výhodnější použít pouze jeden (ten „selektivnější“) z obou selektorů.

Nicméně, jak je uvedeno v *Publikaci I*, ve skutečnosti mohou parametry r a s v rovnici (13) nabývat jak kladných, tak záporných hodnot a výše zmíněné závěry tedy nejsou obecně platné. To je názorně demonstrováno na hypotetickém (nicméně reálně možném) systému chirálního analytu a dvou selektorů: V tomto případě mají oba selektory souhlasný vliv na mobilitu (interakce s oběma pohyb enantiomerů zpomaluje) a opačný rozpoznávací vzorec – podle výše uvedených pravidel odvozených z rovnice (13) by smísení takových dvou selektorů mělo separaci pouze zhoršovat. Bylo ale ukázáno (*Publikace I*, Figure 2), že směs těchto dvou selektorů může generovat větší rozdíl efektivních mobilit enantiomerů i větší selektivitu (poměr efektivních mobilit) ve srovnání s optimální koncentrací jednoho nebo druhého selektoru použitého samostatně.

Rozšířením modelu (4) (respektive (12)) získali Peng *et al.* [60] vztah popisující efektivní mobilitu analytu v S_AM_S systému s libovolným počtem selektorů, *N*, (každý tvoří s analytem komplex o stechiometrii 1 : 1):

$$\mu_{A,eff} = \frac{\mu_A + \mu_{AS1}K'_{AS1}c_{S1} + \mu_{AS2}K'_{AS2}c_{S2} + \ldots + \mu_{ASN}K'_{ASN}c_{SN}}{1 + K'_{AS1}c_{S1} + K'_{AS2}c_{S2} + \ldots + K'_{ASN}c_{SN}} \tag{15}$$

Zjevnou nevýhodou modelu (15) je jeho *N*-dimenzionalita, která by značně komplikovala jeho použití k optimalizaci separace v praxi. Karanack *et al.* [61] později ukázali, jak lze tento model výrazně zjednodušit. Koncentraci každého ze selektorů v systému lze vyjádřit jako:

$$c_{Sj} = \chi_{Sj}c_{tot} \tag{16}$$

kde χ_{Sj} je molární zlomek *j*-tého selektoru ve směsi a c_{tot} je celková koncentrace selektorů (součet koncentrací všech přítomných selektorů). Dosazením z rovnice (16) do rovnice (15) a následnou úpravou vznikne vztah:

$$\mu_{A,eff} = \frac{\mu_A + (\mu_{AS1}K'_{AS1}\chi_{S1} + \mu_{AS2}K'_{AS2}\chi_{S2} + \ldots + \mu_{ASN}K'_{ASN}\chi_{SN})c_{tot}}{1 + (K'_{AS1}\chi_{S1} + K'_{AS2}\chi_{S2} + \ldots + K'_{ASN}\chi_{SN})c_{tot}} \tag{17}$$

V případě, že složení směsi (vzájemný poměr koncentrací selektorů vyjádřený molárními zlomky χ_{Sj}) je konstantní, pak zavedením následující substituce:

$$K^M_{AS} = K'_{AS1}\chi_{S1} + K'_{AS2}\chi_{S2} + \ldots + K'_{ASN}\chi_{SN} = \sum_{j=1}^{N} K'_{ASj}\chi_{Sj} \tag{18}$$

$$\mu^M_{AS} = \frac{\mu_{AS1}K'_{AS1}\chi_{S1} + \mu_{AS2}K'_{AS2}\chi_{S2} + \ldots + \mu_{ASN}K'_{ASN}\chi_{SN}}{K'_{AS1}\chi_{S1} + K'_{AS2}\chi_{S2} + \ldots + K'_{ASN}\chi_{SN}} = \frac{\sum_{j=1}^{N}\mu_{ASj}K'_{ASj}\chi_{Sj}}{K^M_{AS}} \tag{19}$$

lze získat výsledný výraz pro efektivní mobilitu analytu interagujícího se směsí selektorů:

$$\mu_{A,eff} = \frac{\mu_A + \mu_{AS}^{M} K_{AS}^{\prime M} c_{tot}}{1 + K_{AS}^{\prime M} c_{tot}} \tag{20}$$

Rovnice (20) je formálně shodná s výrazem (4) popisujícím systém, kde analyt interaguje pouze s jedním selektorem. Pokud je složení směsi selektorů konstantní, lze na směs selektorů pohlížet jako na selektor jediný, jehož interakce s analytem je charakterizována M-souhrnnou (*M-overall*) komplexační konstantou $K_{AS}^{\prime M}$ a M-souhrnnou mobilitou komplexu μ_{AS}^{M}. Tyto parametry lze pro danou směs změřit experimentálně metodou afinitní kapilární elektroforézy (ACE, *affinity capillary electrophoresis*) [20, 62] a následně je použít k hledání optimální celkové koncentrace selektoru – a to bez ohledu na fakt, že konkrétní složení směsi (χ_{Sj}) a komplexační parametry pro její jednotlivé složky nejsou známy.

Karanack *et al.* ve své práci [61] používali k separaci směs dvou derivatizovaných cyklodextrinů, z nichž každý byl ve skutečnosti sám směsí selektorů lišících se stupněm substituce a polohou substituentů. Modelem (18) – (20) demonstrovali, že pro popis takového systému může být použit vztah (12) (odvozený původně pro směs dvou „čistých“ selektorů) a dále se souhrnným modelem (18) – (20) nepracovali. Pravděpodobně z toho důvodu model zapadl, dokud nebyl nezávisle znovu odvozen a publikován naší skupinou [63, 64].

Z modelu (18) – (20) (dále bude označován jako M-souhrnný model) vyplývá, že optimalizační strategie odvozené pro S_AS_S systémy lze použít pro optimalizaci celkové koncentrace směsi selektorů v S_AM_S systémech – ovšem opět s touž důležitou výjimkou jako v případě pH-souhrnného popisu (7) – (10): V případě chirálních separací nelze *a priori* předpokládat, že M-souhrnná mobilita komplexu μ_{AS}^{M} bude stejná pro oba enantiomery. Tento parametr nelze chápat jako mobilitu nějaké částice fyzicky přítomné v roztoku, ale jednoduše jako parametr μ_{AS}^{M} závislosti (20), tedy mobilitu, ke které se limitně blíží efektivní mobilita analytu se vzrůstající celkovou koncentrací směsi selektorů. Z rovnice (19) vyplývá, že hodnota tohoto parametru závisí jak na mobilitách jednotlivých komplexů μ_{ASj}, tak na komplexačních konstantách a složení směsi. I pokud budou pro každý jednotlivý selektor *j* mobility komplexu stejné pro oba enantiomery, ale ty budou různé pro různé selektory, pak se budou výsledné μ_{AS}^{M} u obou enantiomerů lišit (pokud se alespoň pro jeden selektor budou lišit komplexační konstanty obou enantiomerů). Tímto mechanismem je možné vysvětlit velkou separační schopnost nedefinovaně sulfatovaných cyklodextrinů [64], která je velmi významná v analytické praxi.

M-souhrnný model poskytl užitečný vhled do mechanismu separace se směsmi selektorů, jako jsou komerčně dodávané derivatizované cyklodextriny, u kterých uživatel nezná přesné složení směsi. Využití tohoto přístupu také pro popis záměrně připravovaných směsí dvou selektorů, stejně jako experimentální ověření, je ukázáno v *Publikaci II*.

Na rozdíl od systémů s jedním selektorem, pro které existují M_AS_S modely zmiňované výše, publikované modely elektromigrace v systémech s více selektory dosud nezahrnovaly možnou acidobazickou disociaci analytu. Takové rozšíření modelu (18) - (20) na M_AM_S (*multi-free-analyte-form multi-selector*) systémy, kde více volných forem analytu interaguje s více selektory je představeno v *Publikacích III* a *IV*.

1.2 Stanovení správné efektivní mobility

Všechny elektromigrační modely rozebírané v předešlé kapitole pracují s parametry komplexace – komplexačními konstantami a mobilitami komplexu. Ty je nutné stanovit experimentálně, zpravidla proložením závislosti efektivních mobilit daného analytu na koncentraci selektoru vhodnou funkcí (ACE metoda [20, 62]). Určení správné efektivní mobility analytu je proto klíčové pro stanovení komplexačních parametrů a jejich následnou využitelnost v různých optimalizačních strategiích.

Tato dizertační práce se detailněji věnuje dvěma úskalím, se kterými se experimentátor při stanovování správné efektivní mobility může potýkat:

(i) stanovení mobility elektroosmotického toku v základních elektrolytech obsahujících nabitou interagující složku;

(ii) určení migračního času u píků deformovaných elektromigrační disperzí.

Elektroosmotický tok a jeho stanovení

Elektroosmotický tok (EOF, *electroosmotic flow*) v elektroforéze je způsoben nábojem na vnitřní stěně kapiláry (ten vzniká například disociací silanolových skupin na povrchu nemodifikované křemenné kapiláry) a projevuje se pohybem celého obsahu kapiláry směrem k jedné z elektrod [65]. Rychlost analytu vůči kapiláře a detektoru je tak dána součtem jeho pohybu skrz roztok způsobeného elektromigrací, a pohybu roztoku jako celku způsobeného elektroosmotickým tokem. Pro určení efektivní mobility analytu (rychlosti pohybu skrz roztok vztažené na jednotkovou intenzitu elektrického pole) je tedy třeba správně stanovit

mobilitu EOF a tu odečíst od celkové, zjevné mobility analytu. V literatuře je popsána řada způsobů stanovení mobility EOF, které jsou shrnuty například v přehledovém článku Wanga *et al.* [66].

Nejčastější je použití neutrálního markeru (značkovače), který nemá vlastní elektroforetickou mobilitu, pohybuje se pouze působením EOF, a z jeho píku zaznamenaného detektorem je pak rychlost EOF stanovena. V případě komplexujících systémů s nabitými selektory ale tato metoda může selhat, protože selektor může vedle analytu interagovat i s EOF markerem – ten pak díky této interakci získává nenulovou efektivní mobilitu, která se navíc (obdobně jako u analytu) s koncentrací selektoru mění. Stanovené efektivní mobility analytu jsou pak zatížené systematickou chybou.

Fuguet *et al.* [67] porovnávali, nakolik různé EOF markery interagují či neinteragují s nabitými micelami v BGE a které markery jsou tedy vhodné ke stanovení mobility EOF v micelární elektrokinetické chromatografii. Takové srovnání pro nabité cyklodextriny (zejména cyklodextriny nedefinovaně sulfatované, které patří k nejoblíbenějším selektorům v CE [4, 68, 69, 70]) nebylo k dispozici.

V roce 1997 vyvinuli Williams a Vigh [71] metodu pro stanovení efektivní mobility v BGE obsahujících interagující složku. Zóna neutrálního EOF markeru byla obklopena širokými zónami BGE bez interagující složky, zóna analytu se pak nacházela v zóně BGE, který nabitou interagující složku obsahoval. Analytem mohla být, a často byla, látka běžně sloužící jako EOF marker. Metoda umožňovala odhalit její případnou „mobilizaci“ interakcí s nabitou interagující složkou BGE – s nabitým selektorem. Konkrétně se jednalo o definované (*single-isomer*) sulfatované cyklodextriny [72-74]. Metoda byla založena na určení vzdálenosti mezi EOF markerem a analytem před a po krátké aplikaci napětí. Její velkou nevýhodou nicméně bylo, že UV detektor musel být umístěn přibližně uprostřed délky kapiláry, což v komerčních přístrojích zpravidla není možné.

V *Publikaci V* je představena metoda stanovení efektivní mobility v BGE s nabitou interagující složkou, kterou lze použít v komerčně dostupném přístroji pro CE bez potřeby dodatečných úprav. Pomocí této metody byla porovnána vhodnost čtyř často používaných EOF markerů pro využití v BGE obsahujícím nedefinovaně sulfatovaný β-cyklodextrin (směs selektorů o různém stupni derivatizace a poloze substituentů) hojně používaný v analytické praxi.

Elektromigrační disperze a parametry HVL funkce

Pokud v zóně analytu závisí pohyblivost analytu na jeho vlastní koncentraci, pak dochází k deformaci tvaru jeho píku z Gaussovského na trojúhelníkový (za předpokladu, že původně byl vzorek dávkován jako velmi úzká zóna). Tento jev se nazývá elektromigrační disperze (EMD) a může k němu docházet z následujících příčin:

(i) změna vodivosti (a tedy i intenzity pole) ve srovnání s BGE v důsledku přítomnosti analytu [75];

(ii) nedostatečná pufrační kapacita BGE (a tedy změna zastoupení jednotlivých disociačních stavů analytu se změnou jeho koncentrace v zóně) [75];

(iii) významný úbytek volného selektoru v zóně analytu v důsledku komplexace (a tedy nárůst frakce volného analytu s rostoucí celkovou koncentrací analytu) [14, 15].

Z linearizovaného modelu elektromigrace s malou nelineární poruchou bylo odvozeno, že tvar píku deformovaného EMD dobře vystihuje HVL funkce [16, 17, 18]:

$$HVL(t) = \frac{\frac{a_0}{a_2 a_3 \sqrt{2\pi}} \exp\left(-\frac{1}{2}\left(\frac{t-a_1}{a_2}\right)^2\right)}{\frac{1}{\exp(a_3)-1} + \frac{1}{2}\left(1 + \mathrm{erf}\left(\frac{t-a_1}{\sqrt{2}a_2}\right)\right)} \tag{21}$$

kde t je čas, parametr a_0 odpovídá ploše píku, a_1 jeho poloze vyplývající z efektivní mobility analytu při jeho nekonečném zředění, a_2 popisuje difuzní (symetrické) rozšíření píku a a_3 charakterizuje nesymetrickou deformaci píku[*]. Na Obrázku 1 je ukázáno, jak se u píku deformovaného EMD mění poloha jeho maxima s celkovou koncentrací analytu, zatímco parametr a_1 se nemění. Právě z parametru a_1 je tedy vhodné stanovovat efektivní mobilitu analytu, která je následně využita například k určení komplexačních parametrů.

V případě Gaussovského píku jsou známy vztahy mezi jeho geometrickými vlastnostmi (poloha maxima, šířka v polovině výšky) a parametry příslušné Gaussovy funkce (střední

[*] V literatuře se užívají dva různé způsoby parametrizace HVL funkce, které se ovšem liší pouze v definici parametru a_3. V této práci je používán způsob uvedený v práci Hrušky *et al.* [18].

hodnota, rozptyl). Pro HVL pík ale dosud takové vztahy nebyly odvozeny. Jediným způsobem, jak pro daný pík analytu stanovit parametry odpovídající HVL funkce, byl export experimentálních dat a jejich proložení HVL funkcí pomocí vhodného softwaru pro nelineární regresi – což vyžaduje vymezení rozsahu dat pro analýzu, odečtení základní linie a především prvotní odhad parametrů HVL funkce, které jsou následně softwarem optimalizovány. Odhad parametrů je klíčový pro úspěšné vyhodnocení experimentálních dat a vyžaduje jistou míru zkušenosti.

Vztahy mezi „viditelnými“ charakteristikami píku – geometrickými vlastnostmi HVL funkce, a jejími parametry, které umožňují výpočet těchto parametrů bez použití nelineární regrese, jsou odvozeny v *Publikaci VI.*

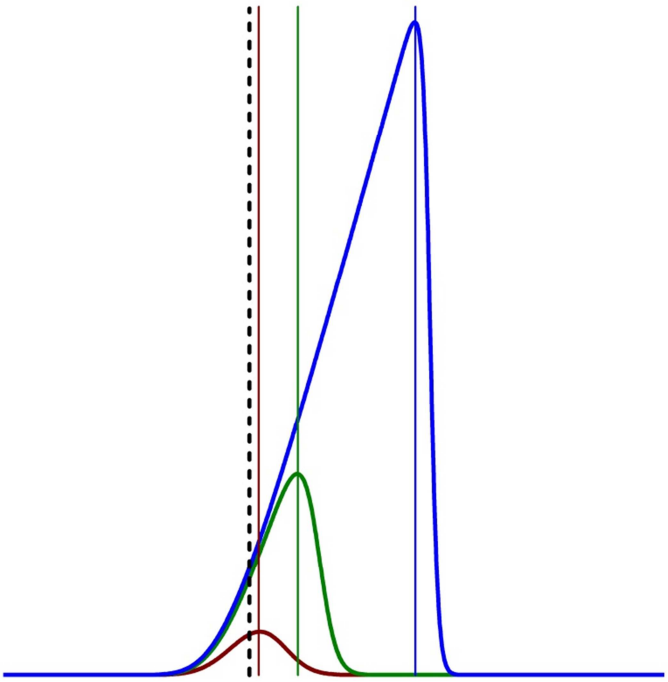

Obrázek 1: Změna tvaru píku deformovaného elektromigrační disperzí s rostoucí koncentrací analytu; plnými svislými čarami jsou vyznačena maxima píků, svislá přerušovaná čára značí polohu parametru a_1 příslušné HVL funkce – hodnota tohoto parametru se s koncentrací analytu nemění a je tedy stejná pro všechny tři zobrazené píky.

Publikace I

Twenty years of development of dual and multi-selector models in capillary electrophoresis: A review

L. Müllerová, P. Dubský, B. Gaš

Electrophoresis 2014, *35*, 2688-2700.

Ludmila Müllerová
Pavel Dubský
Bohuslav Gaš

Department of Physical and Macromolecular Chemistry, Faculty of Science, Charles University in Prague, Prague, Czech Republic

Received March 18, 2014
Revised May 28, 2014
Accepted May 29, 2014

Review

Twenty years of development of dual and multi-selector models in capillary electrophoresis: A review

It has been 20 years since Lurie et al. first published their model of electromigration of an analyte under simultaneous interaction with two cyclodextrins as chiral selectors. Since then, the theory of (enantio)separation in dual and complex mixtures of (chiral) selectors is well understood. In spite of this, a trial-and-error approach still prevails in analytical practice. Such a situation is likely caused by the fact that the entire theory is spread over numerous papers and the relations between various models are not always clear. The present review condenses the theory for the first time. Available mathematical models and feasible practical approaches are summarized and their advantages and limitations discussed.

Keywords:
Capillary zone electrophoresis / Complexation / Dual selector system / Electrokinetic chromatography / Mixture of selectors DOI 10.1002/elps.201400149

1 Scope of the review

A variety of mathematical models describing electromigration of an analyte interacting with a single selector (single-selector models) have been published and are summarized in general CE reviews or reviews focused on chiral separations [1–4]. Models dealing with separation systems containing two or more selectors (dual-selector and multiselector models) have also been proposed in the literature. However, even though some of these models were cited in reviews [2, 3, 5, 6], there is apparently no up-to-date review in which the dual- and multiselector models are thoroughly discussed and summarized.

Practical applications of dual separation systems, mainly with cyclodextrins, can be found in specialized reviews [5,7] or in comprehensive reviews on chiral CE separations [3,6,8–12]. In the present paper, we provide an overview of mathematical models that describe by means of closed mathematical formulas the electromigration behavior of analytes under an interaction with two or more selectors.

2 Introduction

The effective mobility of an analyte interacting with a single selector, μ_{Aeff}, is given by a weighted average of mobilities of the individual forms the analyte has in the solution. In this case, in the separation system, these are the free (uncomplexed) form of the analyte with the mobility μ_{Af}, and the complex of analyte and the selector with the mobility μ_{AC} [13]:

$$\mu_{Aeff} = \frac{1}{1 + K_{AC}[C]}\mu_{Af} + \frac{K_{AC}[C]}{1 + K_{AC}[C]}\mu_{AC} = \frac{\mu_{Af} + \mu_{AC}K_{AC}[C]}{1 + K_{AC}[C]} \quad (1)$$

where K_{AC} is the apparent complexation constant characterizing strength of interaction of the analyte with the selector:

$$K_{AC} = \frac{[AC]}{[A][C]} \quad (2)$$

where [A], [C], and [AC] are equilibrium concentrations of the free analyte, the free selector and the formed complex, respectively. Note that the apparent complexation constant K_{AC} is defined by concentrations (conversely to the true thermodynamic complexation constant defined by activities). The Eq. (1) is valid if the complexation equilibrium is established much faster compared to the speed of the electrophoretic movement and the complexation stoichiometry is 1:1 (analyte:selector). The stoichiometry of the complexation can be determined by various methods reviewed elsewhere [2,3] (e.g. NMR or UV-Vis spectroscopy utilizing the Job's plot method, MS with soft ionization). The 1:1 stoichiometry is typical for cyclodextrins [2,4]. Alternatively, the interaction of an analyte with a selector may be characterized with a capacity factor

Correspondence: Dr. Pavel Dubský, Charles University in Prague, Faculty of Science, Albertov 6, 128 40 Prague 2, Czech Republic
E-mail: pavel.dubsky@natur.cuni.cz

Abbreviation: EMO, electromigration order

Colour Online: See the article online to view Figs. 1 and 2 in colour.

k'_A (or the affinity factor analogous to the retention factor in chromatography) [14]:

$$k'_A = \frac{n_{AC}}{n_{Af}} \tag{3}$$

where n_{Af} and n_{AC} are molar amounts of the free and the complexed form of the analyte in the separation system, respectively. Consequently, the effective mobility of the analyte may be expressed in terms of the capacity factor:

$$n_{AC} = \frac{1}{1+k'_A}\mu_{Af} + \frac{k'_A}{1+k'_A}\mu_{AC} \tag{4}$$

In the case of 1:1 complexation, the Eq. (4) is mathematically equivalent to the Eq. (1) ($k'_A = K_{AC}[C]$). When adopting the simplification stating that the equilibrium concentration of the free selector [*C*] is approximately equal to its analytical concentration, c_C, (i.e. the complexation affects the selectors' concentration only negligibly) the Eq. (1) results in the form published by Wren and Rowe in 1992 [13]:

$$\mu_{Aeff} = \frac{\mu_{Af} + \mu_{AC}K_{AC}c_c}{1 + K_{AC}c_c} \tag{5}$$

A high concentration of CD increases the viscosity of the solution that, in turn, influences the effective mobility of an analyte. Therefore, on the right-hand side of the Eq. (5), the effective mobility should be multiplied by a viscosity correction factor (see e.g. [15]). The viscosity correction will be omitted in formulas presented in this work for simplicity. Similarly, all the individual complexation constants and mobilities of complexes are considered under the constant ionic strength. If a mixture of selectors is used, from which at least one is charged, the ionic strength of the buffer depends strongly on both the mixture composition and its total concentration. This problem can be overcome by decreasing the buffer concentration as a compensation for increasing concentration of the charged selector [16, 17].

3 Dual selector models

3.1 Extension of Wren and Rowe model

3.1.1 Two-concentration model

A quantitative description of the effective mobility of an analyte in a dual-selector system stems from the Wren and Rowe's single-selector Eq. (5). Its natural extension lies in integrating the second selector so that the effective mobility becomes a function of two concentrations c_1 and c_2 of the first and the second selector, respectively. In general, it is assumed that the analyte interacts with the two selectors independently. Thus it is sometimes mentioned explicitly that no formation of mixed complexes between the analyte and the two selectors is allowed. In fact, 1:1 complexation is required along with all the other requirements for validity of the Wren and Rowe's model. Under this assumption, the equilibria is characterized by two individual complexation constants, K_{AC1} and K_{AC2} and the two analyte-selector complexes migrate with their respective mobilities, μ_{AC1} and μ_{AC2}, so the Eq. (5) becomes:

$$\mu_{Aeff} = \frac{\mu_{Af} + \mu_{AC1}K_{AC1}c_1 + \mu_{AC2}K_{AC2}c_2}{1 + K_{AC1}c_1 + K_{AC2}c_2.} \tag{6}$$

Similar to Eq. (4), Eq. (6) can alternatively be expressed in terms of the capacity factors k'_1 and k'_2; $k'_i = K_{ACi}c_i$.

To our knowledge, Lurie et al. [18] were the first who published the Eq. (6) in 1994. The authors used it for semiquantitative analysis of their dual-CD system, which consisted of positively charged chiral analytes $A^{[+]}$ and neutral and highly negatively charged cyclodextrins $CD^{[0]}$ and $CD^{[-]}$, respectively. Thus the analytes migrating toward the cathode were slowed down by complexation with the $CD^{[0]}$, and could possibly reverse the direction of electromigration when complexed with $CD^{[-]}$. The authors concluded that it is the numerator in Eq. (6) that controls the sign of the final expression and thus proved mathematically that the direction of electromigration of the analyte in a dual mixture consisting of a neutral and a counter-migrating selector is governed by both the individual complexation constants and concentrations of the two selectors.

The pioneering work continued with the group of Peng, Bowser, Kranack and Chen. Besides the theoretical description of the system, they also discovered the existence of the so-called "dengsu" point [19]. "Dengsu" means "equal speed" in Chinese and refers to a rather curious property of some dual-selector systems where the effective mobility of the analyte may not change at a certain (dengsu) concentration of one of the selectors, regardless of the presence of the other selector. Peng et al. [19] were also the first who provided the experimental verification of the theory (6). The reported data gave a good agreement between the observed and predicted effective mobilities of three $A^{[-]}$ analytes in a $CD^{[0]}/CD^{[0]}$ dual mixture (Table 1). Kranack et al. [20] then compared, measured and predicted effective mobilities in a $CD^{[0]}/CD^{[-]}$ system for three $A^{[-]}$ analytes (Table 1).

Two dual selector models have also been developed that are focused on the separation of neutral hydrophobic analytes—polycyclic aromatic hydrocarbons—by mixtures of the charged and the neutral CD (a $A^{[0]}/CD^{[-]}/CD^{[0]}$system) [21–23]. Due to the high hydrophobicity of polycyclic aromatic hydrocarbons, the authors supposed that the concentration of the free form of the analytes is negligible. Therefore, the analytes are considered to be present only in the form of the complexes with either the neutral or the charged CD.

The approach proposed by Szolar et al. [23] is very similar to the model (6), except that the concentration of the free form of the analyte is neglected and not only 1:1 stoichiometry of the formed complexes is allowed. Formation of the mixed complexes was not taken into account in the model. The authors observed that the 1:1 (analyte:selector) stoichiometry for both selectors was in the best agreement with their experimental results. Conversely, Whitaker et al. [21, 22] based their model on the approach developed for MEKC [24]. The authors expected that the analytes would be present only in the

Table 1. Experimental verifications of dual selector models

Type of separation	Model verified	Quantity predicted and measured	Analyte(s)		CD_1	CD_2	Difference |measured-predicted|		Range	Number of values compared	Reference
							Median	Maximum			
Nonchiral	**(6)**	μ_{Aeff} ($10^{-9}m^2V^{-1}s^{-1}$)	Phenol, p-nitrophenol, benzoate	$A^{[-]}$	β-$CD^{[0]}$	HP-β-$CD^{[0]}$	0.05	0.17	(–1)–(–18)	18	[19]
Nonchiral	**(6)**	μ_{Aeff} ($10^{-9}m^2V^{-1}s^{-1}$)	Phenol, 1-naphthol, 2-naphthol	$A^{[-]}$	SBE-β-$CD^{[-]}$	HP-β-$CD^{[0]}$	0.2	0.7	(–3)–(–15)	24	[20]
Chiral	**(6)**+**(18)**	α_{AB}	Fenoprofen, flurbiprofen, ibuprofen	$A^{[0]}$	HS-β-$CD^{[-]}$	TM-β-$CD^{[0]}$	0.004	0.011	1.04–1.10	17	[31]
Chiral	**(6)**+**(18)**	α_{AB}	Ketoprofen	$A^{[0]}$	HS-β-$CD^{[-]}$	TM-β-$CD^{[0]}$	0.06	0.13	1.10–1.28	6	[31]
Chiral	**(6)**+**(18)**	α_{AB}	Fenoprofen, flurbiprofen, ibuprofen	$A^{[0]}$	PMMA-β-$CD^{[+]}$	HS-β-$CD^{[-]}$	0.010	0.015	1.05–1.10	6	[32]
Chiral	**(6)**+**(18)**	α_{AB}	Aminoglutethimide	$A^{[+]}$	γ-$CD^{[0]}$	α-$CD^{[0]}$ or β-$CD^{[0]}$	0.001	0.002	1.01–1.04	5	[33]
Chiral	**(19)**	$\Delta\mu_{AB}$ ($10^{-9}m^2V^{-1}s^{-1}$)	Amphetamine, methamphetamine, pseudoephedrine, ephedrine, norephedrine	$A^{[+]}$	β-$CD^{[0]}$	DM-β-$CD^{[0]}$	Graphical comparison				[34]
Chiral	**(20)**	α_{AB}	Amphetamine, methamphetamine, pseudoephedrine, ephedrine, norephedrine	$A^{[+]}$	β-$CD^{[0]}$	DM-β-$CD^{[0]}$	Graphical comparison				[34]
Nonchiral	**(11)**	K_{AC}^{over} M^{-1}	Ibuprofen, flurbiprofen	$A^{[-]}$	DM-β-$CD^{[0]}$	β-$CD^{[0]}$ or Malt-β-$CD^{[0]}$	190	500	4200–6900	14	[26]
Nonchiral	**(12)**	μ_{AC}^{over} ($10^{-9}m^2V^{-1}s^{-1}$)	Ibuprofen, flurbiprofen	$A^{[-]}$	DM-β-$CD^{[0]}$	β-CD or Malt-β-$CD^{[0]}$	0.06	0.23	(−7.4)–(−8.4)	14	[26]
Nonchiral	**(10)**+**(18)**	α_{AB}	Ibuprofen, flurbiprofen	$A^{[-]}$	DM-β-$CD^{[0]}$	β-CD or Malt-β-$CD^{[0]}$	Graphical comparison				[26]

DM-β-CD, dimethyl-β-cyclodextrin; HP-β-CD, hydroxypropyl-β-cyclodextrin; HS-β-CD, heptakis-6-sulfato-β-cyclodextrin; Malt-β-CD, 6-O-maltosyl-β-cyclodextrin; PMMA-β-CD, permethyl-6-monoamino-6-monodeoxy-b-CD; SBE-β-CD, sulfobutyl ether-β-cyclodextrin, TM-β-CD, heptakis-(2,3,6-tri-O-methyl)-β-cyclodextrin.

hydrophobic cavities of the CDs and that the transfer of the analytes between the "phases" would occur only during collisions of the CD molecules. Therefore, when loss of the separation efficiency at the low total concentration of the selectors was observed, the authors explained this effect by the lower frequency of the collisions and thus the slower exchange of the analyte between the "phases." This consideration is in contrast with the other dual selector models discussed in this review, in which the complexation equilibrium is always supposed to be infinitely fast.

3.1.2 Overall equilibrium

In addition, Bowser et al. expressed the effective mobility of the analyte in terms of the "adapted" mobilities and complexation constants. Provided that one of the selector concentrations (c_2) is kept constant, the effective mobility of an analyte can be expressed as [25]:

$$\mu_{Aeff} = \frac{\mu^*_{Af} + K^*_{AC1}\mu_{AC1}c_1}{1 + K^*_{AC1}c_1} \tag{7}$$

$$\mu^*_{Af} = \frac{\mu_{Af} + K_{AC2}\mu_{AC2}c_2}{1 + K_{AC2}c_2} \tag{8}$$

$$K^*_{AC1} = \frac{K_{AC1}}{1 + K_{AC2}c_2} \tag{9}$$

Quantities μ^*_{Af} and K^*_{AC1} were referred to as "apparent" values in the original work, but we use the term "adapted" instead. Equation (7) is formally identical to that of Wren and Rowe (5). Noticeably, it implies that if the analyte is supposed to interact with only one selector but another interacting compound is present in the BGEs at constant concentration, the "hidden" complexation will not be revealed and incorrect complexation constant and mobility of free analyte will be determined.

A similar, but conceptually different, scheme was recently published by our group [26]. We deduced that it is not the individual concentrations of the two selectors in the mixture but rather their molar fraction that governs the dual selector system behavior. In all other aspects the system should obey the simple Wren and Rowe's equation with certain overall complexation constants and overall mobility of the complex:

$$\mu_{Aeff} = \frac{\mu_{Af} + K^{over}_{AC}\mu^{over}_{AC}c_{tot}}{1 + K^{over}_{AC}c_{tot}} \tag{10}$$

$$K^{over}_{AC} = (1-\chi_2)\,K_{AC1} + \chi_2 K_{AC2} \tag{11}$$

$$\mu^{over}_{AC} = \frac{(1-\chi_2)\,\mu_{AC1}K_{AC1} + \chi_2\mu_{AC2}K_{AC2}}{K^{over}_{AC}} \tag{12}$$

where $c_{tot} = c_1 + c_2$ is the total concentration of the mixture and $\chi_2 = c_2/c_{tot}$ is the molar fraction of the second selector in the mixture.

Several advantages of switching from $\{c_1; c_2\}$ to $\{\chi_2; c_{tot}\}$ coordinates are discussed in the original paper [26]. They all basically originate from the following two points: First, the system behaves according to the familiar single-selector-like pattern of μ_{Aeff} versus c_{tot} dependency as far as the mixture composition χ_2 is constant. Consequently, the entire theory, which has been extensively developed for the single-selector systems in recent years, can be applied in dual-selector systems as well when the overall complexation parameters are substituted into the original Wren and Rowe's Eq. (5). Also, the molar fraction χ_2 can only attain values from zero to one. In turn, the μ_{Aeff} versus c_{tot} pattern can be inspected as a function of the well-bounded parameter χ_2 over the whole range of all possible mixture compositions.

3.2 Predicting separation characteristics

3.2.1 Intrinsic selectivity

Lelievre et al. [27] used the concept of intrinsic selectivity to characterize the separation ability of a dual-selector system. For a single selector interacting with a pair of enantiomers A and B, the intrinsic selectivity is defined as [28]:

$$\kappa = \frac{k'_A}{k'_B} = \frac{K_{AC}}{K_{BC}} \tag{13}$$

where k'_A and k'_B are the capacity factors (see Eq. (3)) and K_{AC} and K_{BC} are the respective complexation constants. For a dual-selector system, the authors defined the intrinsic selectivity $\kappa^*_1$of the first selector in the presence of a particular concentration of the second selector, which we will call the adapted intrinsic selectivity in terms defined in Section 3.1.2:

$$\kappa^*_1 = \frac{K^*_{AC1}}{K^*_{BC1}} = \frac{K_{AC1}}{K_{BC1}}\frac{1 + K_{BC2}c_2}{1 + K_{AC2}c_2} \tag{14}$$

K^*_{AC1} and K^*_{BC1} are the adapted complexation constants (see Eq. (9)) of the respective analytes A and B with the first selector at a fixed concentration, $c_{2,}$ of the second selector. Other symbols have the same meaning as in (6). If $K_{AC2}c_2 \gg 1$ and $K_{BC2}c_2 \gg 1$, then the adapted intrinsic selectivity of the first selector is equal to the ratio of the intrinsic selectivities of the two selectors $\kappa^*_1 = \kappa_1/\kappa_2$.

The adapted intrinsic selectivity, κ^*_1, is independent of the concentration of the first selector and therefore should characterize the influence of this selector on a separation at a given concentration of the second selector. This approach reflects the common analytical practice, where one selector is used as a (stereo-)selective agent, the concentration of which is optimized, while the other is used as a mobilizing agent at a constant concentration.

In addition, the global intrinsic selectivity of a dual-selector mixture, κ^{glob}, is defined:

$$\kappa^{glob} = \frac{k'^{glob}_A}{k'^{glob}_B} = \frac{K_{AC1}c_1 + K_{AC2}c_2}{K_{BC1}c_1 + K_{BC2}c_2} = \frac{K_{AC1} + K_{AC2}z}{K_{BC1} + K_{BC2}z}$$
$$k'^{glob}_j = \frac{n_{jC1} + n_{jC2}}{n_{jf}} \tag{15}$$

where $k_j'^{glob}$ is the global capacity factor of the analyte j (j referring to the analyte A or B) in the dual-selector mixture (see also Eq. (3)), n_{jC1} is the molar amount of the complex of the analyte with the first selector, n_{jC2} is the molar amount of the complex of the analyte with the second selector, n_{jf} is the molar amount of the free analyte, and z is the ratio of concentrations of the two selectors $z = c_1/c_2$. The global intrinsic selectivity is therefore constant for a given ratio of selector concentrations. It may not be obvious, but comparison of the Eqs. (15) and (11) shows, that the global intrinsic selectivity is actually a ratio of the overall complexation constants of the analytes A and B. The authors also concluded [27] that above a certain concentration threshold, the analytical resolution does not change significantly with increasing concentration of the selector mixture, but can be tuned by altering the ratio of the selector concentrations. A formula was also presented for mobility of an analyte completely complexed with a dual-selector mixture. Though expressed in a slightly different way, it was mathematically equivalent to the Eq. (12) given in the overall complexation model.

The model by Lelievre et al. does not offer any formula that could be directly used for the search for optimum separation conditions but it can be helpful in considering the separation ability of a particular dual-selector system. On the other hand, the intrinsic selectivity only takes into account the contribution of complexation constants to the selectivity of the system and omits the influence of the mobilities of the complexes, which can be crucial [29].

3.2.2 Mobility difference, selectivity

Based on the effective mobilities of the two analytes, various quantities ranking the separation efficiency can be calculated. These are ordinary measures used in single-, dual-, and possibly, multiselector systems and their common advantages and disadvantages are thoroughly discussed in the review by Chankvetadze [30]. Their adaptation and applicability in the dual-selector systems is reviewed in the rest of this section.

The mobility difference $\Delta\mu_{AB}$ (16), the mobility factor MF (17), the selectivity α_{AB}(18), as well as any other characteristic, can be straightforwardly calculated from the effective mobilities μ_{Aeff} and μ_{Beff} of the two analytes A and B expressed in terms of either of the dual-selector Eqs. (6), (7), or (10).

$$\Delta\mu_{AB} = \mu_{Aeff} - \mu_{Beff} \tag{16}$$

$$MF = \frac{2(\mu_{Aeff} - \mu_{Beff})}{\mu_{Aeff} + \mu_{Beff}} \tag{17}$$

$$\alpha_{AB} = \frac{\mu_{Aeff}}{\mu_{Beff}} \tag{18}$$

Abushoffa et at. [31–33] experimentally verified that the selectivity in a dual-selector system can be predicted utilizing the Eqs. (6) and (18) (Table 1).

Nhujak et al. [34] chose the selectivity and the mobility difference as the measures of the chiral separation efficacy. However, instead of using parameters of complexation of each individual analyte with each individual selector (i.e. individual complexation constants and mobilities of complexes), they defined the following parameters to characterize the interaction of a pair of enantiomers with one selector: (i) a geometric average of the complexation constants of the selector with the two enantiomers $\overline{K_{Ci}} = (K_{ACi} \cdot K_{BCi})^{\frac{1}{2}}$, (ii) the intrinsic selectivity $\kappa_i = K_{ACi}/K_{BCi}$(the same as (13), the parameter was called "enantioselectivity" by the authors), (iii) the mobility of the diastereomeric complex (supposed to be the same for both enantiomers in this model) $\mu_{Ci} = \mu_{ACi} = \mu_{BCi}$, and (iv) the ratio of the mobilities of the free analyte and the diastereomeric complex, $\beta_i = \mu_f/\mu_{Ci}$ (note that the two enantiomers have the same mobility μ_f). Substituting these parameters into the Eq. (6), the authors expressed the mobility difference $\Delta\mu_{AB}$ and the selectivity α_{AB} in a dual selector mixture:

$$\begin{aligned} \Delta\mu_{AB} &= \frac{G_1 + G_2 + H_{12}}{\left(1 + \overline{K_{C1}}c_1 + \overline{K_{C2}}c_2\right)^2} \\ G_i &= 2\left(\frac{\kappa_i - 1}{\kappa_i + 1}\right)\overline{K_{Ci}}c_i\left(\mu_f - \mu_{Ci}\right) \\ H_{12} &= \left(\frac{4\left(\kappa_2 - \kappa_1\right)}{\left(\kappa_1 + 1\right)\left(\kappa_2 + 1\right)}\right)\overline{K_{C1}}c_1\,\overline{K_{C2}}c_2\left(\mu_{C1} - \mu_{C2}\right) \end{aligned} \tag{19}$$

$$\begin{aligned} \alpha_{AB} &= \frac{V}{V_\beta}, \quad V = \frac{1 + \overline{K_{C1}}c_1\sqrt{\kappa_1} + \overline{K_{C2}}c_2\sqrt{\kappa_2}}{1 + \overline{K_{C1}}c_1\dfrac{1}{\sqrt{\kappa_1}} + \overline{K_{C2}}c_2\dfrac{1}{\sqrt{\kappa_2}}} \\ V_\beta &= \frac{1 + \overline{K_{C1}}c_1\beta_1\sqrt{\kappa_1} + \overline{K_{C2}}c_2\beta_2\sqrt{\kappa_2}}{1 + \overline{K_{C1}}c_1\beta_1\dfrac{1}{\sqrt{\kappa_1}} + \overline{K_{C2}}c_2\beta_2\dfrac{1}{\sqrt{\kappa_2}}} \end{aligned} \tag{20}$$

where subscripts 1 and 2 refer to the first and the second selector, respectively. It should be reemphasized that the model is preferably aimed at enantioseparation ($\mu_{Af} = \mu_{Bf}$) and valid only under the assumption of $\mu_{ACi} = \mu_{BCi}$. The model was also verified experimentally (Table 1). The main advantage of this approach, stressed by the authors, is that the parameters κ_i and β_i are dimensionless and thus can be used for comparison among various selectors. In this way they identified five different kinds of dual-selector systems. Unfortunately, the parameters β_1 and β_2 (that reflect the mobilities of the complexes with the first and second selector, μ_{C1} and μ_{C2}) were not accounted for in the classification. Therefore it suffers from the same drawback as the intrinsic selectivity concept and is only of limited value in practice.

3.2.3 Resolution

Resolution of analytes A and B can be expressed as follows (adapted from [30]):

$$R_S^{AB} = \frac{\sqrt{N}}{4}\frac{(\mu_{Aeff} - \mu_{Beff})}{\frac{1}{2}\left(\mu_{Aeff} + \mu_{Beff}\right) + \mu_{EOF}} \tag{21}$$

where N is the number of theoretical plates and μ_{EOF} is the mobility of EOF. Interestingly, a modification of the resolution equation for a $A^{[+]}/CD^{[0]}/CD^{[-]}$dual-selector system was reported already by Lurie et al. [18] but without any further use.

Shaeper et al. [35] made an attempt to optimize their separation based on a prediction of the resolution. They used a dual-selector system consisting of two neutral CDs to separate five enantiomeric pairs of dansylated amino acids in one run ($A^{[+]}/CD^{[0]}/CD^{[0]}$ system). For a particular selector mixture composition, they calculated the effective mobilities of all their analytes by Eq. (6). Then, they roughly estimated the resolution of each pair of subsequent analytes based on the calculated effective mobilities and the approximation that the number of theoretical plates, N, is the same for all analytes and separations. Consequently, a "chromatographic response function" CRF was calculated that served as a measure of the success of the separation:

$$CRF = a\sum_{AB}\ln\frac{R_S^{opt}}{R_S^{AB}} + b\sum_{AB}\ln\frac{R_S^{AB}}{R_S^{opt}} \tag{22}$$

where R_S^{opt} is the optimum resolution ($R_S^{opt} = 1.5$ was chosen by the authors). The parameter a weights those pairs of neighboring peaks that have higher resolution than necessary ($R_S^{AB} > R_S^{opt}$), b weights insufficiently resolved peaks ($R_S^{AB} < R_S^{opt}$).The values of the parameters a and b are arbitrarily chosen according to the needs of a particular separation ($a = 5$, $b = 50$ were used by the authors). The CRF values should be always negative and approach zero for the ideal separation. The authors optimized the CRF value by varying concentrations of both selectors. Even though the resolution was estimated very roughly in this work, the concept of the chromatographic response function is of general applicability for separations of higher numbers of analytes.

More accurate calculation of resolution was used by Surapaneni et al. [36] in order to optimize the chiral separation in the $A^{[0]}/CD^{[0]}/CD^{[-]}$ system (three different $CD^{[0]}$ were tested). When the EOF is assumed to be negligible (as was the case in [36]) and only the longitudinal diffusion is taken into account as a source of the peak broadening, the Eq. (21) can be rewritten in terms of the effective mobilities μ_{Aeff} and μ_{Beff} and effective charges z_{Aeff} and z_{Beff} of the analytes A and B [37]:

$$R_S^{AB} = \frac{(\mu_{Aeff} - \mu_{Beff})(z_{Aeff}z_{Beff})^{\frac{1}{2}}}{\mu_{Aeff}(z_{Aeff})^{\frac{1}{2}} + \mu_{Beff}(z_{Beff})^{\frac{1}{2}}}\left(\frac{eU}{8kT}\right)^{1/2} \tag{23}$$

where U is the applied voltage, e is the elementary charge, k is the Boltzmann constant, T is thermodynamic temperature. Surapaneni et al. calculated the effective mobilities by Eq. (6). The effective charges can be calculated analogously as a weighted sum of charges of the individual forms of the analyte. In the case of the $A^{[0]}/CD^{[0]}/CD^{[charged]}$ system, it applies:

$$z_{Aeff} = \frac{z_{AC1}K_{AC1}c_1}{1 + K_{AC1}c_1 + K_{AC2}c_2} \tag{24}$$

where subscript 1 refers to the charged selector and z_{AC1} is its charge. The predicted resolution was plotted as a 3D function of the concentrations of the two selectors (see also Section 3.3.2) and the dual-selector system with optimum concentrations of selectors was chosen. Nevertheless, the authors admit that the experimental resolution was only 60% of that predicted, and attributed this observation to the longer time the analyte spent in the capillary when interacting with a lower amount of the charged (mobilizing) selector. However, the loss of the resolution could just as likely be caused by a complexation-induced electromigration dispersion, as demonstrated recently for single-selector systems [38, 39]. This study showed that the unusual electromigration-like dispersion of the analyte peak may occur, especially when it interacts with a relatively low amount of the selector. Therefore, Eq. (23) must be used with care, especially in case of the strongly complexing selectors.

3.3 Graphical analysis

3.3.1 Binding isotherms and counter plots

Visualizing the expected trends in dual- selector systems may help to overcome the mathematical difficulty of dealing with the two-parametric model (6). Most straightforward are the 3D plots of μ_{Aeff} versus c_1 and c_2 dependence (Fig. 1A) as originally used by Peng et al. [19, 20, 25]. These dependences were referred to as binding isotherm surfaces by the authors. Nevertheless, such graphs suffer from their rather hard readability when printed. The graphs must be explored from various projections and perspectives, in order to get insight into the properties of the system. On the other hand, the binding isotherms are readily constructible by means of modern software tools, where they can be further inspected without any limitation.

Another strategy adopted by the authors was the description of the system by contour plots (Fig. 1B). The concentration, c_2, can be calculated at which the analyte attains a certain effective mobility μ_{Aeff} as a function of c_1. Thus the contour plot shows the "iso-mobility" curves (the term not originally used by the authors). By expressing the partial derivative of c_2 *vs.* c_1, the authors showed that the iso-mobility curves form straight lines with the slopes (depending on chosen μ_{Aeff}):

$$\frac{\partial c_2}{\partial c_1} = -\frac{K_{AC1}(\mu_{Aeff} - \mu_{AC1})}{K_{AC2}(\mu_{Aeff} - \mu_{AC2})} \tag{25}$$

Notably, in the light of the contour plots, the dengsu point (*cf.* Section 3.1.1) is only a special case of such iso-mobility lines. In principle, any achievable μ_{Aeff} value can be attained in an infinite number of mixtures at various concentrations c_2 and the corresponding concentration c_2

3.3.2 Separation characteristics

Separation characteristics of dual selector systems, such as the mobility difference, selectivity, resolution, etc. were also

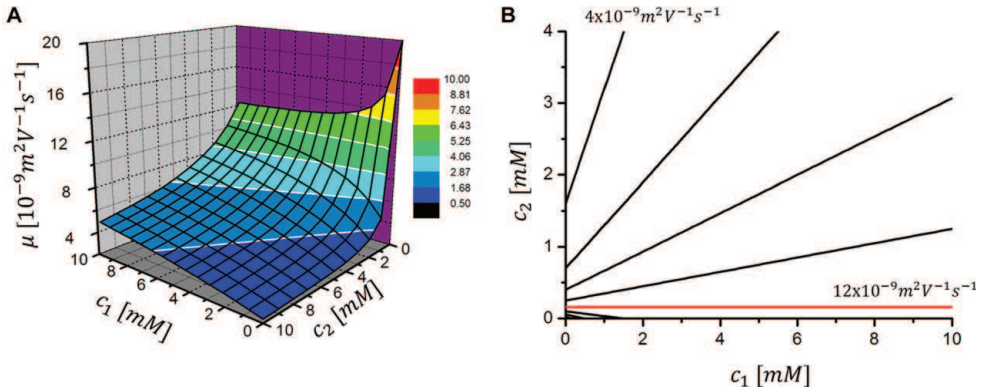

Figure 1. Graphical analysis of the mobility dependence in the dual-selector system. Model data from Table 2, analyte A, selectors 2 and 3. (A) 3D plot, Eq. (6). (B) Counter plot, Eq. (25). The counter lines are displayed in 2×10^{-9} $m^2V^{-1}s^{-1}$ steps. The dengsu point is indicated in red ($12 \cdot 10^{-9}m^2V^{-1}s^{-1}$).

inspected theoretically by means of the graphical analysis (Fig. 2 A). Surapaneni et al. [36] plotted the resolution surfaces (Eqs. 6 and 24 combined with (23) in the $A^{[0]}/CD^{[0]}/CD^{[-]}$ system using three different $CD^{[0]}$ selectors. All the resulted plots exhibited simple monotonous trends. Abushoffa et al. [32] combined Eq. (6) with that for the selectivity (18) or with that for the mobility factor (17) in order to observe the respective 3D surface plots in their $A^{[0]}/CD^{[-]}/CD^{[+]}$ dual-CD separation system. These plots were far more complex than the previous ones observed by Surapaneni et al. [36] but still served well for both the qualitative picture of the system behavior (identification of the extremes or the electromigration order reversal (EMO)) as well as the quantitative assessment of favorable mixture compositions.

Simplification of the 3D complexity lies in plotting the separation characteristics as a function of one parameter, while keeping the second parameter constant. Most often, the separation characteristics are plotted against c_1 at constant c_2 [32, 34, 36, 40]. Nhujak et al. [34] utilized such an analysis to describe their dimensionless classification system (cf. Section 3.2.2). Similarly Zhu et al. [40] used the graphs for the theoretical explanation of the observed EMO reversal in the $A^{[+]}/CD^{[0]}/CD^{[0]}$ system.

Introduction of the overall model (Eqs. 10–12) enables us to plot various characteristics of the dual selector system as a function of its composition χ_2 (Fig. 2B–D). Interestingly, Zhu et al. [40] already plotted the mobility difference and selectivity in terms of the molar fraction χ_2 at a constant total mixture concentration c_{tot}, but without a further theoretical substantiation. We demonstrated this approach in our recent study [26]. Advantageously, the molar ratio χ_2 can only attain the values between one and zero and thus the exploration is needed no more than within this limited constraint. As the example, the total mixture concentration c_{tot} at which (if any) the EMO reversal occurs was plotted as the function of the mixture composition χ_2 in two model $A^{[-]}/CD^{[0]}/CD^{[0]}$ systems. The regions of a possible EMO reversal are easily identified in this way (Fig. 2B); model data). A similar strategy can be adopted for the optimum mixture concentration with respect to the maximum mobility difference, selectivity or other separation characteristics. Furthermore, the optimization characteristics of interest can be plotted as the function of the overall mixture concentration c_{tot} at several levels of mixture compositions χ_2 (Fig. 2C and D). Such curves obey the patterns familiar from single-selector models, which generally exhibit the clear limit (as c_{tot} grows to infinity) and possible extremes (e.g. maximum selectivity etc.). The selectivity curves were also validated in the cited paper [26]. Such a graphical analysis thus helps the analysts in choosing the favorable separation conditions.

3.4 Weighted mobility difference concept

The approaches summarized up to now were based on the extended Wren and Rowe's Eq. (6). Conversely, Chankvetadze et al. [33, 41, 42] proposed a rather different strategy to understanding the chiral separation mechanism in the dual-selector systems. The mobility difference in the dual selector system, $\Delta\mu_{AB}$, was expressed as a weighted sum of mobility differences generated by the first, $\Delta\mu_{AB,C1}$, and the second, $\Delta\mu_{AB,C2}$ selector:

$$\Delta\mu_{AB} = r \cdot \Delta\mu_{AB,C1} + s \cdot \Delta\mu_{AB,C2} \tag{26}$$

where r and s were referred to as the statistical weights of the mobility difference, which the first and the second selector, respectively, would generate if it was in the system alone. This mobility difference generated by the individual selector is then expressed based on the single-selector model of Wren and Rowe:

$$\Delta\mu_{AB,Ci} = \frac{(\mu_{Ci} - \mu_f)(K_{BCi} - K_{ACi})c_{Ci}}{1 + (K_{ACi} + K_{BCi})c_{Ci} + K_{ACi}K_{BCi}c_{Ci}^2} \tag{27}$$

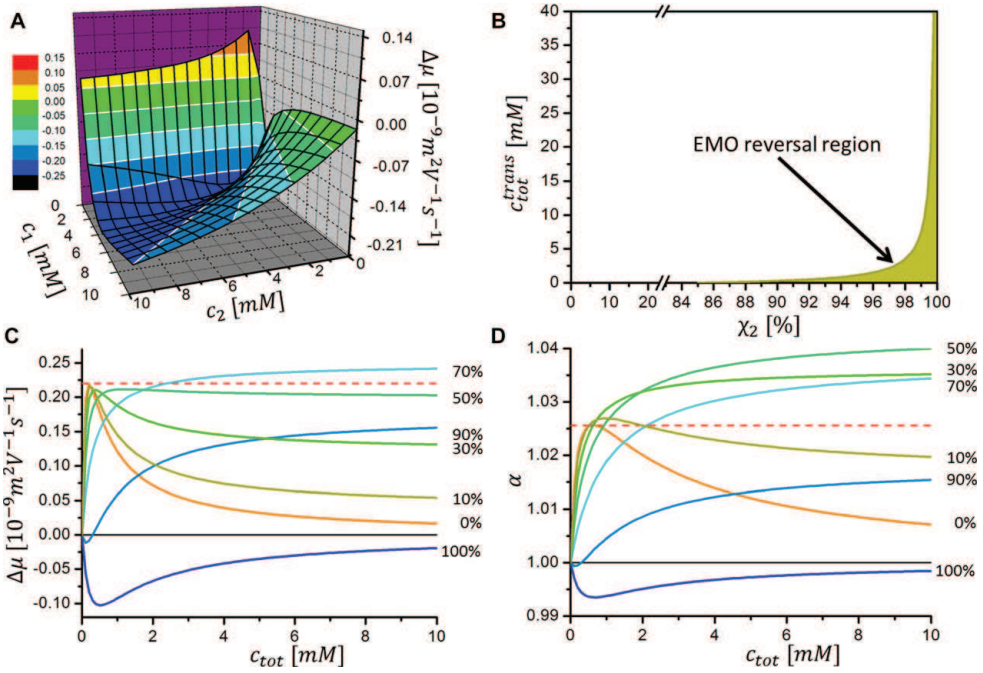

Figure 2. Graphical analysis of the separation characteristics in the dual-selector system. Model data from Table 2, analytes A and B, selectors 2 and 3. (A) Mobility difference 3D plot, Eq. (18). (B) EMO reversal plot. Transient state total mixture concentration, c_{tot}^{trans}, as a function of the 2nd selector molar fraction, χ_2. Region of the EMO reversal (compared to the single-selector system 1) shaded, *x*-axis scale-changing break is present at $\chi_2 = 20\%$. (C) Mobility difference plot using the overall model, Eqs. (10) and (18). Molar fractions of the 2nd selector, χ_2, indicated by percentage. The highest (absolute) value observable in either the 1st or the 2nd selector system alone indicated by the red dashed line. (D) The same as C but selectivity, Eq. (20), is depicted.

As the model focuses on the chiral separations, the mobilities of the free analytes A and B are the same: $\mu_{Af} = \mu_{Bf} = \mu_f$. Also the mobilities of the diastereomeric complexes formed between either of the analytes and the selector are supposed to be the same: $\mu_{AC1} = \mu_{BC1} = \mu_{C1}$ and $\mu_{AC2} = \mu_{BC2} = \mu_{C2}$.

The authors used Eqs. (26) and (27) to consider which selectors should be combined in the dual selector mixture. The complexation effect is reflected by the so-called recognition pattern. Two selectors can exhibit either the same ($K_{BC1} > K_{AC1}$ and $K_{BC2} > K_{AC2}$) or the opposite ($K_{BC1} > K_{AC1}$ and $K_{BC1} < K_{AC1}$) recognition pattern (one may choose the analyte A such that $K_{BC1} > K_{AC1}$ for simplicity). Besides the recognition pattern, the effect the complexation has on the analyte's mobility must be taken into account. Again, two possibilities can happen. Either both the selectors accelerate or decelerate the analytes, thus exhibiting the same effect on the analyte's mobility ($\mu_{C1} > \mu_f$ and $\mu_{C2} > \mu_f$ or vice versa). Or one selector accelerates and the other decelerates the analytes, thus having the opposite effects ($\mu_{C1} > \mu_f$ and $\mu_{C2} < \mu_f$ or vice versa).

Accordingly, the authors concluded that the mobility differences $\Delta\mu_{AB,C1}$ and $\Delta\mu_{AB,C2}$ must have the same sign (either positive or negative) should the dual selector system improve the separation compared to the two separate single-selector systems. This follows from Eq. (26) and from the fact that the statistical weights *r* and *s* were claimed to be positive numbers. As can be seen from Eq. (27), the sign of $\Delta\mu_{AB,Ci}$ generated by the particular selector depends on its effect on the analyte's mobility, $\mu_{Ci} - \mu_f$, and the recognition pattern, $K_{BCi} - K_{ACi}$. Thus the second conclusion is that if the two selectors have the same/opposite effects on analyte's mobility, they should also possess the same/opposite recognition patterns in order to increase the mobility difference when employed together. Later on [33], the authors further deduced, that if both the selectors have the same effects on the analyte's mobility, their combination is still unlikely to enhance the separation since using either the first or the second selector alone would probably yield better results. Thus usually the opposite mobility effects and recognition patterns are considered advantageous. This was also stated in the review by Fillet and Crommen [7].

Based on this model, Matthijs et al. [43] clarified the observed effects of the complexation on the electromigration order of the enantiomers and efficacy of separation. Other authors, e.g. [44–47], used a similar approach to choose the suitable dual-selector system for the particular separation. On the other hand, some authors also concluded [42, 43] that not all experimentally obtained results could be explained by the (26) concept.

In spite of its indisputable usefulness in practice, the seeming transparency of the model (26) may however seduce one to incorrect interpretations. It can be shown that the coefficients r and s in the Eq. (26) can in reality attain any value, both positive and negative. This does not force the individual mobility difference contributors, $\Delta\mu_{AB,C1}$ and $\Delta\mu_{AB,C2}$, to be of the same sign in order to positively influence the final mobility difference, $\Delta\mu_{AB}$. Figure 2C illustrates the model dual-selector system with reasonable input parameters, which not only exhibits the same effects on the analyte's mobility but simultaneously combines the same effects with the opposite selectivity patterns. Consequently, $\Delta\mu_{AB,C1} > 0$ and $\Delta\mu_{AB,C2} < 0$. When the mixture composition is about 30:70 (c_1:c_2 ratio) and the total mixture concentration is above 4 mM, the mixture provides a higher mobility difference than the highest value obtainable in any of the two single-selector systems alone. The same result is even more pronounced for the selectivity (Fig. 2D).

3.5 Electromigration order reversal

The electromigration order of two analytes may reverse in certain single-selector systems with changing the selector concentration [48]. During the process, a transient state occurs at a certain selector concentration, c^{trans}, at which the two analytes are inseparable. The same applies to dual-selector systems, where the EMO generally depends on the concentrations of both selectors in the mixture, c_1 and c_2. The transient state concentrations c_1^{trans} and c_2^{trans} in a specific dual-selector system may be predicted analogously to the single-selector systems. The transient state corresponds to the zero mobility difference (16), the zero mobility factor (17), or to the selectivity (18) equal to one at the nonzero concentration of the selectors.

However, in cases where the EMO reversal was discussed in the dual-selector chiral separations, the authors made mostly qualitative considerations regarding each selector's recognition pattern and the effect on the analytes' mobility [18, 44, 46, 49–51]. Similarly, the weighted mobility difference Eq. (26) (Section 3.4) was utilized to clarify the transient state occurrence in the dual-selector systems [33, 43, 52]. All these qualitative approaches can be briefly summarized as follows: Existence of a transient state in the dual selector system is expected, if the EMO is opposite in the two single selector systems, i.e. if the two selectors exhibit either opposite recognition patterns and the same effects on the analytes' mobility, or the same recognition patterns and opposite effects on the mobility (see also Section 3.4). It is worth noting that in the mobility difference concept (Section 3.4), a dual-selector system showing the transient state is not expected to be able to improve the separation.

Zhu et al. [40] studied the transient state in the dual selector system $A^{[+]}/CD^{[0]}/CD^{[0]}$. In agreement with the above mentioned weighted mobility difference concept, they stated that the two selectors alone must provide the different EMO of the analytes should their combination lead to the mixture-composition-dependent EMO reversal. Simultaneously, they made the observation that (within the experimental error) for the two selector concentrations at the transient state, c_1^{trans} and c_2^{trans}, it applies:

$$\mu_{Aeff,C1}\left(c_1^{trans}\right) = \mu_{Beff,C2}\left(c_2^{trans}\right)$$
$$\mu_{Aeff,C2}\left(c_2^{trans}\right) = \mu_{Beff,C1}\left(c_1^{trans}\right) \quad (28)$$

where the effective mobilities of the analytes A and B in the first or the second single-selector system are observed at the corresponding concentrations c_1^{trans}or c_2^{trans}. The authors further proved mathematically that the aforementioned condition (both equalities must apply simultaneously) truly results in the zero mobility difference $\Delta\mu_{AB}\left(c_1^{trans}, c_2^{trans}\right) = 0$ in the dual-selector systems. The mathematical treatment assumed the equal mobilities of the free analytes, the equal mobilities of the complexes of the two analytes with the first selector as well as those with the second selector (an approximation often adopted for enantioseparations). However, Eq. (28) represents just one particular solution of the problem, while a virtually infinite number of other mixture compositions exists in the system that also lead to the transient state. Moreover, if the two free analytes do not have the same mobilities (as each other) or the mobilities of their complexes, the Eq. (28) cannot be applied.

It should be noted that although any of the above approaches has its validity in certain cases, none of them covers the problem of the EMO reversal in the dual-selector systems in its full complexity. Firstly, dual-selector systems may exist in which the two individual selectors have the same selectivity patterns and the same effects on the analyte's mobility but still exhibit the EMO reversal. The model system given in Table 2, Analytes A and B, Selectors 1 and 3, forms one such an example resulting in, e.g. $c_1^{trans} = 9.22$ mM and $c_2^{trans} = 0.29$ mM. If the concentration is kept at roughly 9 mM, only a tiny addition of the second selector causes the EMO reversal and the analytes will further migrate in the opposite order compared to either of the single selectors alone. Secondly, it is natural that if $\Delta\mu_{AB,C1} > 0$ and $\Delta\mu_{AB,C1} < 0$ then the system must lead to the EMO reversal at a certain mixture composition as suggested by the weighted mobility difference concept. However, this itself does not exclude the mixture from being advantageous for the (enantio)separation as discussed in the previous section and demonstrated in Fig. 2C and D.

Finally, it can be summarized that at any mixture composition, the transient state can be solved as a result of a quadratic equation. Thus none, one or even two EMO reversals may occur in the dual-selector mixture, either by

Table 2. Model data used for calculations. Mobilities are given in 10^{-9} $m^2V^{-1}s^{-1}$. Complexation constants are given in M^{-1}

System		Analyte A	Analyte B
Free	μ_{Af}	20	20
Selector 1	μ_{Ci}	12	12
	K_C	2000	2250
	Mobility effect[a)]	$\mu_{Ci} < \mu_f$	
	Selectivity pattern[a)]	$K_{BC} > K_{AC}$	
Selector 2	μ_{Ci}	12	12
	K_C	2000	1900
	Mobility effect[a)]	$\mu_{Ci} < \mu_f$	
	Selectivity pattern[a)]	$K_{BC} < K_{AC}$	
Selector 3	μ_{Ci}	2	2
	K_C	5000	5250
	Mobility effect[a)]	$\mu_{Ci} < \mu_f$	
	Selectivity pattern[a)]	$K_{BC} > K_{AC}$	

a) Selectivity pattern and mobility effect are discussed with Eq. (27).

changing its composition at a constant total concentration or vice versa. The constitution of the quadratic equation does not seem to allow any simple generalization. The convenience of the graphical analysis of the overall complexation model (10)–(12), which expresses the transient state mixture concentration, c_{tot}^{trans}, as a function of its composition, χ_2 was demonstrated in our recent study [26] (*cf.* also Section 3.3 and Fig. 2B).

4 Multiselector models

A need for a theoretical description of multiselector systems arises mainly from the fact that most of the commercially available cyclodextrin derivatives, which are of high practical importance in analytical chemistry, are produced as mixtures of various degrees of substitution and various positions of substituents [3, 30, 48, 53, 54].

Essentially, the dual-selector model reported by Peng et al. [19] resulted as a specialization of their multiselector model:

$$\mu_{Aeff} = \frac{\mu_{Af} + \mu_{AC1} K_{AC1} c_1 + \mu_{AC2} K_{AC2} c_2 + \cdots + \mu_{ACn} K_{ACn} c_n}{1 + K_{AC1} c_1 + K_{AC2} c_2 + \cdots + K_{ACn} c_n} \tag{29}$$

where there are n selectors in the mixture, all interacting with the analyte in the 1:1 ratio without any formation of mixed complexes (the original formula was expressed in terms of the capacity factors, $k_i' = K_{ACi} c_i$). The obvious difficulty of the model (29) is its n-dimensional complexity, which effectively excludes it from any practical use. Later Kranack et al. [20] realized that the formula can be substantially simplified when each of the individual selector concentrations, c_i is expressed as:

$$c_i = \chi_i c_{tot} \tag{30}$$

where χ_i is the molar fraction of the i-th selector in the mixture and $c_{tot} = \sum c_i$ is the total mixture concentration. By substituting Eq. (30) into Eq. (29) and after some simple algebra, Eq. (29) becomes:

$$\mu_{Aeff} = \frac{\mu_0 + K^{over} \mu^{over} c_{tot}}{1 + K^{over} c_{tot}} \tag{31}$$

where:

$$K^{over} = \sum \chi_i K_{ACi} \tag{32}$$

is an overall complexation constant for the mixture as a whole and:

$$\mu^{over} = \frac{\sum \chi_i K_{ACi} \mu_{ACi}}{K^{over}} \tag{33}$$

is the "overall mobility of complex" parameter. We use the formalism differently from the original paper by Kranack et al. for clarity. Equation (31) clearly shows that a mixture of selectors acts as a single selector with the related overall complexation constant and overall mobility of the (ostensible) complex. Actually, the authors derived the above equations rather as an aside, just to justify their approach to deal with a commercial mixture of CD derivatives as if the mixture was a single isomer, but without any profound discussion. This might be the reason why this idea was forgotten until it was independently rediscovered in our group 10 years later [55].

When applied to the dual-selector systems, Eqs. (31)–(33) turn into the overall equilibrium described by Eqs. (10)–(12). Equations (31)–(33) thus offer help in choosing optimal composition of the mixture and its optimal total concentration if the individual complexation constants and mobilities of complexes are determined. Naturally, the mixture composition cannot be optimized neither can the individual complexation constants and mobilities of complexes measured in the commercial mixtures of selectors. Nevertheless, in such a case, Eqs. (31)–(33) still allow us to treat the mixture as a single selector and thus to find its optimal total concentration in the standard way. Additionally, the overall model reveals one key difference between the single-selector and multiselector systems. The overall mobility of the complex (Eq. 33) inseparably blends the individual complexation constants and mobilities of the complexes together. This effect (referred to as the mixed thermodynamic/electrophoretic separation mechanism) has a significant consequence [29], particularly in the light of enantioseparation. When two enantiomers of one compound interact with a single selector, the mobilities of the two complexes are likely to be similar since the two complexes do not differ in charge and probably not much in sizes. On the other hand, the overall mobilities in the mixture of various selectors will most often differ due to the mixed thermodynamic/electrophoretic separation mechanism (cf. Eq. 33). First, this generally leads to a better enatioseparative capability of the commercial mixtures of selectors compared to single isomers as often observed in the analytical practice indeed. In fact, this effect is also responsible for the unexpected separation ability of the dual-selector system depicted in Fig. 2C (cf. discussion in Section 3.4). Second, the approximation of the same mobilities of complexes, as applied in

some enantioseparation method optimization strategies, becomes inappropriate when dealing with mixtures of selectors (including dual systems and not-well-defined "single" selector commercial mixtures).

5 Practical considerations and future challenges

Several models for optimization of dual-selector separation systems have been reviewed in this paper. However, among 55 examined publications, in which dual selector systems were employed for separation, only three of them [33, 35, 36] adopted the electromigration model to search for the optimum separation conditions. In another four, statistical tools were utilized for the method optimization [56–59]. In most cases, the trial-and-error approach remains the first and the only choice. As a matter of fact, the electromigration models require input parameters (complexation constants, mobilities of complexes, mobilities of free analytes) that have to be measured experimentally. Therefore, it may seem that the number of experiments needed for optimization is not much reduced by utilizing the electromigration models. However, in many studies (e.g. [60–64]) all data needed for the evaluation of the complexation parameters were actually gathered during the (semi-)qualitative method optimization process. In several cases [46,47,49,56,65,66] the complexation parameters were even determined but not used for the optimization (the complexation parameters were used, e.g. to optimize the single selector systems only [65,66] or to clarify the electromigration order of the analytes [49]). When lucky, the trial-error approach may be quicker compared to the optimization by mathematical modeling. However, the luck is never guaranteed and the above-mentioned models offer a substantial help in the optimization of the separation when a sufficient separation is not achieved instantly.

On the other hand, the theory of the dual- and multiselector systems is still not fully complete. In our opinion, further development is required especially in the following areas:

(i) The models for method optimization introduced in the dual-selector systems often need a certain level of approximation (e.g. zero EOF, equal mobilities of analytes, equal mobilities of complexes). The overall model (Eq. 10) suggests that such limitations are not necessary. The optimization strategies known from single-selector systems can easily be adopted in dual-systems using the overall parameters, which can further be tuned by changing the mixture composition. We have recently introduced this approach [26] but have not yet fully tested it in practice.

(ii) The single-selector model has been developed for weak acidic or basic analytes [67, 68]. Unfortunately, the acid/base equilibrium brings additional complexity into the theory and thus no such model is available for dual- and multiselector systems so far.

(iii) The single-, dual-, and multiselector models utilize (apparent) complexation constants, mobilities of complexes and mobilities of free analytes, which are specific for a particular ionic strength of the BGE. Therefore, an increase in concentration of a charged selector must be either compensated by a decrease in buffer concentration or an appropriate correction must be applied [16,17]. To our knowledge, the ionic strength-related effects in electrophoresis in BGE solutions of highly charged big molecules (such as multiply charged cyclodextrins) or even their mixtures has not been sufficiently described yet.

(iv) We have shown that complexation with a single selector (even neutral) may significantly contribute to the electromigration dispersion of the analyte [38,39]. The effect can completely disturb the otherwise promising separation. As a matter of fact, none of the above-mentioned theoretical models accounts for electromigration dispersion.

6 Conclusion

Dual-selector separation systems are of high importance in practice. They are simple enough to be treated in a rational way and complex enough to offer a broad range of possibilities for the method development. While their potential has been recognized in analytical practice, the available theory is only sparsely used for the method optimization. The description of electromigration of a single analyte in dual-selector systems already reveals their interesting properties such as the existence of the dengsu point or the iso-mobility counter lines. Separation of two analytes in the dual-selector systems can also be easily inspected. The difference in mobilities of the separated analytes, the selectivity and resolution of the separation can be predicted in a quantitative way. The graphical analysis provides a quick overview of the separation space and identifies its extremes and limits. The weighed mobility difference approach helps in recognizing the expected selectivity mechanism and thus choosing appropriate selectors. The overall model is promising in searching for the dual-selector mixture composition and its total concentration in order to obtain the desired separation. Notably, just as helpful may be the conclusion that no mixture of the chosen selectors exists that would satisfy the analysts' needs.

The commercial mixtures of various derivatives of selectors are often regarded as a single selector. The multiselector model justifies such an approach but simultaneously reveals some distinct aspects of the complex mixtures of selectors. The most important aspect is that the mixed thermodynamic/electrophoretic separation mechanism generally enables better separation ability when compared to the systems with single selectors. Secondly, the overall mobilities of the complexes of the two analytes in the multiselector systems must not be assumed to be the same as they are often approximated in the single-selector systems.

In spite of this progress, some important theoretical tasks still remain unresolved after 20 years of development.

The quantitative approach to the method optimization in dual-selector systems has not been fully tested yet. The model of electromigration of week acidic/basic analytes in dual- and multiselector systems is missing. The ionic strength and electromigration dispersion may significantly bias the predictions made by the contemporary models but such effects have not yet been sufficiently studied and described.

The authors acknowledge the financial support of this work from the Grant Agency of the Charles University, grant number 669412, the Grant Agency of the Czech Republic, grant number P206/12/P630, and financial support of the Charles University UNCE204025/2012.

The authors have declared no conflicts of interest.

7 References

[1] Rizzi, A., *Electrophoresis* 2001, *22*, 3079–3106.

[2] Scriba, G. K. E., *J. Pharm. Biomed. Anal.* 2001, *27*, 373–399.

[3] Chankvetadze, B., Blaschke, G., *J. Chromatogr. A* 2001, *906*, 309–363.

[4] Jac, P., Scriba, G. K. E., *J. Sep. Sci.* 2013, *36*, 52–74.

[5] Lurie, I. S., *J. Chromatogr. A* 1997, *792*, 297–307.

[6] Scriba, G. K. E., *J. Sep. Sci.* 2008, *31*, 1991–2011.

[7] Fillet, M., Hubert, P., Crommen, J., *J. Chromatogr. A* 2000, *875*, 123–134.

[8] Fillet, M., Hubert, P., Crommen, J., *Electrophoresis* 1998, *19*, 2834–2840.

[9] Gubitz, G., Schmid, M. G., *Electrophoresis* 2000, *21*, 4112–4135.

[10] Guebitz, G., Schmid, M. G., *Electrophoresis* 2007, *28*, 114–126.

[11] Guebitz, G., Schmid, M. G., *J. Chromatogr. A* 2008, *1204*, 140–156.

[12] Lu, H. A., Chen, G. N., *Anal. Methods* 2011, *3*, 488–508.

[13] Wren, S. A. C., Rowe, R. C., *J. Chromatogr.* 1992, *603*, 235–241.

[14] Britz-McKibbin, P., Chen, D. D. Y., *J. Chromatogr. A* 1997, *781*, 23–34.

[15] Penn, S. G., Goodall, D. M., Loran, J. S., *J. Chromatogr.* 1993, *636*, 149–152.

[16] Benes, M., Zuskova, I., Svobodova, J., Gas, B., *Electrophoresis* 2012, *33*, 1032–1039.

[17] Uselova-Vcelakova, K., Zuskova, I., Gas, B., *Electrophoresis* 2007, *28*, 2145–2152.

[18] Lurie, I. S., Klein, R. F. X., Dal Cason, T. A., LeBelle, M. J., Brenneisen, R., Weinberger, R. E., *Anal. Chem.* 1994, *66*, 4019–4026.

[19] Peng, X., Bowser, M. T., Britz-McKibbin, P., Bebault, G. M., Morris, J. R., Chen, D. D. Y., *Electrophoresis* 1997, *18*, 706–716.

[20] Kranack, A. R., Bowser, M. T., Britz-McKibbin, P., Chen, D. D. Y., *Electrophoresis* 1998, *19*, 388–396.

[21] Sepaniak, M. J., Copper, C. L., Whitaker, K. W., Anigbogu, V. C., *Anal. Chem.* 1995, *67*, 2037–2041.

[22] Whitaker, K. W., Copper, C. L., Sepaniak, M. J., *J. Microcolumn Sep.* 1996, *8*, 461–468.

[23] Szolar, O. H. J., Brown, R. S., Luong, J. H. T., *Anal. Chem.* 1995, *67*, 3004–3010.

[24] Terabe, S., Otsuka, K., Ando, T., *Anal. Chem.* 1985, *57*, 834–841.

[25] Bowser, M. T., Kranack, A. R., Chen, D. D. Y., *Anal. Chem.* 1998, *70*, 1076–1084.

[26] Mullerova, L., Dubsky, P., Gas, B., *J. Chromatogr. A* 2014, *1330*, 82–88.

[27] Lelievre, F., Gareil, P., Bahaddi, Y., Galons, H., *Anal. Chem.* 1997, *69*, 393–401.

[28] Lelievre, F., Gareil, P., Jardy, A., *Anal. Chem.* 1997, *69*, 385–392.

[29] Dubsky, P., Svobodova, J., Tesarova, E., Gas, B., *Electrophoresis* 2010, *31*, 1435–1441.

[30] Chankvetadze, B., *J. Chromatogr. A* 1997, *792*, 269–295.

[31] Abushoffa, A. M., Fillet, M., Hubert, P., Crommen, J., *J. Chromatogr. A* 2002, *948*, 321–329.

[32] Abushoffa, A. M., Fillet, M., Servais, A., Hubert, P., Crommen, J., *Electrophoresis* 2003, *24*, 343–350.

[33] Abushoffa, A. M., Fillet, M., Marini, R. D., Hubert, P., Crommen, J., *J. Sep. Sci.* 2003, *26*, 536–542.

[34] Nhujak, T., Sastravaha, C., Palanuvej, C., Petsom, A., *Electrophoresis* 2005, *26*, 3814–3823.

[35] Schaeper, J. P., Fox, S. B., Sepaniak, M. J., *J. Chromatogr. Sci.* 2001, *39*, 411–419.

[36] Surapaneni, S., Ruterbories, K., Lindstrom, T., *J. Chromatogr. A* 1997, *761*, 249–257.

[37] Friedl, W., Kenndler, E., *Anal. Chem.* 1993, *65*, 2003–2009.

[38] Hruska, V., Svobodova, J., Benes, M., Gas, B., *J. Chromatogr. A* 2012, *1267*, 102–108.

[39] Benes, M., Svobodova, J., Hruska, V., Dvorak, M., Zuskova, I., Gas, B., *J. Chromatogr. A* 2012, *1267*, 109–115.

[40] Zhu, X., Ding, Y., Lin, B., Jakob, A., Koppenhoefer, B., *J. Chromatogr. A* 2000, *888*, 241–250.

[41] Chankvetadze, B., *TrAC, Trends Anal. Chem.* 1999, *18*, 485–498.

[42] Fillet, M., Chankvetadze, B., Crommen, J., Blaschke, G., *Electrophoresis* 1999, *20*, 2691–2697.

[43] Matthijs, N., Van Hemelryck, S., Maftouh, M., Luc Massart, D., Vander Heyden, Y., *Anal. Chim. Acta* 2004, *525*, 247–263.

[44] Chankvetadze, B., Burjanadze, N., Crommen, J., Blaschke, G., *Chromatographia* 2001, *53*, S296-S301.

[45] Tabi, T., Magyar, K., Szoeko, E., *Electrophoresis* 2003, *24*, 2665–2673.

[46] Nemeth, K., Varga, E., Ivanyi, R., Szeman, J., Visy, J., Jicsinszky, L., Szente, L., Forro, E., Fueloep, F., Peter, A., Simonyi, M., *J. Pharm. Biomed. Anal.* 2010, *53*, 382–388.

[47] Beni, S., Sohajda, T., Neumajer, G., Ivanyi, R., Szente, L., Noszal, B., *J. Pharm. Biomed. Anal.* 2010, *51*, 842–852.

[48] Chankvetadze, B., *Electrophoresis* 2002, *23*, 4022–4035.

[49] Calvet, C., Cuberes, R., Perez-Maseda, C., Frigola, J., *Electrophoresis* 2002, *23*, 1702–1708.

[50] Lin, C., Lin, S., Fang, I., Liao, W., Chen, C., *Electrophoresis* 2004, *25*, 2786–2794.

[51] Lin, C., Lin, S., Cheng, H., Fang, I., Kuo, C., Liu, Y., *Electrophoresis* 2005, *26*, 4187–4196.

[52] Chankvetadze, B., *J. Chromatogr. A* 2007, *1168*, 45–70.

[53] Chen, F. T. A., Shen, G., Evangelista, R. A., *J. Chromatogr. A* 2001, *924*, 523–532.

[54] Schmitt, U., Ertan, M., Holzgrabe, U., *Electrophoresis* 2004, *25*, 2801–2807.

[55] Dubsky, P., Svobodova, J., Gas, B., *J. Chromatogr. B* 2008, *875*, 30–34.

[56] Perez-Maseda, C., Calvet, C., Cuberes, R., Frigola, J., *Electrophoresis* 2003, *24*, 1416–1421.

[57] Jimidar, M. I., Vennekens, T., Van Ael, W., Redlich, D., De Smet, M., *Electrophoresis* 2004, *25*, 2876–2884.

[58] Jamali, B., Bjoernsdottir, I., Cornett, C., Honore Hansen, S., *Electrophoresis* 2009, *30*, 2853–2861.

[59] Danel, C., Chaminade, P., Odou, P., Bartelemy, C., Azarzar, D., Bonte, J., Vaccher, C., *Electrophoresis* 2007, *28*, 2683–2692.

[60] Fillet, M., Fotsing, L., Bonnard, J., Crommen, J., *J. Pharm. Biomed. Anal.* 1998, *18*, 799–805.

[61] Tsunoi, S., Harino, H., Miura, M., Eguchi, M., Tanaka, M., *Anal. Sci.* 2000, *16*, 991–993.

[62] Grard, S., Morin, P., Dreux, M., Ribet, J., *Electrophoresis* 2000, *21*, 3028–3034.

[63] Martinez-Giron, A. B., Dominguez-Vega, E., Garcia-Ruiz, C., Crego, A. L., Marina, M. L., *J. Chromatogr. B* 2008, *875*, 254–259.

[64] Chu, B., Guo, B., Zuo, H., Wang, Z., Lin, J., *J. Pharm. Biomed. Anal.* 2008, *46*, 854–859.

[65] Sohajda, T., Szakacs, Z., Szente, L., Noszal, B., Beni, S., *Electrophoresis* 2012, *33*, 1458–1464.

[66] Sohajda, T., Hu, W. H., Zeng, L. L., Li, H., Szente, L., Noszal, B., Beni, S., *Electrophoresis* 2011, *32*, 2648–2654.

[67] Rawjee, Y. Y., Staerk, D. U., Vigh, G., *J. Chromatogr.* 1993, *635*, 291–306.

[68] Williams, B. A., Vigh, G., *J. Chromatogr. A* 1997, *777*, 295–309.

2 Cíle dizertační práce

Cílem této práce bylo především rozšířit poznatky o elektromigraci v systémech s více selektory:

(i) Experimentálně ověřit využitelnost M-souhrnného modelu pro popis a predikci vlastností separačních systémů připravených smísením dvou definovaných cyklodextrinů a demonstrovat výhody tohoto přístupu (*Publikace II*).

(ii) Rozšířit M-souhrnný model o možnost acidobazické disociace analytu a experimentálně demonstrovat platnost rozšířeného modelu na systému slabé jednosytné kyseliny jako analytu a dvou definovaných cyklodextrinů jako selektorů (*Publikace III* a *IV*).

Další cíle pak souvisely se stanovením správné efektivní mobility analytu:

(i) Navrhnout metodu pro stanovení efektivní mobility v systému s interagující složkou BGE použitelnou v komerčně dostupném přístroji pro CE a s její pomocí posoudit vhodnost populárních EOF markerů pro použití v BGE s nedefinovaně sulfatovaným cyklodextrinem (*Publikace V*).

(ii) Odvodit vztahy mezi geometrickými charakteristikami elektroforetického píku deformovaného elektromigrační disperzí a parametry HVL funkce popisující tento pík, především migračním časem odpovídajícím efektivní mobilitě analytu při jeho nekonečném zředění (*Publikace VI*).

3 Experimentální podmínky

Elektroforetické experimenty byly prováděny na přístroji Agilent ^{3D}CE pro kapilární elektroforézu (Agilent Technologies, Waldbronn, Německo). Přístroj je vybaven vestavěným UV/Vis detektorem s diodovým polem a bezkontaktním vodivostním detektorem vyvinutým v naší laboratoři [76]. K ovládání přístroje a sběru dat sloužil software ChemStation (Agilent Technologies). K měření pH sloužil PHM 240 pH/ION metr (Radiometer analytical, Kodaň, Dánsko).

Byly používány křemenné kapiláry z vnější strany pokryté polyimidovým potahem. Použité chemikálie byly vysoké čistoty, voda byla deionizována systémem Rowapur a Ultrapur (Watrex, San Francisco, USA).

Ke zpracování a vyhodnocení dat sloužily programy Origin 8.1 (OriginLab Corporation, Northampton, USA) a Microsoft Office Excel.

Detailní experimentální podmínky jsou vždy popsány v příslušné publikaci, a proto zde nejsou podrobně uváděny.

4 Výsledky a diskuze

4.1 Použití M-souhrnného modelu pro definované směsi dvou selektorů

Podle M-souhrnného modelu (18) – (20) lze směs selektorů o konstantním složení (konstantním poměru molárních koncentrací jednotlivých selektorů ve směsi) pokládat za selektor jeden. Model také ukazuje, jak jsou komplexační parametry tohoto „souhrnného“ selektoru provázány s komplexačními parametry jednotlivých složek směsi. V případě, že jsou do BGE záměrně přidávány dva různé selektory za účelem dosažení lepší separace, pak je složení směsi známo a komplexační parametry směsi mohou být předpovězeny na základě komplexačních parametrů obou čistých selektorů pomocí M-souhrnného modelu.

Pro směs toliko dvou selektorů přecházejí vztahy (18) a (19) do následujících tvarů:

$$K'^{M}_{AS} = K'_{AS1}\chi_{S1} + K'_{AS2}\chi_{S2} = K'_{AS1}\chi_{S1} + K'_{AS2}(1-\chi_{S1}) \tag{22}$$

$$\mu^{M}_{AS} = \frac{\mu_{AS1}K'_{AS1}\chi_{S1} + \mu_{AS2}K'_{AS2}\chi_{S2}}{K'^{M}_{AS}} = \frac{\mu_{AS1}K'_{AS1}\chi_{S1} + \mu_{AS2}K'_{AS2}(1-\chi_{S1})}{K'^{M}_{AS}} \tag{23}$$

kde χ_{S1} a $\chi_{S2} = (1-\chi_{S1})$ jsou molární zlomky prvního a druhého selektoru ve směsi. Efektivní mobilita analytu pro konkrétní složení směsi a celkovou koncentraci selektoru je pak dána vztahem (20). Pokud je stejným způsobem vyjádřena i efektivní mobilita druhého analytu, lze pomocí M-souhrnného modelu zkoumat, jak se mění separační potenciál směsi se změnou jejího složení, případně zvolit optimální χ_{S1} a c_{tot} pro danou separaci.

V *Publikaci II* byl tento přístup experimentálně ověřen. Jako modelové analyty byly zvoleny ibuprofen a flurbiprofen. Přestože se jedná o chirální látky, v tomto případě nebyla prováděna chirální separace (při zvoleném pH není interakce s CD enantioselektivní), ale ibuprofen byl brán jako první analyt a flurbiprofen jako analyt druhý. Dále jsou při daném pH oba tyto analyty plně disociovány s vlastní mobilitou $\mu_A \neq 0$ a neúčastní se žádné acidobazické rovnováhy (jedná se tedy o S_AM_S systém). V práci byla zkoumána jejich elektromigrace v systémech se dvěma různými dvojicemi selektorů: heptakis(2,6-di-O-methyl)-β-cyclodextrinu (DM-β-CD) s 6-O-α-maltosyl-β-cyclodextrinem (Malt-β-CD) tvořily první dvojici cyklodextrinů a DM-β-CD s nativním β-cyclodextrinem (β-CD) dvojici druhou.

Nejprve byly metodou ACE stanoveny komplexační parametry K'_{AS} a μ_{AS} obou analytů s jednotlivými selektory (v S_AS_S systémech). Následně byly experimentálně změřeny M-

souhrnné komplexační parametry K'^{M}_{AS} a μ^{M}_{AS} pro různá složení směsi (reprezentovaná frakcí prvního selektoru χ_{S1}) a pro obě zkoumané dvojice selektorů. Pro experimentální stanovení těchto souhrnných komplexačních parametrů byla opět použita metoda ACE – se směsí dvou selektorů o konstantním χ_{S1} se zacházelo jako s jedním selektorem. Takto změřené M-souhrnné parametry byly porovnány s parametry vypočtenými pomocí rovnic (22) a (23) z parametrů jednotlivých selektorů (*Publikace II*, Table 2). Shoda mezi změřenými a spočtenými parametry byla velmi dobrá, pozorované rozdíly mezi nimi byly, podle dlouhodobých zkušeností naší výzkumné skupiny, srovnatelné s přesností ACE metody.

Za zmínku také stojí porovnání kvality fitu, jmenovitě chyb parametrů stanovených ACE metodou, v S_AS_S a S_AM_S systémech. Závislost efektivní mobility na (celkové) koncentraci selektoru je v obou případech prokládána stejnou funkcí. Pokud by chyby stanovení byly v systémech se dvěma selektory významně vyšší ve srovnání se S_AS_S systémy, zpochybňovalo by to závěr M-souhrnného modelu, že směs selektorů o konstantním složení lze pokládat za selektor jediný. Výsledky ale ukazují (*Publikace II*, Table 1 a Table 2), že chyby stanovení se nijak neliší, bez ohledu na to, zda byla metoda ACE aplikována na S_AS_S nebo S_AM_S systém, což správnost M-souhrnného modelu potvrzuje.

Schopnost M-souhrnného modelu předpovídat kvalitu separace je demonstrována graficky (*Publikace II*, Fig. 4A a 4B) – v tomto případě byl jako parametr kvantifikující kvalitu separace použit poměr efektivních mobilit separovaných analytů neboli selektivita. Selektivity ve směsi selektorů předpovězené pomocí M-souhrnného modelu z komplexačních parametrů obou čistých selektorů (plné čáry) jsou v dobré shodě se selektivitami změřenými experimentálně (symboly). Přestože některé experimentální body se s predikcí neshodují zcela přesně, tvar závislosti a důležité charakteristiky daného separačního systému (přítomnost a přibližná poloha maxima, záměna migračního pořadí) jsou předpovězeny správně.

Má-li být M-souhrnný model použit k optimalizaci separačního systému se dvěma selektory, je třeba optimalizovat dvě nezávisle proměnné: celkovou koncentraci selektoru c_{tot} a molární frakci prvního selektoru ve směsi χ_{S1} (frakce druhého selektoru je jednoznačně určena vztahem $\chi_{S2} = 1 - \chi_{S1}$). To je obdobná situace jako v případě původního modelu elektromigrace v systému se dvěma selektory (12), kde jsou nezávislými proměnnými koncentrace obou selektorů c_{S1} a c_{S2}. Nicméně, přechod od c_{S1} a c_{S2} v původním modelu k c_{tot} a χ_{S1} v M-souhrnném modelu přináší významné výhody.

Především koncentrace selektorů c_{S1} a c_{S2} mohou obě v principu růst do nekonečna a je náročné představit si chování systému při všech jejich možných kombinacích. Na druhou stranu M-souhrnný model ukazuje, že chování směsi selektorů je závislé na poměru jejich koncentrací, respektive na frakci χ_{S1}, která může nabývat pouze hodnot od nuly do jedné. V rámci takto dobře definovaného rozsahu složení směsi lze studovat vlastnosti systému – to bylo jednak ukázáno na experimentálních výsledcích v *Publikaci II*, a dále je demonstrováno na Obrázku 2 pro hypotetický (nicméně reálně možný) systém.

Z modelu (18) – (20) vyplývá, že M-souhrnná komplexační konstanta může nabývat pouze hodnot mezi hodnotami komplexačních konstant prvního a druhého selektoru (*Publikace II*, Fig. 3A; Obrázek 2E, přerušované čáry). Totéž platí i pro M-souhrnnou mobilitu komplexu, která se ale na rozdíl od komplexační konstanty nemění s χ_{S1} lineárně (*Publikace II*, Fig. 3B; Obrázek 2E, plné čáry). Stejně tak i efektivní mobilita jednoho analytu při dané celkové koncentraci selektoru se bude vždy nacházet v rozmezí daném efektivními mobilitami tohoto analytu v BGE obsahujícím ekvivalentní koncentraci prvního respektive druhého selektoru (Obrázek 2A a 2B). Nicméně toto už neplatí pro rozdíl efektivních mobilit dvou analytů (Obrázek 2C), nebo jejich poměr (*Publikace II*, Fig. 4; Obrázek 2D) – jinak by směs dvou selektorů nikdy nemohla zlepšovat separaci ve srovnání s jednotlivými selektory. Tento efekt je možné pozorovat v případě dvojice selektorů DM-β-CD a β-CD při vyšších koncentracích c_{tot} (*Publikace II*, Fig. 4A). V případě hypotetického systému na Obrázku 2 pak směs poskytuje jak větší rozdíl mezi mobilitami analytů (Obrázek 2C, $\chi_{S1} = 0{,}7$) tak i lepší selektivitu (Obrázek 2D, $\chi_{S1} = 0{,}3$; 0,5 a 0,7) ve srovnání s optimální koncentrací obou čistých selektorů. Tyto grafy ilustrují, jak se průběh závislosti selektivity na celkové koncentraci mění s měnícím se složením směsi – a že změny tvarů těchto závislostí mohou být značně „neintuitivní“.

Dalším jevem, na němž lze demonstrovat vhodnost M-souhrnného modelu pro popis separačního systému se dvěma selektory je záměna elektromigračního pořadí analytů (EMO, *electromigration order*). Zda a při jaké koncentraci selektoru dojde k záměně EMO analytů A a B, lze zjistit nalezením takové koncentrace c_{tot}, která pro dané složení směsi (χ_{S1}) splňuje podmínku $\mu_{A,eff} = \mu_{B,eff}$. Za efektivní mobility obou analytů $\mu_{A,eff}$ a $\mu_{B,eff}$ lze dosadit ze vztahu (20), což vede ke kvadratické rovnici, jejímž řešením jsou koncentrace, při kterých k záměně EMO dochází – ty pak lze vynést jako funkci složení směsi χ_{S1} (*Publikace II*, Fig. 2; Obrázek 2F). Stejným způsobem lze graficky pracovat s dalšími charakteristikami systému, jako je například koncentrace odpovídající maximálnímu rozdílu mobilit.

M-souhrnný model je vhodným nástrojem pro popis separačních systémů se dvěma selektory. Zejména umožňuje snadno identifikovat, zda smísení dvou konkrétních selektorů může vést ke zlepšení separace a pokud ano, lze jej využít k nalezení optimálního složení a celkové koncentrace směsi selektorů vzhledem k podílu (nebo rozdílu) efektivních mobilit analytů nebo například i z hlediska jejich migračního pořadí. Výhodou tohoto modelu také je, že se nejedná o rozšíření jednoduššího modelu o přítomnost druhého selektoru, ale spíše o speciální případ obecného modelu popisujícího komplexaci s libovolným počtem selektorů. Model tak nabízí užitečný vhled do mechanismů, které se v S_AM_S systémech podílejí na separaci.

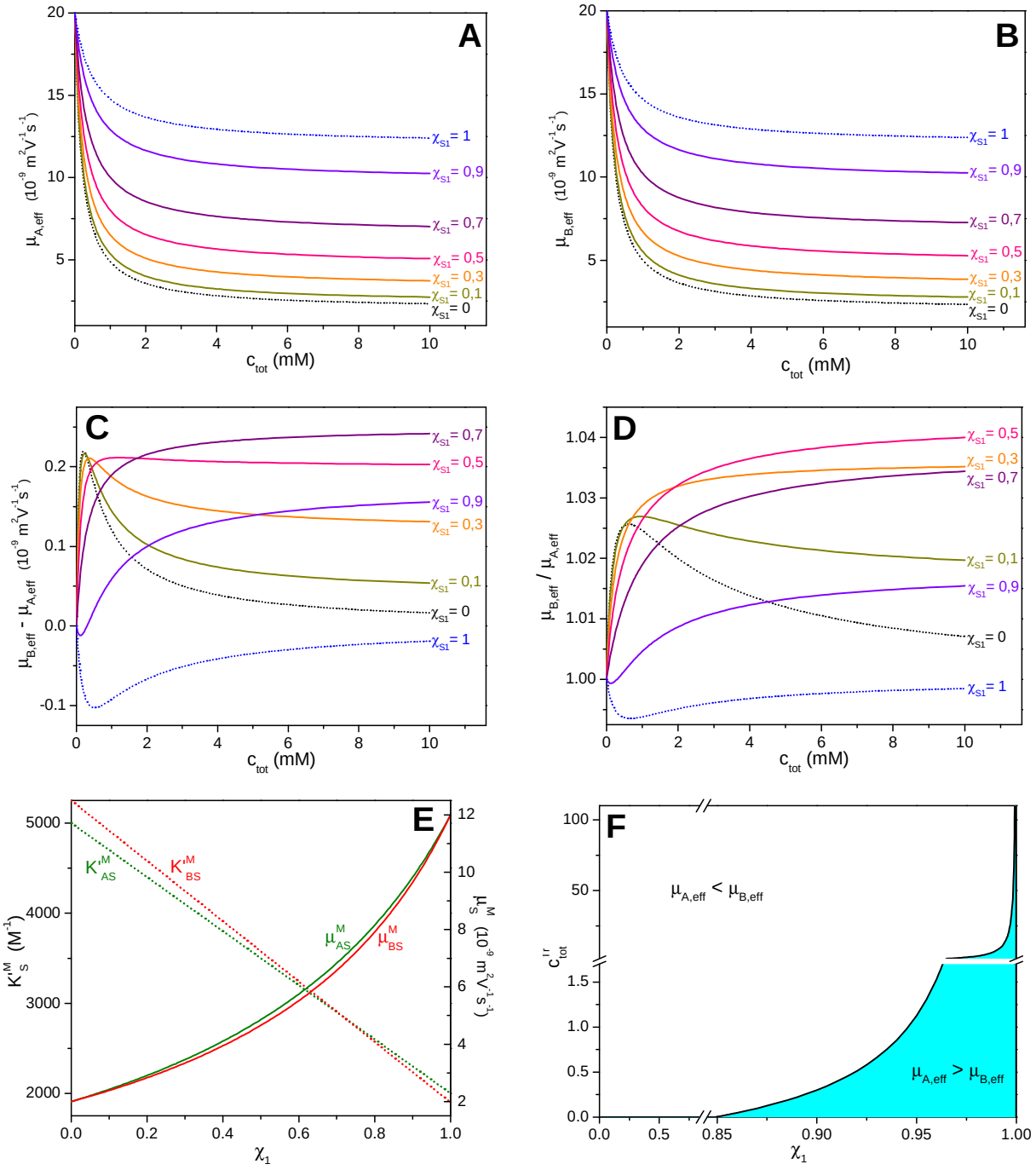

Obrázek 2: Grafická analýza vlastností hypotetického separačního systému pomocí M-souhrnného modelu. Závislost efektivní mobility prvního (A) a druhého (B) analytu, rozdílu efektivních mobilit (C) a poměru efektivních mobilit (D) na celkové koncentraci selektoru v systémech s jednotlivými čistými selektory (přerušované čáry, c_{tot} odkazuje na koncentraci čistého selektoru) a se směsmi těchto selektorů (plné čáry), složení směsi (frakce prvního selektoru, χ_{S1}) uvedeno v grafech; (E) závislost M-souhrnných komplexačních konstant (přerušované čáry) a M-souhrnných mobilit komplexů (plné čáry) na složení směsi; (F) závislost koncentrace c^{Tr}_{tot}, při které dochází k záměně EMO, na složení směsi. Mobility volných analytů $\mu_A =$ $= \mu_B = 20 \cdot 10^{-9}$m^{2}V^{-1}s^{-1}; mobility komplexů s prvním selektorem a se druhým selektorem $\mu_{AS1} =$ $= \mu_{BS1} = 12 \cdot 10^{-9}$ m^{2}V^{-1}s^{-1}, $\mu_{AS2} = \mu_{BS2} = 2 \cdot 10^{-9}$m^{2}V^{-1}s^{-1}; konstanty komplexace analytů s prvním selektorem K'_{AS1} = 1900 M^{-1}, K'_{BS1} = 2000 M^{-1} a se druhým selektorem K'_{BS2} = 5250 M^{-1}, K'_{BS2} = 5000 M^{-1}.

Publikace II

Separation efficiency of dual-selector systems in capillary electrophoresis

L. Müllerová, P. Dubský, B. Gaš

Journal of Chromatography A 2014, *1330*, 82-88.

Journal of Chromatography A, 1330 (2014) 82–88

Contents lists available at ScienceDirect

Journal of Chromatography A

journal homepage: www.elsevier.com/locate/chroma

Separation efficiency of dual-selector systems in capillary electrophoresis☆

Ludmila Müllerová, Pavel Dubský*, Bohuslav Gaš

Charles University in Prague, Faculty of Science, Department of Physical and Macromolecular Chemistry, Prague, Czech Republic

ARTICLE INFO

Article history:
Received 24 October 2013
Received in revised form 3 January 2014
Accepted 6 January 2014
Available online 13 January 2014

Keywords:
Capillary zone electrophoresis
Complexation
Dual selector system
Model of electromigration

ABSTRACT

We introduce an easy but highly descriptive model of separation efficiency of dual-selector systems in capillary electrophoresis. The model expresses effective mobilities of analytes in dual-selector mixtures as a function of mixture composition and total concentration. The effective mobility follows the pattern familiar from single-selector systems, while complexation constant and mobility of the complex are replaced by the same but "overall" parameters and a total concentration of the mixture takes the role of a selector concentration. The overall parameters can be either calculated from the individual ones (an arbitrary mixture) or measured directly (a particular mixture). We inspected two model dual-selector systems consisting of heptakis(2,6-di-O-methyl)-β-CD and β-CD and of heptakis(2,6-di-O-methyl)-β-CD and 6-O-α-maltosyl-β-CD, and ibuprofen and flurbiprofen as model analytes (pH 8.2, non-enantioselective separation). Adopting any optimization strategy typically used in single-selector systems and finding an optimal mixture composition and total concentration is perhaps the prime benefit of the model. We demonstrate this approach on the selectivity parameter and show that the model is precise enough to be used in analytical practice. It also results that an electromigration order (reversal) of analytes can exhibit a rather curious dependency on the mixture composition and concentration. Last, the model can be used for better understanding of separation principles in dual-selector systems in general.

1. Introduction

In capillary electrophoresis (CE), interaction of analytes with selectors added into the background electrolyte (BGE) makes it possible to achieve enantioseparation or separation of neutral analytes as well as it is widely used to improve ordinary achiral separations. Additionally, combination of two selectors employed in a mixture (dual systems) proved advantageous when a single selector does not serve efficiently enough. Several mathematical models have been derived describing the mechanism of the separation. While these models provide help with finding optimal separation conditions in single selector systems [1–5], a lack of similarly systematic approach can still be identified when coming to dual systems.

In 1992, Wren and Rowe described electromigration behavior of chiral analytes interacting with one chiral selector as follows [6]:

$$\mu_{A,eff} = \frac{\mu_{A,f} + \mu_C K_C[S]}{1 + K_C[S]} \quad (1)$$

where $\mu_{A,eff}$ is the effective mobility of the analyte, $\mu_{A,f}$ the mobility of the free analyte (the effective mobility of the analyte in a BGE containing no selector), μ_C the mobility of the complex of the analyte with the selector, [S] is the equilibrium concentration of the selector and K_C is the apparent equilibrium complexation constant:

$$K_C = \frac{[C]}{[A][S]} \quad (2)$$

where [A] and [C] are the equilibrium concentrations of the free analyte and the complex of the analyte with the selector, respectively. The model is valid under 1:1 complexation stoichiometry and if the exchange between the complexed and free form of the analyte is much faster than electrophoretic movement. Even though this model originally aimed at chiral separations, it serves just as well for characterization of selector-assisted achiral separations [7,8]. Later published models were in their majority based on the approach by Wren and Rowe [7,9–15] (or a mathematically equivalent one [8,16–18]) extended with acido-base equilibria and

☆ Presented at the 20th International Symposium on Electro- and Liquid Phase-Separation Techniques (ITP 2013), 6–9 October 2013, Puerto de la Cruz, Tenerife, Canary Islands, Spain.

* Corresponding author at: Charles University in Prague, Faculty of Science, Albertov 6, 128 40 Prague 2, Czech Republic. Tel.: +420 221 951 296.
E-mail address: pavel.dubsky@natur.cuni.cz (P. Dubský).

0021-9673/$ – see front matter © 2014 Elsevier B.V. All rights reserved.
http://dx.doi.org/10.1016/j.chroma.2014.01.006

various objective measures of the goodness of separation (mobility difference, selectivity, resolution) with respect to separation conditions, namely the selector concentration and possibly pH.

Dual separation systems (chiral [19–30] and achiral [31–35]) have been also described mathematically [2,3,36–38]. In many cases [19,21,23–26,36,38], authors extend the equation by Wren and Rowe (1) by the second selector, which finally results in equation (3):

$$\mu_{A,eff} = \frac{\mu_{A,f} + \mu_{C1}K_{C1}[S_1] + \mu_{C2}K_{C2}[S_2]}{1 + K_{C1}[S_1] + K_{C2}[S_2]} \quad (3)$$

where symbols have the same meaning as those in Eq. (1) and indexes 1 and 2 stays for the 1st and the 2nd selector, respectively. A different approach based on the chromatographic model developed originally for micellar electrokinetic chromatography separations [39] was used to describe separation of highly hydrophobic analytes by a dual selector system of neutral and charged cyclodextrin (CD) [31,33]. Several authors also described difference between effective mobilities of two enantiomers separated by a dual selector system, $\Delta\mu_d$, as a weighted sum of mobility differences generated by the first, $\Delta\mu_1$, and the second, $\Delta\mu_2$, selector [22,27,28,37]: $\Delta\mu_d = i\Delta\mu_1 + j\Delta\mu_2$. The (not quantitatively specified) coefficients i and j generally depend on the concentration of the selectors and their complexation constants. This approach can be utilized to judge qualitatively which affinity patterns and effects on analyte mobilities offer separation improvement (compared to single selectors) or lead to inversion of the electromigration order. Models have been also derived describing complexation of an analyte with more than two selectors [30,34,35].

The main drawback of the dual models is their higher complexity in comparison with the single models. With two independent variables (concentration of two selectors) it is more difficult to optimize the separation or even get an insight into the separation mechanism. Therefore, simplifications are often used which, however, result in mathematical models valid only for specific cases [21,31–33], or the models are used only for qualitative explanations of observed effects [19,22,28,38].

Recently, we have shown that Eq. (3) can be expressed in a form identical to that of complexation with a single selector (1) even when extended to an arbitrary number of constituents [40,41]:

$$\mu_{A,eff} = \frac{\mu_{A,f} + \mu_C^{over}K_C^{over}c_{tot}}{1 + K_C^{over}c_{tot}} \quad (4)$$

where $\mu_{A,eff}$ and $\mu_{A,f}$ have the same meaning as in Eq. (1), c_{tot} is the total molar concentration of the selector mixture (sum of molar concentrations of all present selectors) and K_C^{over} is the overall complexation constant:

$$K_C^{over} = \sum_i \chi_i K_i \quad (5)$$

and μ_C^{over} is the overall mobility of the complex:

$$\mu_C^{over} = \frac{\sum_i \chi_i \mu_i K_i}{\sum_i \chi_i K_i} = \frac{\sum_i \chi_i \mu_i K_i}{K_C^{over}} \quad (6)$$

Finally, χ_i in Eqs. (5) and (6) is the molar fraction of the ith selector in the mixture and K_i and μ_i are corresponding complexation constant and mobility of the complex, respectively. Note that the "overall mobility of the complex" actually does not refer to the mobility of any single specific compound in the solution, but should be understood as the limiting mobility of the analyte in BGE containing infinite concentration of the mixture of the selectors.

Equation (4) is valid under the following conditions: (i) the complexation is much "faster" than the electrophoretic movement, (ii) the analyte can interact with no more than one single selector at a time with 1:1 stoichiometry, (iii) consumption of each single selector by the complexation is negligible. The overall complexation parameters (overall complexation constant and overall mobility of the complex) can be either measured experimentally (in the same way as those of a single selector) or calculated (using Eqs. (5) and (6)) and can serve as input parameters for the already-well-developed single-selector models.

The objective of this work is both to verify our model experimentally and to demonstrate its potency to systematically characterize separation properties of dual-selector systems. We compare the calculated overall complexation parameters with the measured ones and use them to predict and measure the separation efficacy of various dual mixtures.

2. Materials and methods

2.1. Chemicals

All chemicals used, namely: (±)-ibuprofen, (±)-flurbiprofen, tris(hydroxymethyl)aminomethane (tris), N-[Tris(hydroxymethyl) methyl]glycine (tricine), nitromethane, heptakis(2,6-di-O-methyl)-β-cyclodextrin (DM-β-CD), 6-O-α-maltosyl-β-cyclodextrin hydrate (Malt-β-CD) and β-cyclodextrin (β-CD); were purchased from Sigma-Aldrich (Prague, Czech Republic) and were of analytical-grade purity. Water used for preparation of all solutions was purified by Rowapur and Ultrapur water purification system (Watrex, San Francisco, USA).

2.2. Instrumentation

All experiments were performed using an Agilent ^{3D}CE capillary electrophoresis operated by ChemStation software (Agilent Technologies, Waldbronn, Germany). The instrument is equipped with a built-in photometric diode array detector (UV detector). Fused-silica capillary of 50 μm i.d. and 375 μm o.d. was provided by Polymicro Technologies (Phoenix, AZ, USA). The total length of the capillary and distance from inlet to UV detector were 52.1 and 43.6 cm, respectively. PHM 240 pH/ION Meter (Radiometer analytical, Lyon, France) was used for pH measurements.

2.3. Experimental conditions

The running buffer not containing any selector was composed of 50 mM tris and 50 mM tricine, pH of 8.2 (tris–tricine buffer). The stock solution of each single selector was prepared by dissolving the selector directly in the tris–tricine buffer to obtain the highest selector concentration used. BGEs containing a single selector at lower concentrations were prepared by diluting the stock solution of the particular selector with the tris–tricine buffer. The concentration ranges used were 0–8 mM, 0–10 mM and 0–5 mM for β-CD, DM-CD and Malt-CD, respectively. To prepare BGEs containing two different selectors, firstly stock solutions of the single selectors were mixed in required ratio to obtain the highest concentration of the desired mixture. Then the mixture was diluted with the pure tris–tricine buffer to obtain BGEs containing the mixture in lower concentrations. The concentration ranges used were 0–8 mM and 0–5 mM for dual system consisted of β-CD and DM-β-CD and of DM-β-CD and Malt-β-CD, respectively. All the BGEs used in this work had the same ionic strength of 26 mM according to the calculation by PeakMaster software [42]. Samples contained (±)-ibuprofen or (±)-flurbiprofen (0.4 mM and 0.2 mM, respectively), nitromethane serving as EOF marker (0.02%, v/v) and running buffer constituents. Samples did not contain any selector. All solutions were filtered using syringe filters, pore size 0.45 μm (Sigma-Aldrich, Prague, Czech Republic).

The capillary was thermostated at 25 °C. Prior to use, a new capillary was flushed with water for 5 min, then with 1 M NaOH for 5 min and then twice with water for 5 min. Prior to each run, the capillary was flushed at least for 3 min with the actual BGE. Samples were injected hydrodynamically, 150 mbar s. Applied voltage was 15 kV (anode at the injection side). Each experiment was repeated at least four times. The software ChemStation (Agilent Technologies) was used for data collection and acquisition. The mathematical software Origin 8.1 (OriginLab Corporation, Northampton, USA) was used for fitting analyte peaks with the Haarhoff van der Linde (HVL) function [43,44] and marker peaks with the Gaussian function, and for nonlinear regression of effective mobilities (Eqs. (1) and (4)). Calculations were performed by means of Microsoft Office Excel 2010 (Microsoft).

3. Results and discussion

We chose ibuprofen and flurbiprofen as our model analytes. Although both of these analytes are chiral compounds, chiral separation was not in our scope of interest and their interaction with CDs is not enantioselective at the pH used (as published for native β-CD [10] and verified by us for the β-CD isomers used in this study). Consequently, (±)-ibuprofen is regarded as the first analyte and (±)-flurbiprofen as the second analyte. Additionally, both compounds are fully charged under this pH so that they have their own electrophoretic mobilities $u_{A,f} \neq 0$ and no acido-base equilibrium is considered. Interaction of these analytes with two dual systems, one consisting of DM-β-CD and β-CD and the second of DM-β-CD and Malt-β-CD, was quantified.

3.1. Model verification

As described in Section 1, a mixture of a particular ratio of two individual selectors can be regarded as a new selector with its own overall complexation parameters. If so, these overall parameters can be either calculated based on our model, or measured directly as usual for single systems.

Calculation of the overall complexation parameters uses the individual parameters of both the single selector systems (cf. Eqs. (5) and (6)). These parameters were determined by means of affinity capillary electrophoresis (ACE) [45,46]: dependence of the analyte's effective mobility on the selector concentration was obtained and fitted with equation (1). Exactly the same procedure – including fitting equation (1) with $[S] \equiv c_{tot}$ – was applied to the dual systems. Here, c_{tot} refers to the concentration of the mixture, instead of a single selector, and varying c_{tot} means that the total molar concentration of the two selectors is changed while the ratio of their individual concentrations remains the same.

Several circumstances should be considered prior to/during the ACE measurements:

- Peak distortion due to electromigration dispersion that affects reading of the right peak position.
- Selector consumption due to complexation that should be low enough as to satisfy condition (iii) of equation (4) but is also prerequisite for fitting Eq. (1) (or otherwise the proper value of [S] is unknown).
- Ionic strength, viscosity and temperature that influence physical–chemical parameters of the system, namely complexation constants and electrophoretic mobilities.

The first two issues are both solved by fitting the analyte peak with HVL function [47]. As a parameter of this function, we obtain migration time of the analyte at its infinite dilution (Fig. 1). This exactly corresponds to the conditions where neither

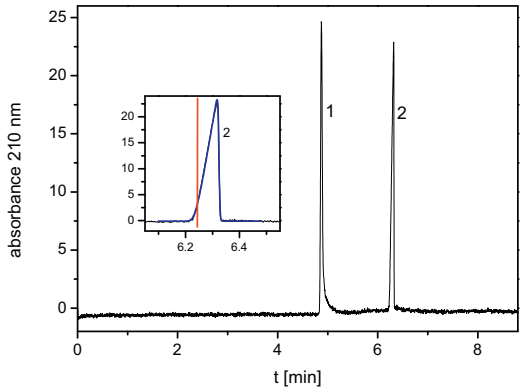

Fig. 1. Sample electropherogram. Peak 1: EOF marker (nitromethane); peak 2: flurbiprofen; the insert shows an extension of the analyte's peak fitted with HVL function, migration time obtained as a parameter of this function is marked by the vertical line; BGE: 50 mM tris, 50 mM tricine, 0.1 mM DM-β-CD and 0.4 mM β-CD (0.5 mM of dual selector mixture composed of DM-β-CD and β-CD, molar fraction of DM-β-CD being 0.2); sample contained 0.2 mM flurbiprofen and 0.02% (v/v) nitromethane; for other experimental conditions see Section 2.3.

electromigration dispersion nor the selector consumption occurs. Furthermore, as all the selectors used are neutral compounds and do not interact in a significant way with the buffer constituents (buffer pH remained unchanged after addition of the CD, see also [48]), all the corresponding BGEs had the same ionic strength regardless of the selector or the mixture concentration. Consequently complexation constants obtained in this study are apparent (non-thermodynamic) equilibrium constants, valid only for the ionic strength of 26 mM (see Section 2.3), and the same applies to the electrophoretic mobilities. The constant ionic strength over all single and dual systems also ensures that the apparent parameters measured in the single systems can be used to predict the apparent overall parameters in the dual systems. Further, according to our best knowledge, viscosity changes do not significantly affect the determined complexation parameters as far as the concentration of the CD does not exceed approximately 10 mM. Finally, at least 80% of the migration path (due to physical limitation of the instrumentation) was efficiently thermostated and electrical current did not exceed 8 μA in the 50 μm i.d. capillary so that no significant Joule heating is expected.

DM-β-CD and Malt-β-CD were bought as single isomers. Although isomeric purity is always an issue when dealing with CD derivatives, the actual purity of the "single" derivative does not matter since if it were a mixture of derivatives, the mixture could yet again be treated as a single derivative with the overall complexation constant and mobility of complex. Such overall parameters can once more appear at the right-hand side of Eqs. (5) and (6) without compromising their validity. The obtained complexation parameters for single systems β-CD, DM-β-CD and Malt-β-CD and the two analytes ibuprofen and flurbiprofen are given in Table 1. These parameters, when substituted into Eqs. (5) and (6), serve for calculation of overall parameters for possible mixtures of these selectors. As mentioned above, two dual-selector systems consisting of DM-β-CD and β-CD and of DM-β-CD and Malt-β-CD were examined. Notice that the overall parameters do not depend on the chosen pair of selectors only, but also on their particular ratio. Therefore, several mixtures differing in molar ratio of the selectors were examined per each model dual-selector system. Simultaneously, the same overall parameters were determined experimentally treating each individual mixture of a particular

Table 1
Complexation parameters of single systems: apparent complexation constants (K_C) and effective mobilities of complexes ($u \equiv u_C$). Bottom: effective mobilities of free analytes ($u \equiv u_{A,f}$). Tris–tricine buffer, pH 8.2, ionic strength 26 mM.

Selector	Analyte	K_C [M^{-1}]	u [$m^2\ s^{-1}\ V^{-1}$]
β-CD	Ibuprofen	7074 ± 105	−8.63 ± 0.02
β-CD	Flurbiprofen	5093 ± 87	−8.71 ± 0.03
DM-β-CD	Ibuprofen	5334 ± 208	−7.37 ± 0.07
DM-β-CD	Flurbiprofen	7040 ± 333	−7.47 ± 0.08
Malt-β-CD	Ibuprofen	5480 ± 61	−7.41 ± 0.03
Malt-β-CD	Flurbiprofen	3912 ± 75	−7.44 ± 0.05
–	Ibuprofen	–	−19.60 ± 0.04
–	Flurbiprofen	–	−19.71 ± 0.05

molar ratio, χ_i, as virtually one selector. The calculated and measured data are given in Table 2.

Generally, the predicted values of the overall parameters are proven to be in a good accord with the measured ones. Difference between calculated and measured overall complexation constants does not exceed 10% and varies around 5%. In case of overall complex mobilities, the difference is even below 3% and varies around 1%. Based on our long-term experience, we can conclude that such relative errors are well comparable to what one would expect to be an intermediate precision of the ACE method. Additionally, using Eq. (1) for either single systems or dual systems yields virtually the same errors of estimate indicating that the equation works for mixtures of selectors just as well as it originally does for single-selector systems. This, consequently, further supports the idea that the mixture behaves like a single selector with the corresponding overall parameters.

3.2. Selectivity in dual systems

When an analyte interacts with a mixture of only two selectors, their molar fractions in the mixture, χ_1 and χ_2, must satisfy $\chi_1 = 1 - \chi_2$. Thus the multi-selector model (4) can be rewritten in terms of χ_1 (or equivalently χ_2) and c_{tot}. Although this procedure leads to a two-parametric model similar to Eq. (3), a transformation from {[S1], [S2]} to {c_{tot}, χ_1} brings several advantages, which we shall demonstrate in this section.

One of the advantages is that both [S1] and [S2] can, in principle, go to infinity and it is nearly impossible to see what would happen at their various combinations. Conversely, the multi-selector model shows that it is in fact their molar ratio (and consequently χ_1) that matters. When constant, the system follows the familiar pattern of u_{eff} vs. c_{tot} dependency. The molar fraction, χ_1, can only attain values between zero and one and thus the pattern can easily be inspected within these constraints. For instance, electromigration order (EMO) is one example of practically relevant characteristics studied in the literature [4].

Whether an interaction of two analytes with a particular selector leads to EMO reversal can be answered by solving the expression of $u_{1,eff} = u_{2,eff}$. This condition leads to a quadratic equation resulting in selector concentration(s) at which (if any) the EMO reversal occurs. The solution (and its existence) depends on the corresponding mobilities and complexation constants. In dual systems, the entire range of all possible overall mobilities of complex and complexation constants is obtained via Eqs. (5) and (6) (with $0 \le \chi_1 \le 1$ and $\chi_2 = 1 - \chi_1$) and thus the EMO reversal condition can be examined with respect to the mixture composition, χ_1. Such an examination is depicted in Fig. 2 where the total concentration at which the EMO reversal should occur is plotted for each of the two dual-selector systems against their respective composition. This examination indicates that the EMO of the two model analytes can be remarkably tuned when DM-β-CD is mixed up with β-CD, while it mostly remains the same when DM-β-CD is combined with Malt-β-CD. Similar approach can be adopted for other characteristics such as, e.g., optimal selector concentration in terms of maximal effective mobility difference, selectivity (mobility ratio) or resolution.

Another advantage is the fact that the dual-selector model results as a special case of a more general multi-selector model, rather than an extension of a specific single-selector model. This gives it a possibility to view the mechanism of separation in a more general context, similarly as we already demonstrated for multi-selector systems elsewhere [41].

Detailed mathematical analysis of the model is provided in supplementary information to this paper. The equations lead to an expectable conclusion that no mixture can form a hypothetic selector with its overall complexation constant and overall mobility of the complex outside of the range of the particular values of K_C and u_C of the two individual selectors in the mixture. The same, yet not so straightforwardly apparent consequence applies to the effective mobilities. Namely, the effective mobility of an analyte in a dual-selector system is always kept within the range of those obtained in one or the other selector at an equivalent selector concentration. Equivalently, it can be stated that the u_{eff} vs. c_{tot} dependence curve is always bounded by the individual curves valid for the two single selectors.

Fig. 3 depicts K_C^{over} and u_C^{over} vs. $\chi_{DM\text{-}\beta\text{-}CD}$ dependences for our two dual-selector systems and analytes. DM-β-CD/β-CD system has the same values of overall complexation constant for both analytes at 54% of DM-β-CD thus resulting in the "pure electrophoretic separation mechanism" (cf. [41]) under this composition. The same

Table 2
Overall parameters of complexation of ibuprofen and flurbiprofen with dual selector systems calculated according to Eqs. (5) and (6) and measured directly by ACE (see text for details); χ_{DM} is the molar ration of DM-β-CD in a particular dual system.

Dual system	χ_{DM}	Analyte	K_C^{over} calculated [M^{-1}]	K_C^{over} measured [M^{-1}]	Difference	u_C^{over} calculated [$m^2\ s^{-1}\ V^{-1}$]	u_C^{over} measured [$m^2\ s^{-1}\ V^{-1}$]	Difference
DM-β-CD + β-CD	0.2	Ibuprofen	6726	6802 ± 215	+1%	−8.43	−8.43 ± 0.05	0.0%
	0.2	Flurbiprofen	5482	5325 ± 121	−3%	−8.39	−8.39 ± 0.04	0.0%
	0.4	Ibuprofen	6378	6882 ± 173	+7%	−8.21	−8.30 ± 0.04	1.1%
	0.4	Flurbiprofen	5872	6277 ± 161	+6%	−8.11	−8.23 ± 0.04	1.4%
	0.7	Ibuprofen	5856	6057 ± 228	+3%	−7.83	−8.00 ± 0.07	2.2%
	0.7	Flurbiprofen	6456	6905 ± 217	+7%	−7.76	−7.99 ± 0.06	2.8%
	0.85	Ibuprofen	5595	5535 ± 153	−1%	−7.61	−7.68 ± 0.05	0.9%
	0.85	Flurbiprofen	6748	6713 ± 217	−1%	−7.61	−7.70 ± 0.06	1.2%
DM-β-CD + Malt-β-CD	0.2	Ibuprofen	5451	5034 ± 47	−8%	−7.40	−7.37 ± 0.02	−0.4%
	0.2	Flurbiprofen	4538	4246 ± 62	−7%	−7.45	−7.49 ± 0.03	0.5%
	0.5	Ibuprofen	5407	5247 ± 107	−3%	−7.39	−7.40 ± 0.05	0.2%
	0.5	Flurbiprofen	5476	5342 ± 52	−3%	−7.46	−7.49 ± 0.02	0.4%
	0.8	Ibuprofen	5363	5179 ± 49	−4%	−7.38	−7.44 ± 0.02	0.8%
	0.8	Flurbiprofen	6415	6193 ± 68	−4%	−7.46	−7.52 ± 0.02	0.8%

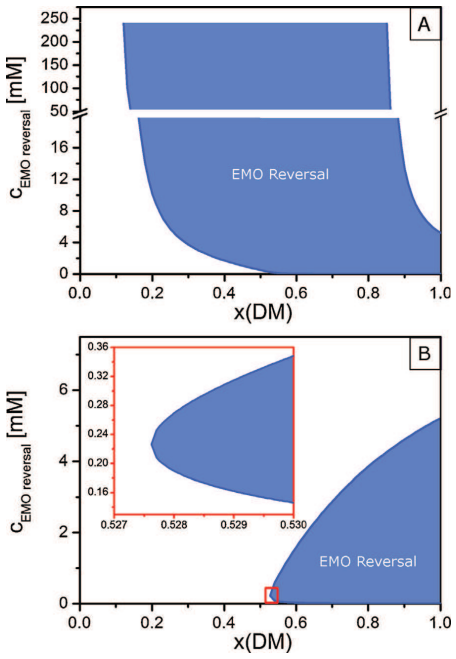

Fig. 2. EMO reversal concentration (y-axis) at various mixture compositions (x-axis). (A) Dual systems composed of DM-β-CD and β-CD; (B) dual systems composed of DM-β-CD and Malt-β-CD; calculation based on Table 1. (A) y-axis scale-changing break is present at $y = 20$ mM; (B) a zoomed area is inserted focusing on x-values between 0.527 and 0.530.

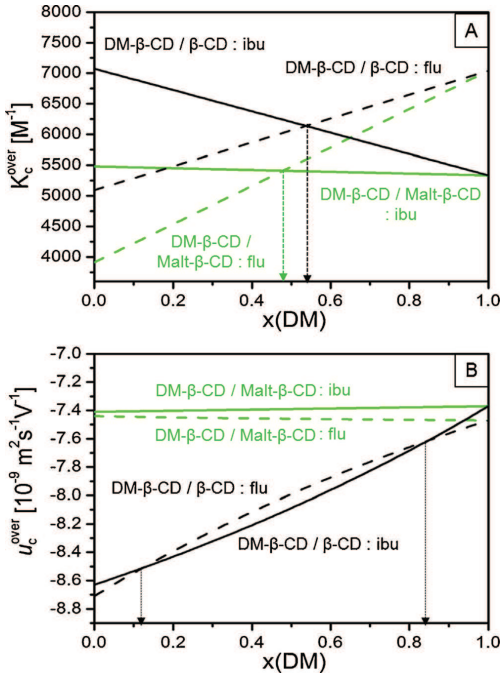

Fig. 3. Overall parameters of complexation of ibuprofen (solid) and flurbiprofen (dashed) with dual-selector systems DM-β-CD/β-CD (black) and DM-β-CD/Malt-β-CD (green) depending on mixture composition (x(DM), molar fraction χ_{DM} of DM-β-CD in the mixture); calculation based on Table 1. (A) Overall complexation constants; mixture compositions at which overall complexation constants of the two analytes equal each other indicated with arrows. (B) Overall mobilities; mixture compositions at which overall mobilities of complexes of the two analytes equal each other indicated with arrows.

applies to the second system of DM-β-CD/Malt-β-CD at 46% of DM-β-CD. To the contrary, the "pure chromatographic separation mechanism" ([41]) controls the separation at 13% and at 85% of DM-β-CD in the first dual-selector system, where both the overall mobilities of the complex become the same, while it never happens in the second dual-selector system. Notice however that the equality/non-equality of the overall complex mobilities is not a result of different complex sizes or effective charges but, instead, is a consequence of the mixed chromatographic-electrophoretic mechanisms as also discussed in [41].

The most illustrative – from the practical point of view – is the advantage of treating the individual mixtures as a single selector and utilizing the up-to-now well developed concepts for single-selector systems. For example, selectivity (i.e. the ratio of effective mobilities of the analytes being separated) is regarded as an objective measure of optimal separation by many authors [10,15,17,18,25–27]. Therefore, we examined dependences of selectivity on total concentration of the mixtures. Effective mobilities of the analytes in the mixtures were both measured and predicted according to Eq. (4) using the calculated overall complexation parameters. Predicted or actual selectivity of the separation was then obtained as a ratio of the predicted or measured effective mobilities. Fig. 4 shows comparison of these theoretical dependences (solid lines) with experimentally measured selectivities (points). Selectivity in single systems is also plotted (dot lines) using complexation parameters given in Table 1.

It is worth noting that the selectivity of the separation in the mixture of the selectors does not necessarily lie between selectivities provided by the single selectors (see namely Fig. 4A, higher c_{tot} values). This result might seem rather counterintuitive as we have already concluded that the effective mobilities of analytes in any dual system must always lie between those in the individual single systems. However, the selectivity – as a ratio of these effective mobilities – is a nonlinear parameter that does not obey this simple limitation. This is indeed the very reason why mixing selectors in dual-systems could ever have improved the separation.

A good agreement between the predicted and observed selectivity curves is apparent. Although some experimental points do not always lie exactly at the expected curves, the prediction is actually precise enough to get the true picture of the selectivity patterns even in these systems of very small nuances in selectivity (notice selectivity changes in order of less than 0.01 units only). All the practically important characteristics of the selectivity profiles, such as an existence and quantity of the optimal mixture concentration (in terms of maximal selectivity), the electromigration order of the analytes as well as the trends in selectivity as mixture composition and its overall concentration change, are correctly reflected. The EMO reversal is also observed in accordance with the discussion above.

This all makes the herein introduced strategy promising for identifying benefits that might be gained by mixing two particular selectors along with quantitative estimations of the optimal molar ratio of selectors and the total mixture concentration. The same kind of reasoning could be also made using mobility difference or relative mobility difference instead of selectivity. Qualitatively the

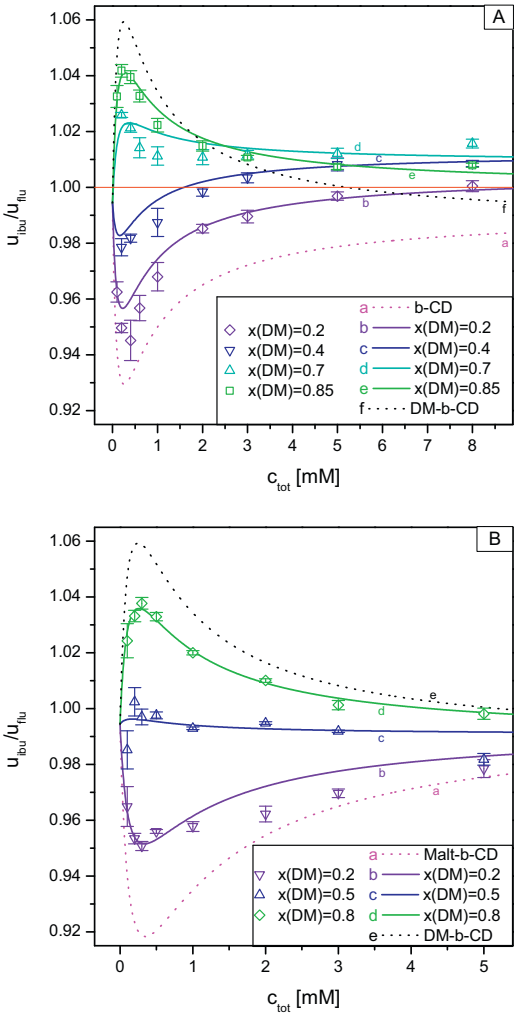

Fig. 4. Dependences of selectivity on total concentration of dual selector mixture (separating ibuprofen and flurbiprofen). (A) Dual systems composed of DM-β-CD and β-CD; (B) dual systems composed of DM-β-CD and Malt-β-CD; solid lines: selectivity of dual selector mixtures predicted based on calculated overall complexation parameters (Table 2); dot lines: selectivity of single selectors (calculated using their complexation parameters, Table 1); points: experimental selectivities obtained as ratio of effective mobilities of ibuprofen and flurbiprofen; x(DM), molar fraction χ_{DM} of DM-β-CD in a particular dual selector mixture; description of individual lines an symbols given in the figure.

figure would be just the same, only extremes of the dependences would be slightly shifted towards lower concentrations in our case.

4. Concluding remarks

Determination of the complexation constants and the mobilities of complexes by the ACE method typically requires measurements at five to nine selector concentration levels per selector and analyte. This study shows that such a limited number of rather easy experiments is sufficient to completely characterize any particular dual-selector system with its virtually infinite number of possible mixture compositions and concentrations.

Having these parameters measured, the model is ready for the straightforward graphical and/or mathematical analysis of the basic separation characteristics of the dual-selector system. Optimal mixture composition and total concentration can be advantageously found in terms of maximal selectivity or (relative) mobility difference. Additionally, a potency of the model to find optimal separation conditions at the desired electromigration order of the analytes (or to show that none such a condition exists) in a given dual-selector system was demonstrated. Finally, the model describes general mechanism that controls separation in various mixtures that form dual-selector systems. This can lead to better understanding of which classes of selectors are principally promising to combine in order to achieve better separation in analytical practice.

The results are encouraging in using a systematic approach to method optimization in dual-selector systems as outlined in this study, which is in contrast to still prevailing trial-and-error or semi-quantitative approaches.

Conflict of interest

All authors declare no conflicts of interest.

Acknowledgements

The authors acknowledge the financial support of this work from the Grant Agency of the Charles University, grant number 669412, the Grant Agency of the Czech Republic, grant number P206/12/P630, long-term research plan of the Ministry of Education of the Czech Republic, MSM 0021620857 and financial support of the Charles University UNCE204025/2012.

Appendix A. Supplementary data

Supplementary data associated with this article can be found, in the online version, at http://dx.doi.org/10.1016/j.chroma.2014.01.006.

References

[1] S. Terabe, K. Otsuka, H. Nishi, J. Chromatogr. A 666 (1994) 295.
[2] T. de Boer, R.A. de Zeeuw, G.J. de Jong, K. Ensing, Electrophoresis 21 (2000) 3220.
[3] G.K.E. Scriba, J. Pharm. Biomed. Anal. 27 (2001) 373.
[4] B. Chankvetadze, Electrophoresis 23 (2002) 4022.
[5] P. Jáč, G.K.E. Scriba, J. Sep. Sci. 36 (2013) 52.
[6] S.A.C. Wren, R.C. Rowe, J. Chromatogr. 603 (1992) 235.
[7] P. Britz-McKibbin, D.D.Y. Chen, J. Chromatogr. A 781 (1997) 23.
[8] M. Rogan, K.D. Altria, D.M. Goodall, Electrophoresis 15 (1994) 808.
[9] S.A.C. Wren, Electrophoresis 16 (1995) 2127.
[10] Y.Y. Rawjee, D.U. Staerk, G. Vigh, J. Chromatogr. 635 (1993) 291.
[11] B.A. Williams, G. Vigh, J. Chromatogr. A 777 (1997) 295.
[12] T.H. Seals, C. Sheng, J.M. Davis, Electrophoresis 22 (2001) 1957.
[13] W. Yang, A. Yu, X. Yu, H. Chen, Electrophoresis 22 (2001) 2025.
[14] N. Mofaddel, H. Krajian, D. Villemin, P.L. Desbene, Talanta 78 (2009) 631.
[15] M. Hammitzsch-Wiedemann, G.K.E. Scriba, Anal. Chem. 81 (2009) 8765.
[16] S.G. Penn, D.M. Goodall, J.S. Loran, J. Chromatogr. 636 (1993) 149.
[17] F. Lelievre, P. Gareil, A. Jardy, Anal. Chem. 69 (1997) 385.
[18] A.M. Rizzi, L. Kremser, Electrophoresis 20 (1999) 2715.
[19] I.S. Lurie, R.F.X. Klein, T.A. Dal Cason, M.J. LeBelle, R. Brenneisen, R.E. Weinberger, Anal. Chem. 66 (1994) 4019.
[20] F. Lelievre, P. Gareil, Y. Bahaddi, H. Galons, Anal. Chem. 69 (1997) 393.
[21] S. Surapaneni, K. Ruterbories, T. Lindstrom, J. Chromatogr. A 761 (1997) 249.
[22] M. Fillet, B. Chankvetadze, J. Crommen, G. Blaschke, Electrophoresis 20 (1999) 2691.
[23] X. Zhu, Y. Ding, B. Lin, A. Jakob, B. Koppenhoefer, J. Chromatogr. A 888 (2000) 241.
[24] J.P. Schaeper, S.B. Fox, M.J. Sepaniak, J. Chromatogr. Sci. 39 (2001) 411.
[25] A.M. Abushoffa, M. Fillet, P. Hubert, J. Crommen, J. Chromatogr. A 948 (2002) 321.

[26] A.M. Abushoffa, M. Fillet, A. Servais, P. Hubert, J. Crommen, Electrophoresis 24 (2003) 343.
[27] A.M. Abushoffa, M. Fillet, R.D. Marini, P. Hubert, J. Crommen, J. Sep. Sci. 26 (2003) 536.
[28] N. Matthijs, S. Van Hemelryck, M. Maftouh, D. Luc Massart, Y. Vander Heyden, Anal. Chim. Acta 525 (2004) 247.
[29] T. Nhujak, C. Sastravaha, C. Palanuvej, A. Petsom, Electrophoresis 26 (2005) 3814.
[30] C. Lin, S. Lin, H. Cheng, I. Fang, C. Kuo, Y. Liu, Electrophoresis 26 (2005) 4187.
[31] M.J. Sepaniak, C.L. Copper, K.W. Whitaker, V.C. Anigbogu, Anal. Chem. 67 (1995) 2037.
[32] O.H.J. Szolar, R.S. Brown, J.H.T. Luong, Anal. Chem. 67 (1995) 3004.
[33] K.W. Whitaker, C.L. Copper, M.J. Sepaniak, J. Microcolumn Sep. 8 (1996) 461.
[34] X. Peng, M.T. Bowser, P. Britz-McKibbin, G.M. Bebault, J.R. Morris, D.D.Y. Chen, Electrophoresis 18 (1997) 706.
[35] A.R. Kranack, M.T. Bowser, P. Britz-McKibbin, D.D.Y. Chen, Electrophoresis 19 (1998) 388.
[36] I.S. Lurie, J. Chromatogr. A 792 (1997) 297.
[37] B. Chankvetadze, TrAC, Trends Anal. Chem. 18 (1999) 485.
[38] M. Fillet, P. Hubert, J. Crommen, J. Chromatogr. A 875 (2000) 123.
[39] S. Terabe, K. Otsuka, T. Ando, Anal. Chem. 57 (1985) 834.
[40] P. Dubský, J. Svobodová, B. Gaš, J. Chromatogr., B: Anal. Technol. Biomed. Life Sci. 875 (2008) 30.
[41] P. Dubský, J. Svobodová, E. Tesařová, B. Gaš, Electrophoresis 31 (2010) 1435.
[42] M. Jaroš, V. Hruška, M. Štědrý, I. Zusková, B. Gaš, Electrophoresis 25 (2004) 3080.
[43] P.C. Haarhoff, H.J. van der Linde, Anal. Chem. 38 (1966) 573.
[44] G.L. Erny, E.T. Bergstroem, D.M. Goodall, S. Grieb, Anal. Chem. 73 (2001) 4862.
[45] K. Ušelová-Včeláková, I. Zusková, B. Gaš, Electrophoresis 28 (2007) 2145.
[46] C.X. Jiang, D.W. Armstrong, Electrophoresis 31 (2010) 17.
[47] M. Beneš, I. Zusková, J. Svobodová, B. Gaš, Electrophoresis 33 (2012) 1032.
[48] M. Riesová, J. Svobodová, Z. Tošner, M. Beneš, E. Tesařová, B. Gaš, Anal. Chem. 85 (2013) 8518.

4.2 Generalizovaný model elektromigrace v interagujících systémech ($\mathbf{M_A M_S}$ model)

V minulosti se mnoho autorů zabývalo popisem systémů, ve kterých analyt interaguje s více než jedním selektorem (jak je shrnuto v *Publikaci I*). Nicméně žádný z těchto modelů (včetně M-souhrnného modelu probíraného v předešlé kapitole) nezahrnoval další možné rovnováhy, kterých se analyt může účastnit vedle komplexace – především rovnováhy acidobazické. Na druhé straně elektromigrace analytů, které jsou slabými jednosytnými kyselinami nebo bázemi a interagují s jedním selektorem, byla zevrubně popsána například skupinou profesora Vigha [30-33].

V *Publikaci III* je představen generalizovaný model elektromigrace v interagujících systémech se stechiometrií interakce 1:1 (analyt : selektor). Tento model vychází z M-souhrnného modelu a popisuje efektivní mobilitu analytu, který je přítomný v libovolném počtu L volných (nekomplexovaných) forem, mezi kterými se ustavuje rychlá rovnováha. Tyto rovnováhy nejsou pro potřeby modelu specifikovány, ale z praktického hlediska jsou významné zejména rovnováhy acidobazické a jednotlivými volnými formami analytu se pak míní jednotlivé disociační stavy slabé kyseliny, báze nebo amfolytu. Pro každou volnou formu analytu lze definovat molární zlomek χ_{Ai} jako poměr její molární koncentrace ku celkové molární koncentraci volného analytu. Každá z těchto volných forem analytu interaguje s každým z N přítomných selektorů. Všechny vznikající komplexy mají stechiometrii 1:1 a interakci i-té volné formy analytu s j-tým selektorem charakterizuje komplexační konstanta K'_{AiSj}:

$$\mathrm{A}_i + \mathrm{S}_j \rightleftharpoons \mathrm{A}_i\mathrm{S}_j \qquad K'_{AiSj} = \frac{[\mathrm{A}_i\mathrm{S}_j]}{[\mathrm{A}_i][\mathrm{S}_j]} \tag{24}$$

Pro každý selektor lze definovat molární zlomek χ_{Sj} jako poměr koncentrace tohoto selektoru ku celkové koncentraci všech přítomných selektorů c_{tot} (stejně jako v M-souhrnném modelu). Komplexace sice ovlivňuje celkovou koncentraci volného analytu, ale už ne jeho distribuci mezi jednotlivé volné formy, proto hodnoty χ_{Ai} nezávisí ani na koncentracích přidaných

selektorů, ani na hodnotách komplexačních konstant. Efektivní mobilitu analytu v takovém systému popisuje rovnice:

$$\mu_{A,eff} = \frac{\sum_{i=1}^{L} \chi_{Ai}\mu_{Ai} + \sum_{i=1}^{L}\left(\chi_{Ai} \cdot \sum_{j=1}^{N} K'_{AiSj}\mu_{AiSj}\chi_{Sj}\right) \cdot c_{tot}}{1 + \sum_{i=1}^{L}\left(\chi_{Ai} \cdot \sum_{j=1}^{N} K'_{AiSj}\chi_{Sj}\right) \cdot c_{tot}} \tag{25}$$

kde μ_{Ai} je mobilita *i*-té formy volného analytu a μ_{AiSj} mobilita komplexu mezi *i*-tou formou volného analytu a *j*-tým selektorem.

Pokud je složení směsi selektorů konstantní (nemění se vzájemné poměry koncentrací jednotlivých selektorů, $\chi_{Sj} = konst.$ pro všechna *j*) a jsou konstantní i podmínky, na kterých závisí distribuce volného analytu mezi jeho jednotlivé formy ($\chi_{Ai} = konst.$ pro všechna *i*; v případě, že mezi jednotlivými volnými formami analytu se ustavují acidobazické rovnováhy, je takovou podmínkou konstantní pH základního elektrolytu – přesněji koncentrace oxoniových iontů [H_3O^+]), pak je jedinou nezávisle proměnnou v rovnici (25) celková koncentrace selektorů a rovnice přechází na tvar:

$$\mu_{A,eff} = \frac{\mu_A^{M_A M_S} + K_{AS}^{\prime M_A M_S}\mu_{AS}^{M_A M_S} c_{tot}}{1 + K_{AS}^{\prime M_A M_S} c_{tot}} \tag{26}$$

kde

$$\mu_A^{M_A M_S} = \sum_{i=1}^{L} \chi_{Ai}\mu_{Ai} \tag{27}$$

$$K_{AS}^{\prime M_A M_S} = \sum_{i=1}^{L} \chi_{Ai} \sum_{j=1}^{N} K'_{AiSj}\chi_{Sj} \tag{28}$$

$$\mu_{AS}^{M_A M_S} = \frac{\sum_{i=1}^{L} \chi_{Ai} \sum_{j=1}^{N} K'_{AiSj}\mu_{AiSj}\chi_{Sj}}{K_{AS}^{\prime M_A M_S}} \tag{29}$$

Rovnice (26) je (stejně jako rovnice (20) v M-souhrnném modelu) formálně shodná s původním vztahem (4) pro mobilitu analytu, který je přítomný pouze v jedné volné formě a interaguje pouze s jedním selektorem. Z toho vyplývá, že v tomto případě (konstantní χ_{Ai} a χ_{Sj}) lze libovolný M_AM_S systém (splňující podmínky (i)-(v) uvedené v kapitole 1.1) pokládat za S_AS_S systém: závislost efektivní mobility analytu na celkové koncentraci selektoru má známý hyperbolický tvar. To ukazuje jednak, že pro hledání optimální celkové koncentrace směsi je možné využít optimalizační postupy odvozené pro S_AS_S systémy (s výjimkou předpokladu shodné mobility komplexů při separaci dvojice enantiomerů), jednak univerzální použitelnost hyperbolické závislosti (4) pro elektroforetické systémy se stechiometrií komplexace 1:1.

Stojí za zmínku, že M_AM_S model zůstává aplikovatelný i v případě, kdy acidobazické disociaci podléhá selektor. V takovém případě se definují molární frakce χ_{Sj} pro jednotlivé formy selektoru a je třeba zajistit, aby tyto nezávisely na celkové koncentraci selektoru c_{tot}. Toho lze dosáhnout dostatečnou pufrační kapacitou BGE nebo změnou koncentrací jeho nekomplexujících složek, aby se kompenzovala změna pH a iontové síly způsobená přídavkem selektoru (obdobný způsob se používá k zajištění konstantní iontové síly v systémech s plně nabitými selektory [12]).

Řadu dříve publikovaných elektromigračních modelů popisujících systémy se stechiometrií komplexace 1:1 lze chápat jako speciální případy generalizovaného M_AM_S modelu (25) nebo jeho souhrnné formy (26) – (29):

(i) Pokud je přítomna pouze jedna volná forma analytu a ta interaguje pouze s jedním selektorem ($L = 1$; $N = 1$), přechází rovnice (25) na původní vztah Wrena a Rowa (4).

(ii) V případě že analyt je slabá jednosytná kyselina nebo báze, která interaguje s jedním selektorem ($L = 2$; $N = 1$), a závislost molárních frakcí obou volných forem analytu na $[H_3O^+]$ se vyjádří explicitně, přechází rovnice (25) na vztah publikovaný skupinou profesora Vigha pro slabé kyseliny (5), respektive pro slabé báze [31].

(iii) Pro systém uvedený v bodě (ii) přechází souhrnná forma M_AM_S modelu (26) – (29) na pH-souhrnný model Lelièvra *et al.* (7) – (10). Obdobně pro dvojsytnou kyselinu ($L = 3$; $N = 1$) na model Moffadela *et al.* [37].

(iv) Pokud je přítomna pouze jedna volná forma analytu a ta interaguje s více selektory ($L = 1$; $N > 1$), přechází model (26) – (29) na M-souhrnný model (18) – (20), který je pro případ dvou selektorů podrobněji rozebrán v předešlé kapitole.

V M_AM_S systémech se ustavuje řada navzájem propojených rovnovah, které mají vliv na výslednou efektivní mobilitu analytu. Na Obrázku 3 jsou tyto rovnováhy znázorněny pro nejjednodušší M_AM_S systém: slabou jednosytnou kyselinu interagující se dvěma selektory. Výhodou M_AM_S modelu je, že umožňuje nahlížet na M_AM_S systémy z různých perspektiv. Jak už bylo uvedeno, lze na tento komplikovaný systém nahlížet jako na systém, kde jediná forma volného analytu interaguje s jediným selektorem, a popsat jej pomocí S_AS_S modelu. Obdobně je také možné popsat (a optimalizovat) tento systém pomocí M_AS_S modelů například Lelièvra *et al.* [34] nebo Vigha *et al.* [30-33] (pH-explicitní přístup), nebo pomocí S_AM_S modelů například duálního modelu Lurie *et al.* [44] nebo M-souhrnného modelu (18) – (20) (M-explicitní přístup).

Při pH-explicitním přístupu je složení směsi selektorů konstantní ($\chi_{Sj} = konst.$ pro všechna *j*). Výsledky sumací podle jednotlivých selektorů jsou tedy také konstantní a rovnici (25) lze zapsat:

$$\mu_{A,eff} = \frac{\sum_{i=1}^{L} \chi_{Ai}\mu_{Ai} + \sum_{i=1}^{L} \chi_{Ai}K'^{M}_{AiS}\mu^{M}_{AiS} \cdot c_{tot}}{1 + \sum_{i=1}^{L} \chi_{Ai}K'^{M}_{AiS} \cdot c_{tot}} \tag{30}$$

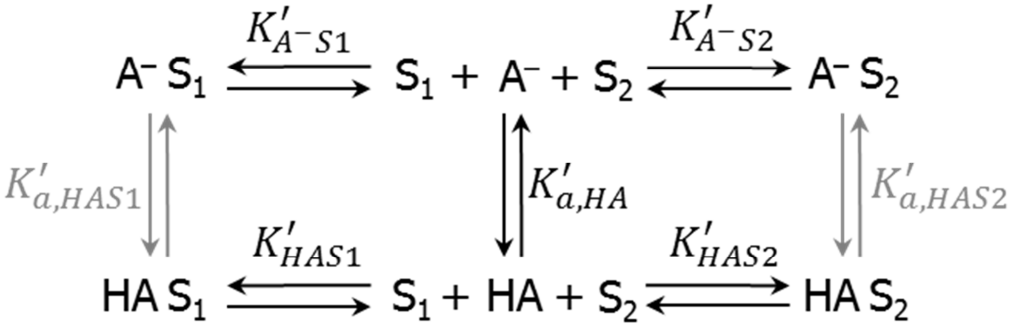

Obrázek 3: Nejjednodušší M_AM_S systém – slabá kyselina (disociovaná, A^-, a protonovaná, HA, forma) interaguje se dvěma selektory (S_1 a S_2); K'_{A^-S1}, K'_{A^-S2}, K'_{HAS1} a K'_{HAS2} jsou komplexační konstanty disociované formy s prvním a druhým selektorem a protonované formy s prvním a druhým selektorem, $K'_{a,HA}$ je acidobazická disociační konstanta volného analytu, $K'_{a,HAS1}$ a $K'_{a,HAS2}$ jsou acidobazické disociační konstanty obou vzniklých komplexů (jejich hodnota je dána rovnicí (11) a není tedy nutné je experimentálně stanovit); pro větší přehlednost nejsou ve schématu uvedeny oxoniové kationty.

kde

$$K'^{M}_{AiS} = \sum_{j=1}^{N} K'_{AiSj}\chi_{Sj} \tag{31}$$

$$\mu^{M}_{AiS} = \frac{\sum_{j=1}^{N} K'_{AiSj}\mu_{AiSj}\chi_{Sj}}{K'^{M}_{AiS}} \tag{32}$$

Komplexační konstanta K'^{M}_{AiS} a mobilita komplexu μ^{M}_{AiS} jsou M-souhrnné komplexační parametry charakterizující interakci *i*-té formy volného analytu s danou směsí selektorů, se kterou tedy lze zacházet jako se selektorem jediným. Tyto parametry lze například stanovit experimentálně při takovém pH základního elektrolytu, kdy je analyt přítomen pouze v této formě. Dále lze v rovnici (30) explicitně vyjádřit závislost molárních frakcí jednotlivých volných forem analytu na $[H_3O^+]$ a optimalizovat separaci vzhledem k pH a celkové koncentraci směsi selektorů, přičemž se systémem se zachází, jako by v něm byl přítomen pouze jeden selektor. Pro nejjednodušší M_AM_S systém je tento pohled schematicky znázorněn na Obrázku 4.

Při M-explicitním přístupu jsou podmínky řídící distribuci volného analytu mezi jeho jednotlivé formy udržovány konstantní ($\chi_{Ai} = konst.$ pro všechna *i*). Konkrétně pro analyt podléhající acidobazické disociaci musí být konstantní pH základního elektrolytu. Po přeorganizování sumací v rovnici (25):

$$\mu_{A,eff} = \frac{\sum_{i=1}^{L} \chi_{Ai}\mu_{Ai} + \sum_{j=1}^{N}\left(\chi_{Sj} \cdot \sum_{i=1}^{L} \chi_{Ai}K'_{AiSj}\mu_{AiSj}\right) \cdot c_{tot}}{1 + \sum_{j=1}^{N}\left(\chi_{Sj} \cdot \sum_{i=1}^{L} \chi_{Ai}K'_{AiSj}\right) \cdot c_{tot}} \tag{33}$$

lze M_AM_S model zapsat jako:

$$\mu_{A,eff} = \frac{\mu_A^{pH} + \sum_{j=1}^{N} \chi_{Sj}K'^{pH}_{ASj}\mu^{pH}_{ASj} \cdot c_{tot}}{1 + \sum_{j=1}^{N} \chi_{Sj}K'^{pH}_{ASj} \cdot c_{tot}} \tag{34}$$

kde

$$\mu_A^{pH} = \sum_{i=1}^{L} \chi_{Ai}\mu_{Ai} \tag{35}$$

$$K_{ASj}^{\prime pH} = \sum_{i=1}^{L} \chi_{Ai}K_{AiSj}^{\prime} \tag{36}$$

$$\mu_{ASj}^{pH} = \frac{\sum_{i=1}^{L} \chi_{Ai}K_{AiSj}^{\prime}\mu_{AiSj}}{K_{ASj}^{\prime pH}} \tag{37}$$

Komplexační konstanta $K_{ASj}^{\prime pH}$ a mobilita komplexu μ_{ASj}^{pH} pak charakterizují interakci (částečně disociovaného/protonovaného) analytu s *j*-tým selektorem. Ty lze stanovit experimentálně z měření v BGE, který obsahuje konkrétní selektor, a následně je použít jako vstupní parametry například M-souhrnného modelu popsaného v předešlé kapitole a optimalizovat separaci vzhledem ke složení a celkové koncentraci směsi selektorů, přičemž se systémem se zachází tak, jako kdyby v něm byla přítomna pouze jedna forma volného analytu. Schematicky je tento přístup znázorněn pro nejjednodušší M_AM_S systém na Obrázku 5.

Experimentálně byly jak pH-explicitní, tak M-explicitní přístup ověřeny v *Publikaci IV* na modelovém systému *R*-flurbiprofenu jako analytu (slabá jednosytná kyselina) a jednomocného kladně nabitého 6-monodeoxy-6-monoamino-β-cyclodextrinu (A-β-CD) spolu s nativním β-CD jako selektory.

pH-explicitní přístup: Pro dvě různá složení směsi byly experimentálně stanoveny $K_{AiS}^{\prime M}$ a μ_{AiS}^{M} disociované a nedisociované formy z měření při takovém pH BGE, kde je *R*-flurbiprofen téměř zcela disociován (pH 6,28) respektive téměř zcela protonován (pH 2,02). Na základě těchto parametrů byly předpovězeny efektivní mobility analytu v těchto směsích při pH 4,01 pomocí modelu Williamse a Vigha (5). Tento model byl původně odvozem pro částečně disociovaný analyt interagující pouze s jedním selektorem (L = 2, N = 1). Nicméně díky pH-explicitnímu přístupu M_AM_S modelu (Obrázek 4) jej lze aplikovat i pro tuto situaci, kdy částečně disociovaný analyt interaguje se směsí selektorů (L = 2, N = 2). Dobrá shoda předpovědi s mobilitami experimentálně změřenými (*Publikace IV*, Table 3A, Fig. 1) správnost tohoto přístupu potvrzuje.

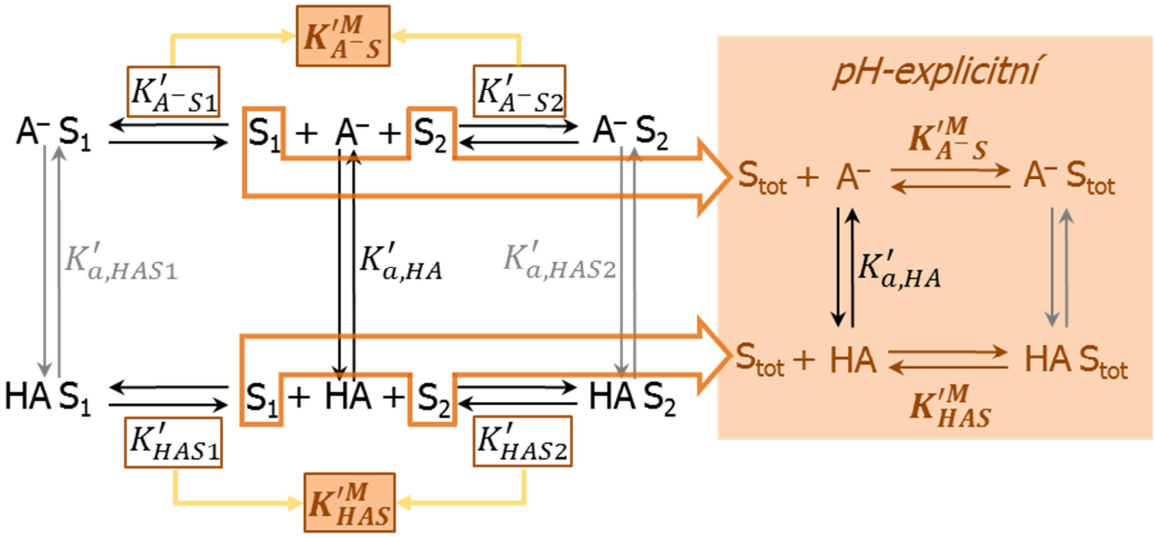

Obrázek 4: Nejjednodušší M_AM_S systém z pH-explicitní perspektivy – na systém se nahlíží, jako by obě volné formy analytu interagovaly pouze s jedním selektorem (S_{tot}), interakci charakterizují M-souhrnné komplexační konstanty $K'^{M}_{A^-S}$ a K'^{M}_{HAS} pro disociovanou a protonovanou formu analytu (význam dalších symbolů je uveden u Obrázku 3; pro větší přehlednost nejsou ve schématu uvedeny oxoniové kationty).

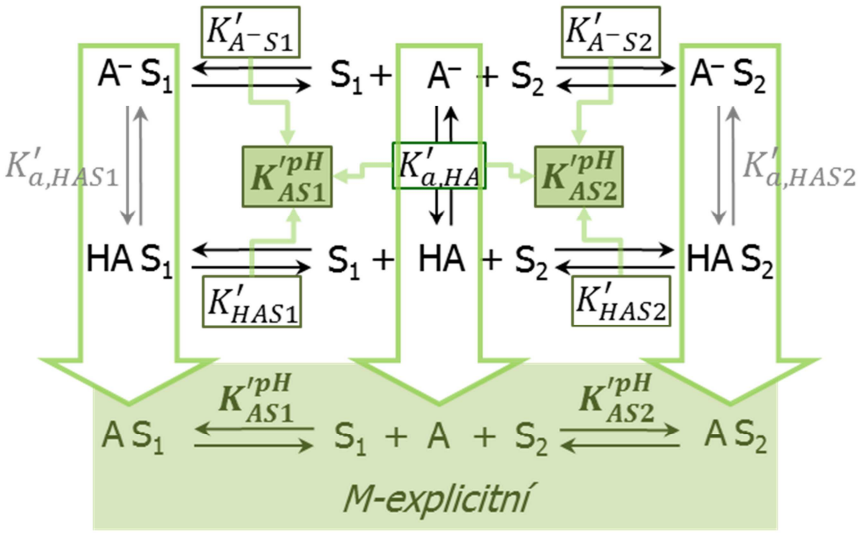

Obrázek 5: Nejjednodušší M_AM_S systém z M-explicitní perspektivy – na systém se nahlíží, jako by s oběma selektory interagovala jen jedna volná forma analytu, jejíž interakce s jednotlivými selektory charakterizují pH-souhrnné komplexační konstanty K'^{pH}_{AS1} a K'^{pH}_{AS2} (význam dalších symbolů je uveden u Obrázku 3; pro větší přehlednost nejsou ve schématu uvedeny oxoniové kationty).

M-explicitní přístup: Při pH 4,01, kdy je analyt pouze částečně disociován a tedy přítomen v obou svých formách, byly změřeny K'^{pH}_{ASj} a μ^{pH}_{ASj} pro oba selektory. Na základě těchto parametrů byly pomocí M-souhrnného modelu (20) – (23) předpovězeny efektivní mobility *R*-flurbiprofenu ve směsích těchto dvou selektorů o čtyřech různých složeních (čtyřech různých χ_{S1}) při tomto pH. Jejich shoda s mobilitami experimentálně stanovenými byla velmi dobrá (*Publikace IV*, Table 3B, Fig. 1). Podobně jako v předchozím případě se tak prokázalo, že model (20) původně platný pro interakci jediné formy analytu se směsí selektorů (L = 1, N > 1) může být díky M-explicitnímu přístupu M_AM_S modelu (Obrázek 5) využit i v případě, kdy se selektory interagují dvě volné formy analytu (L = 2, N = 2).

V *Publikaci IV* je dále ukázáno, že pokud je závislost efektivní mobility analytu na celkové koncentraci selektoru (při konstantním pH a případně složení směsi) prokládána hyperbolickou funkcí (26), pak kvalita proložení (vyjádřená parametrem R^2) se neliší bez ohledu na to, zda se jedná o S_AS_S, M_AS_S, S_AM_S nebo M_AM_S systém (*Publikace IV*, Table 2). To je zcela v souladu s M_AM_S modelem a potvrzuje výše zmíněnou univerzální aplikovatelnost tohoto vztahu na systémy se stechiometrií komplexace 1:1.

M-explicitní a pH-explicitní přístup lze chápat jako svým způsobem „ortogonální“, jak je schematicky naznačeno na vloženém obrázku (*Publikace IV*, Fig. 1). Ve skutečnosti byly tyto přístupy někdy mimoděk používány už v minulosti (například stanovování pH-souhrnných komplexačních parametrů se selektory, které byly ve skutečnosti směsmi selektorů [37]). Generalizovaný model elektromigrace v interagujících systémech se stechiometrií interakce 1:1 představený v *Publikacích III* a *IV* ale poprvé poskytuje teoretický základ pro zacházení s M_AM_S systémy. Model ukazuje, že provázané komplexační a acidobazické rovnováhy, jichž se analyt účastní, od sebe lze separovat a pracovat s nimi odděleně. Experimentátor může zvolit takový způsob optimalizace, který je nejvýhodnější pro konkrétní separaci, a tento model mu poskytuje informace o tom, za jakých podmínek lze kterou optimalizační strategii využít.

Publikace III

Generalized model of electromigration with 1:1 (analyte:selector) complexation stoichiometry: Part I. Theory

P. Dubský, **L. Müllerová**, Martin Dvořák, B. Gaš

Journal of Chromatography A 2015, *1384*, 142-146.

Journal of Chromatography A, 1384 (2015) 142–146

Contents lists available at ScienceDirect

Journal of Chromatography A

journal homepage: www.elsevier.com/locate/chroma

Generalized model of electromigration with 1:1 (analyte:selector) complexation stoichiometry: Part I. Theory

Pavel Dubský*, Ludmila Müllerová, Martin Dvořák, Bohuslav Gaš

Charles University in Prague, Faculty of Science, Department of Physical and Macromolecular Chemistry, Prague, Czech Republic

ARTICLE INFO

Article history:
Received 5 September 2014
Received in revised form 7 January 2015
Accepted 11 January 2015
Available online 19 January 2015

Keywords:
Dissociation
Dual selector system
Cyclodextrins
Enantioseparation
Mixture of selectors
Model of electromigration

ABSTRACT

The model of electromigration of a multivalent weak acidic/basic/amphoteric analyte that undergoes complexation with a mixture of selectors is introduced. The model provides an extension of the series of models starting with the single-selector model without dissociation by Wren and Rowe in 1992, continuing with the monovalent weak analyte/single-selector model by Rawjee, Williams and Vigh in 1993 and that by Lelièvre in 1994, and ending with the multi-selector overall model without dissociation developed by our group in 2008. The new multivalent analyte multi-selector model shows that the effective mobility of the analyte obeys the original Wren and Row's formula. The overall complexation constant, mobility of the free analyte and mobility of complex can be measured and used in a standard way. The mathematical expressions for the overall parameters are provided. We further demonstrate mathematically that the pH dependent parameters for weak analytes can be simply used as an input into the multi-selector overall model and, in reverse, the multi-selector overall parameters can serve as an input into the pH-dependent models for the weak analytes. These findings can greatly simplify the rationale method development in analytical electrophoresis, specifically enantioseparations.

1. Introduction

Selectors have the ability to separate structurally highly related analytes (including enantiomers) with similar mobilities or neutral compounds that would otherwise co-migrate in the (capillary zone) electrophoresis (CZE). For this ability, the interactions between the selectors and the analytes are intensively studied and several models of electromigration under the complexation have been introduced in the CZE theory. The most relevant seems the models assuming 1:1 (selector:analyte) complexation stoichiometry. Although the 1:1 stoichiometry is not guaranteed in general, it results from experimental studies that this is a preferred stoichiometry for many complexes, namely with cyclodextrins, the popular selectors in CZE [1,2].

Under these circumstances, the analyte–selector equilibrium is established as

$$\mathrm{A} + \mathrm{S} \rightleftharpoons \mathrm{AS} \qquad K'_{\mathrm{AS}} = \frac{[\mathrm{AS}]}{[\mathrm{A}][\mathrm{S}]} \tag{1}$$

where A and S represent the free analyte and the free selector in the solution, respectively, AS is the analyte–selector complex, K'_{AS} is the (ionic-strength apparent) complexation constant and the terms in the square brackets, $[\cdot]$, stay for the concentrations. The selector is supposed to be in a high excess over the analyte, so that the complexation does not consume a significant portion of its total concentration, c_{S}. Thus the approximation of

$$[\mathrm{S}] = c_{\mathrm{S}} \tag{2}$$

is generally applied. If an analyte is present in numerous forms among which equilibria much faster compared to the electrophoretic movement exist, its effective mobility becomes

$$\mu_{\mathrm{eff}} = \sum \alpha_i \mu_i \tag{3}$$

where α_i are the molar fractions of the individual forms of the analyte and μ_i are their respective electrophoretic mobilities. Using this relationship, the effective mobility of an analyte under complexation results as published by Wren and Rowe in 1992:

$$\mu_{\mathrm{eff}} = \frac{\mu_0 + \mu_{\mathrm{AS}} K'_{\mathrm{AS}} c_{\mathrm{S}}}{1 + K'_{\mathrm{AS}} c_{\mathrm{S}}} \tag{4}$$

where μ_0 is the electrophoretic mobility of the free analyte and μ_{AS} is the mobility of the analyte–selector complex. The relation (4) can be used to predict separation characteristics such as

* Corresponding author at: Charles University in Prague, Faculty of Science, Albertov 2030, CZ-128 40 Prague 2, Czech Republic. Tel.: +420 221 951 296.
E-mail address: dubsky@natur.cuni.cz (P. Dubský).

http://dx.doi.org/10.1016/j.chroma.2015.01.029
0021-9673/

the effective mobility difference, selectivity and resolution. This is advantageously utilized in analytical chemistry for the rationale method development and optimization [1–5].

The shortcoming of the model (4) is its limitation to the single analyte form interacting with the single selector (as we will further refer to as the S_AS_S system). In reality, the analytes are often weak acids or bases that undergo dissociation equilibria coupled with the complexation. Rawjee, Williams and Vigh partially overcome this limitation in 1993 by extending the model to monovalent weak acidic and basic analytes [6,7]. The theoretical work of this group finally resulted in the "charged resolving agent migration" (CHARM) model, which relates the physical characteristics of the monovalent weak acidic/basic analyte to the fundamental separation characteristics, such as the selectivity and the resolution [8].

Lelièvre et al. [9] has adopted a different strategy, and showed that the effective mobility of the monovalent week acidic/basic analyte can be formally expressed in terms of the simple S_AS_S model (4):

$$\mu_{\mathrm{eff}} = \frac{\mu_0^{\mathrm{pH}} + \mu_{\mathrm{AS}}^{\mathrm{pH}} K'^{\mathrm{pH}}_{\mathrm{AS}} c_S}{1 + K'^{\mathrm{pH}}_{\mathrm{AS}} c_S} \tag{5}$$

with

$$K'^{\mathrm{pH}}_{\mathrm{AS}} = K'_{\mathrm{HAS}} \frac{K'_{a,\mathrm{HAS}} + [H_3O^+]}{K'_{a,\mathrm{HA}} + [H_3O^+]} \tag{6}$$

$$\mu_0^{\mathrm{pH}} = \frac{K'_{a,\mathrm{HA}} \mu_{A^-} + [H_3O^+]\mu_{\mathrm{HA}}}{K'_{a,\mathrm{HA}} + [H_3O^+]} \tag{7}$$

$$\mu_{\mathrm{AS}}^{\mathrm{pH}} = \frac{K'_{a,\mathrm{HAS}} \mu_{A^-S} + [H_3O^+]}{K'_{a,\mathrm{HAS}} + [H_3O^+]} \tag{8}$$

where μ_{A^-}, μ_{A^-S}, μ_{HA}, μ_{HAS}, K'_{A^-S} and K'_{HAS} are respectively mobilities of the free dissociated form of the analyte, its complex with the selector, the free protonated form of the analyte, its complex with the selector, and the (ionic strength apparent) complexation constant for the dissociated, and the protonated forms of the analyte. $K'_{a,\mathrm{HA}}$ is the (ionic strength apparent) acidic dissociation constant of the free analyte and $[H_3O^+]$ is the concentration of the hydroxonium cations. $K'_{a,\mathrm{HAS}}$ is the (ionic strength apparent) acidic dissociation constant of the analyte in the complex. Value of this dissociation constant is determined by dissociation constant of the free analyte and complexation constants of the protonated and deprotonated analyte forms, respectively:

$$K'_{a,\mathrm{HAS}} = K'_{a,\mathrm{HA}} \frac{K'_{A^-S}}{K'_{\mathrm{HAS}}} \tag{9}$$

This model shows that under the constant pH, the two (protonated and deprotonated) forms of the analyte act as a single analyte form with the pH-dependent parameters μ_0^{pH}, $\mu_{\mathrm{AS}}^{\mathrm{pH}}$ and $K'^{\mathrm{pH}}_{\mathrm{AS}}$. Later on, Mofadel et al. [10] expressed the parameters $K'^{\mathrm{pH}}_{\mathrm{AS}}$, μ_0^{pH} and $\mu_{\mathrm{AS}}^{\mathrm{pH}}$ for bivalent acids. We will further call this model (5) a "pH-overall model" and the parameters (6)–(8) "pH-overall parameters".

Somewhat opposite situation arises if a single analyte form (*e.g.* strong, fully deprotonated acid) interacts with a mixture of selectors, which is often encountered in practice [4,11–23]. Luire et al. [24] have first described the interaction of a single analyte with two selectors as a simple extension of Eq. (4) in 1994. This equation has then become a basis for further method optimization in the dual-selector systems, predominantly in enantioseparations [25]. Similarly to the pH-overall model, Kranack et al. [26] and later us [27] have shown that, effective mobility of an analyte (present in a single free form) interacting with a mixture of selectors can be expressed in a form of the S_AS_S Eq. (4):

$$\mu_{\mathrm{eff}} = \frac{\mu_0 + \mu_{\mathrm{AS}}^{\mathrm{M}} K'^{\mathrm{M}}_{\mathrm{AS}} c_{\mathrm{tot}}}{1 + K'^{\mathrm{M}}_{\mathrm{AS}} c_{\mathrm{tot}}} \tag{10}$$

with

$$K'^{\mathrm{M}}_{\mathrm{AS}} = \sum_{j=1}^{N} K'_{S_j} \chi_{S_j} \tag{11}$$

$$\mu_{\mathrm{AS}}^{\mathrm{M}} = \frac{\sum_{j=1}^{N} K'_{S_j} \mu_{S_j} \chi_{S_j}}{K'^{\mathrm{M}}_{\mathrm{AS}}} \tag{12}$$

where c_{tot} is the total concentration of the mixture of N selectors ($c_{\mathrm{tot}} = \sum_{j=1}^{N} c_{S_j}$), χ_{S_j} are fractions of the individual selectors in the mixture, K'_{S_j} and μ_{S_j} complexation constant and mobility of complex of each particular selector with the analyte, and μ_0 is the electrophoretic mobility of the free analyte. Eq. (10) demonstrates that the mixture of selectors of a constant composition, χ_{S_j}, which interacts with the single analyte form, acts as a single selector with an ostensible complexation constant and mobility of complex. We will further call this model "M-overall model" and the parameters (11) and (12) "M-overall parameters". Eq. (10) is applicable to virtually an unlimited number of selectors under the assumption (2). It is useful for describing migration of a single analyte under interaction with a commercial mixture of selectors [28] as well as for investigating separation characteristics, such as mobility difference and selectivity, as a function of mixture composition, namely in the dual selector mixtures [29].

The aim of this paper is to show that the dependence of the effective mobility of the analyte on the selector concentration can always be converted to the S_AS_S formula (4) whenever the various forms of the analyte interact with an arbitrary number of selectors, in 1:1 (analyte:selector) stoichiometry each. The "various forms" of the analyte are not necessarily specified, although the (de)protonated forms of acidic/basic analytes would certainly be of the prime interest. We will denote the systems where multiple forms of the analyte interact with multiple selectors as "M_AM_S systems". This paper focuses on a deep theoretical analysis of such systems. We provide the experimental investigation of the model elsewhere [30].

2. Theory and discussion

2.1. The generalized overall model

Let an analyte A exists in L various (yet not complexed) forms: $A_1, \ldots, A_i, \ldots, A_L$. Next, consider an arbitrary number of N selectors, $S_1, \ldots, S_j, \ldots, S_N$, present in the system. Finally, let every form of the analyte, A_i, undergo an interaction with each of the N selectors, in 1:1 ratio exclusively:

$$A_i + S_j \rightleftharpoons AS_{ij} \qquad K'_{ij} = \frac{[A_i][S_j]}{[AS_{ij}]} \tag{13}$$

where K'_{ij} is the (ionic strength apparent) complexation constant between the ith form of the analyte and the jth selector. Then, for the total (analytical) concentration of the analyte, c_A, it applies

$$c_A = \sum_{i=1}^{L} \sum_{j=0}^{N} [A_{ij}] \tag{14}$$

where $j = 0$ refers to the free analyte form ($[A_{i0}] \equiv [A_i]$) for simplicity. By substituting Eq. (13) into Eq. (14), it results

$$c_A = \sum_{i=1}^{L} [A_{i0}] + \sum_{i=1}^{L} ([A_{i0}] \cdot \sum_{j=1}^{M} K'_{ij}[S_j]) \tag{15}$$

The molar fraction of each individual form of the analyte in the system is expressed as

$$\alpha_{ij} = \frac{[A_{ij}]}{c_A} \tag{16}$$

and the effective mobility of the analyte results according to the relation (3) as

$$\mu_{eff} = \sum_{i=1}^{L}\sum_{j=0}^{N} \frac{[A_{ij}]}{c_A}\mu_{ij} = \frac{\sum_{i=1}^{L}[A_{i0}]\mu_{i0} + \sum_{i=1}^{L}([A_{i0}] \cdot \sum_{j=1}^{N} K'_{ij}\mu_{ij}[S_j])}{\sum_{i=1}^{L}[A_{i0}] + \sum_{i=1}^{L}([A_{i0}] \cdot \sum_{j=1}^{N} K'_{ij}[S_j])} \tag{17}$$

It applies for every individual form, A_{i0},

$$[A_{i0}] = \chi_{i0} c_{A0} \tag{18}$$

where χ_{i0} is the molar fraction of the ith form of the free analyte with respect to the total concentration of the free analyte, c_{A0}. The complexation only controls the total amount of the free analyte, c_{A0}, but not its distribution into its various forms, A_{i0}. Thus, the molar fractions, χ_{i0}, are independent of the complexation. Consequently, Eq. (17) can be rewritten as

$$\mu_{eff} = \frac{\sum_{i=1}^{L}\chi_{i0}\mu_{i0} + \sum_{i=1}^{L}(\chi_{i0} \cdot \sum_{j=1}^{N} K'_{ij}\mu_{ij}[S_j])}{1 + \sum_{i=1}^{L}(\chi_{i0} \cdot \sum_{j=1}^{N} \mu_{ij}[S_j])} \tag{19}$$

where the total concentration of the free analyte, c_{A0}, cancels out and $\sum_{i=1}^{L}\chi_{i0} = 1$.

Using the approximation (2), the amount of every individual selector present in the system can be expressed as [27]

$$[S_j] = \chi_{S_j} c_{tot} \tag{20}$$

where χ_{S_j} is the molar fraction of the jth selector in the selector mixture and c_{tot} is the total concentration of the selector mixture. Then (19) turns into

$$\mu_{eff} = \frac{\sum_{i=1}^{L}\chi_{i0}\mu_{i0} + \sum_{i=1}^{L}(\chi_{i0} \cdot \sum_{j=1}^{N} K'_{ij}\mu_{ij}\chi_{S_j}) \cdot c_{tot}}{1 + \sum_{i=1}^{L}(\chi_{i0} \cdot \sum_{j=1}^{N} K'_{ij}\chi_{S_j}) \cdot c_{tot}} \tag{21}$$

where c_{tot} factors out of the both sums over N and L. Under the constant mixture composition, $\chi_{S_j} = \text{const}$, and constant external conditions governing the $A_1, \ldots, A_i, \ldots, A_L$ equilibria, $\chi_{i0} = \text{const}$, all terms in Eq. (21) are constants, which can be denoted as the M_AM_S-overall mobility of the free analyte, $\mu_0^{M_AM_S}$, the M_AM_S-overall mobility of complex, $\mu_{AS}^{M_AM_S}$, and the M_AM_S-overall complexation constant, $K'^{M_AM_S}_{AS}$:

$$\mu_{eff} = \frac{\mu_0^{M_AM_S} + K'^{M_AM_S}_{AS}\mu_{AS}^{M_AM_S} c_{tot}}{1 + K'^{M_AM_S}_{AS} c_{tot}} \tag{22}$$

Explicitly:

$$K'^{M_AM_S}_{AS} = \sum_{i=1}^{L}\chi_{i0}\sum_{j=1}^{N} K'_{ij}\chi_{S_j} \tag{23}$$

$$\mu_0^{M_AM_S} = \sum_{i=1}^{L}\chi_{i0}\mu_{i0} \tag{24}$$

$$\mu_{AS}^{M_AM_S} = \frac{\sum_{i=1}^{L}\chi_{i0}\sum_{j=1}^{N} K'_{ij}\mu_{ij}\chi_{S_j}}{K'^{M_AM_S}_{AS}} \tag{25}$$

Eq. (21) has the same form as Eq. (4). Therefore, it allows us to treat virtually any system exhibiting 1:1 complexation stoichiometry in the same way as if only one selector and one form of the free analyte were present in the system. Apart from the effective mobility, the effective charges of the analytes affect their analytical resolution. Following the approach described by the group of Rawjee, Williams and Vigh [8], the same formula results for the effective charge of the analyte, z_{eff}, as for the effective mobility, Eqs. (22)–(25), if every mobility is replaced by the respective charge.

2.2. Model assumptions and preconditions

Besides the 1:1 stoichiometry, the approximation (2) along with the constant external conditions (namely temperature, ionic strength, pH and viscosity) are required for the validity of Eq. (22). In reality, the approximation (2) is always fulfilled at the edge of the peak due to the diffusive nature of the analyte zone. Thus the peak distortion, rather than its mobility shift, is observed if the complexation is too strong or there is not a sufficient amount of the selector inside the analyte zone, in general. Recently we have shown that when a fully charged analyte interacts with one neutral selector, the peak distortion caused by the lack of the selector has the same effect as the electromigration dispersion [31]: it generates triangular HVL-shaped peaks [32]. The correct (*i.e.* dispersion unaffected) effective mobility can be determined by a nonlinear regression or approximate solution [33]. Although the same effect can be expected for weak analytes and multiple selectors, the appropriate mathematical theory that would substantiate this expectation has not been formulated yet.

Under the constant external conditions we understand namely constant ionic strength and pH and also viscosity of the BGE and the temperature. Maintaining the constant temperature is not a problem since the temperature control is common in electrophoresis runs. The viscosity correction to the effective mobility is applied in S_AS_S systems if the viscosity is significantly affected by the presence of the selector [34,35]. Since the individual mobilities of the free analyte forms, μ_{i0}, as well as that of the analyte–selector complexes, μ_{ij}, depend on the viscosity to the same extend, Eqs. (24) and (25) guarantee that the same correction applies to the M_AM_S-overall effective mobilities. pH is kept constant using BGEs with defined pH and a sufficient buffer capacity. Nevertheless, a special attention must be paid that none of the BGE constituents interacts with any of the selectors [36,37]. On the other hand, the individual molar ratios, χ_{i0}, can be expressed explicitly as a function of pH and the pH dependence incorporated into the model. Finally, ionic strength may be a serious problem whenever a charged selector is used (either alone or in the mixture). In some cases, appropriate correction can be applied [29,35]. However, ionic strength related effects, particularly in systems containing highly charged big molecules, have not been sufficiently described yet.

Noticeably, the M_AM_S model is not only limited to various forms of the analyte. If it is the selector that undergoes multiple equilibria, the M_AM_S-overall Eq. (22) is applicable whenever the external conditions can secure that the molar ratios, χ_{S_j}, of the various forms of the selector do not change when varying its concentration. *E.g.*, the model is applicable to (a mixture of) weak acidic/basic selector(s) under constant pH and ionic strength.

2.3. The equivalence of the overall models

Inspection of Eq. (21) reveals that the previously published models of electromigration in the presence of selector(s) [25] are

naturally included in the M_AM_S-overall model. Eq. (21) is reduced into the Wren and Row's formula (4) when only one form of the free analyte and one selector are present in the system. In this simplest case, the M_AM_S-overall parameters (22) become the mobility of the free analyte, and the mobility and complexation constant of the analyte–selector complex. If only one selector is present, but multiple equilibria among the L analyte forms take place, the M_AM_S-overall complexation constant, Eq. (23), becomes

$$K'^{M_AM_S}_{AS} = \sum_{i=1}^{L} \chi_{i0} K'_{iS} \tag{26}$$

and similarly the overall mobility of complex (25):

$$\mu^{M_AM_S}_{AS} = \frac{\sum_{i=1}^{L} \chi_{i0} K'_{iS} \mu_{iS}}{\sum_{i=1}^{L} \chi_{i0} K'_{iS}} \tag{27}$$

Eqs. (26), (27) and (24) provide generalized parameters of the pH-overall complexation model (5), K'^{pH}_{AS}, μ^{pH}_{AS} and μ^{pH}_{0}. If the analyte is a simple monovalent weak acid, these formulas result in the original equations by Lelièvre (6)–(9). Finally, in case of a mixture of selectors interacting with a single free form of the analyte, Eq. (21) turns into the formula known from the M-overall model (10).

The M_AM_S model has one important implication, which we discuss in detail in the Supplementary Information. It stays that the pH-overall model remains applicable in multi-selector systems if the individual single selector complexation constants and mobilities in Eqs. (6)–(9) (more generally (24), (26) and (27)) are replaced by the M-overall parameters defined by Eqs. (11) and (12). We refer to this situation as to the "pH-overall" perspective. Reversely, the M-overall model remains applicable in systems with multiple analyte equilibria (*e.g.* weak acidic analytes) if the single-analyte-form parameters in Eqs. (11) and (12) are replaced by the respective pH-overall ones defined by Eqs. (6)–(9) (more generally (24), (26) and (27)). This situation corresponds to the "M-overall" perspective. Although such a conclusion may be anticipated and has in fact been secretly applied in practice (concerning the fact that selectors are mostly produced as actual mixtures) the dissociation/complexation equilibria are highly interconnected (*cf.* Fig. S1 in the Supplementary Information). The herein discussed theory proves for the first time that not only the M_AM_S scheme coalesces into the apparent S_AS_S scheme, but also that the two (dissociation and complexation) equilibria can be decoupled and treated independently of each other.

This all provide us with various alternative approaches to determining the M_AM_S-overall parameters, $K'^{M_AM_S}_{AS}$, $\mu^{M_AM_S}_{AS}$ and $\mu^{M_AM_S}_{0}$, and thus the effective mobilities and separation characteristics for analytes migrating in M_AM_S systems. In the most trivial case of constant selector mixture composition, pH and IS, Eq. (22) tells us that the effective mobility of the analyte can be treated as in a S_AS_S system using the M_AM_S-overall parameters regardless of whether or not the individual complexation/dissociation constants for particular selectors and free analyte forms are available. Alternatively, if for example a monovalent acid interacts with a commercial mixture of selectors of a constant yet unknown composition, the M-overall complexation parameters K'^{M}_{iS} and μ^{M}_{iS} and the free analyte mobilities μ_{i0} can be determined for its protonated and deprotonated (ith) states just as if a single selector was present. The pH-overall perspective then forms a justification for calculating the pH-overall parameters according to the familiar Eqs. (6)–(9). Similarly, if pH-overall parameters are measured at a defined pH and IS with several selectors, one can justifiably combine them into the M-overall parameters as if a single analyte form migrated in the multi-selector environment (11) and (12). Experimental investigation and verification of these approaches is provided in the Part II of this series of papers [30].

3. Conclusion

It has been proven that if an analyte undergoes multiple equilibria among its various free forms and each of this forms complexes with an arbitrary number of selectors in 1:1 ratio, the electromigration of the analyte is equivalent to that of a single analyte form and a single selector. The M_AM_S-overall complexation constant, the M_AM_S-overall mobility of the free analyte and the M_AM_S-overall mobility of the analyte–selector complex play the role of the respective parameters in the single-analyte single-selector model introduced by Wren and Row in 1992. This conclusion is practically relevant for the analytical method optimization since it allows the analysts to treat, *e.g.*, the multivalent week acidic/basic/amphoteric analytes interacting with a commercial mixture of selectors in the same way as if a single form of the free analyte and a single selector were present in the system. The M_AM_S-overall parameters can be measured and used in the currently available optimization strategies. The 1:1 complexation stoichiometry and constant pH and ionic strength are prerequisite for the validity of the model.

Furthermore, the M_AM_S-overall model reveals that the multi-selector overall parameters can serve as an input into the pH-overall model introduced by Lelièvre in 1994 as if only one selector was present in the system. On the contrary, the pH-overall parameters can serve as an input into the multi-selector model introduced by our group in 2008 as if only one form of the free analyte was present (under the constant pH and IS). This enables the analysts to extend the original pH-overall model to the mixtures of selectors as well as the original multi-selector overall model to week multivalent acidic/basic/amphoteric compounds. The model can finally serve for finding the optimal pH and mixture composition for a particular separation setup.

Conflict of interest

The authors declare no conflicts of interest.

Acknowledgements

The authors acknowledge the financial support of this work from Grant no. P206/12/P630 of the Czech Science Foundation, from the Grant nos. 669412 and 570213 of the Grant Agency of the Charles University in Prague, and UNCE 204025/2012.

Appendix A. Supplementary data

Supplementary material related to this article can be found, in the online version, at http://dx.doi.org/10.1016/j.chroma.2015.01.029.

References

[1] G.K.E. Scriba, Selected fundamental aspects of chiral electromigration techniques and their application to pharmaceutical and biomedical analysis, J. Pharm. Biomed. Anal. 27 (2001) 373–399.
[2] P. Jac, G.K.E. Scriba, Recent advances in electrodriven enantioseparations, J. Sep. Sci. 36 (2013) 52–74.
[3] A. Rizzi, Fundamental aspects of chiral separations by capillary electrophoresis, Electrophoresis 22 (2001) 3079–3106.
[4] B. Chankvetadze, G. Blaschke, Enantioseparations in capillary electromigration techniques: recent developments and future trends, J. Chromatogr. A 906 (2001) 309–363.
[5] B. Chankvetadze, Separation selectivity in chiral capillary electrophoresis with charged selectors, J. Chromatogr. A 792 (1997) 269–295.
[6] Y.Y. Rawjee, D.U. Staerk, G. Vigh, Capillary electrophoretic chiral separations with cyclodextrin additives. I. Acids: chiral selectivity as a function of pH and the concentration of β-cyclodextrin for fenoprofen and ibuprofen, J. Chromatogr. 635 (1993) 291–306.
[7] Y.Y. Rawjee, R.L. Williams, G. Vigh, Capillary electrophoretic chiral separations using β-cyclodextrin as resolving agent. II. Bases: chiral selectivity as a function

of pH and the concentration of β-cyclodextrin, J. Chromatogr. A 652 (1993) 233–245.
[8] B.A. Williams, G. Vigh, Dry look at the CHARM (charged resolving agent migration) model of enantiomer separations by capillary electrophoresis, J. Chromatogr. A 777 (1997) 295–309.
[9] F. Lelièvre, P. Gareil, A. Jardy, Selectivity in capillary electrophoresis: application to chiral separations with cyclodextrins, Anal. Chem. 69 (1997) 385–392.
[10] N. Mofaddel, H. Krajian, D. Villemin, P.L. Desbene, Enantioseparation of binaphthol and its monoderivatives by cyclodextrin-modified capillary zone electrophoresis: a mathematical approach, Talanta 78 (2009) 631–637.
[11] E.C. Rickard, R.J. Bopp, Optimization of a capillary electrophoresis method to determine the chiral purity of a drug, J. Chromatogr. A 680 (1994) 609–621.
[12] F.-T.A. Chen, G. Shen, R.A. Evangelista, Characterization of highly sulfated cyclodextrins, J. Chromatogr. A 924 (2001) 523–532.
[13] B. Chankvetadze, K. Lomsadze, N. Burjanadze, J. Breitkreutz, G. Pintore, M. Chessa, K. Bergander, G. Blaschke, Comparative enantioseparations with native β-cyclodextrin, randomly acetylated β-cyclodextrin and heptakis-(2,3-di-O-acetyl)-β-cyclodextrin in capillary electrophoresis, Electrophoresis 24 (2003) 1083–1091.
[14] U. Schmitt, M. Ertan, U. Holzgrabe, Chiral capillary electrophoresis: facts and fiction on the reproducibility of resolution with randomly substituted cyclodextrins, Electrophoresis 25 (2004) 2801–2807.
[15] G. Gubitz, M.G. Schmid, Chiral separation principles in capillary electrophoresis, J. Chromatogr. A 792 (1997) 179–225.
[16] I.S. Lurie, Separation selectivity in chiral and achiral capillary electrophoresis with mixed cyclodextrins, J. Chromatogr. A 792 (1997) 297–307.
[17] M. Fillet, P. Hubert, J. Crommen, Enantiomeric separations of drugs using mixtures of charged and neutral cyclodextrins, J. Chromatogr. A 875 (2000) 123–134.
[18] G.K.E. Scriba, Cyclodextrins in capillary electrophoresis enantioseparations – recent developments and applications, J. Sep. Sci. 31 (2008) 1991–2011.
[19] M. Fillet, P. Hubert, J. Crommen, Method development strategies for the enantioseparation of drugs by capillary electrophoresis using cyclodextrins as chiral additives, Electrophoresis 19 (1998) 2834–2840.
[20] G. Gubitz, M.G. Schmid, Recent progress in chiral separation principles in capillary electrophoresis, Electrophoresis 21 (2000) 4112–4135.
[21] G. Guebitz, M.G. Schmid, Advances in chiral separation using capillary electromigration techniques, Electrophoresis 28 (2007) 114–126.
[22] G. Guebitz, M.G. Schmid, Chiral separation by capillary electromigration techniques, J. Chromatogr. A 1204 (2008) 140–156.
[23] H.A. Lu, G.N. Chen, Recent advances of enantioseparations in capillary electrophoresis and capillary electrochromatography, Anal. Methods 3 (2011) 488–508.
[24] I.S. Lurie, R.F.X. Klein, T.A. Dal Cason, M.J. LeBelle, R. Brenneisen, R.E. Weinberger, Chiral resolution of cationic drugs of forensic interest by capillary electrophoresis with mixtures of neutral and anionic cyclodextrins, Anal. Chem. 66 (1994) 4019–4026.
[25] L. Mullerova, P. Dubsky, B. Gas, Twenty years of development of dual and multi-selector models in capillary electrophoresis: a review, Electrophoresis 35 (2014) 2688–2700.
[26] A.R. Kranack, M.T. Bowser, P. Britz-McKibbin, D.D.Y. Chen, The effects of a mixture of charged and neutral additives on analyte migration behavior in capillary electrophoresis, Electrophoresis 19 (1998) 388–396.
[27] P. Dubsky, J. Svobodova, B. Gas, Model of CE enantioseparation systems with a mixture of chiral selectors. Part I. Theory of migration and interconversion, J. Chromatogr. B 875 (2008) 30–34.
[28] P. Dubsky, J. Svobodova, E. Tesarova, B. Gas, Enhanced selectivity in CZE multi-chiral selector enantioseparation systems: proposed separation mechanism, Electrophoresis 31 (2010) 1435–1441.
[29] L. Mullerova, P. Dubsky, B. Gas, Separation efficiency of dual-selector systems in capillary electrophoresis, J. Chromatogr. A 1330 (2014) 82–88.
[30] L. Mullerova, P. Dubsky, B. Gas, Generalized model of electromigration with 1:1 (analyte:selector) complexation stoichiometry. Part II. Application to dual systems and experimental verification, J. Chromatogr. A (2015, January) (accepted).
[31] V. Hruska, J. Svobodova, M. Benes, B. Gas, A nonlinear electrophoretic model for PeakMaster. Part III. Electromigration dispersion in systems that contain a neutral complex-forming agent and a fully charged analyte. Theory, J. Chromatogr. A 1267 (2012) 102–108.
[32] V. Hruska, M. Riesova, B. Gas, A nonlinear electrophoretic model for PeakMaster. I. Mathematical model, Electrophoresis 33 (2012) 923–930.
[33] P. Dubsky, M. Dvorak, L. Mullerova, B. Gas, Determination of the correct migration time and other parameters of the Haarhoff–van der Linde function from the peak geometry characteristics, Electrophoresis (2015), http://dx.doi.org/10.1002/elps.201400463.
[34] S.G. Penn, D.M. Goodall, J.S. Loran, Differential binding of tioconazole enantiomers to hydroxypropyl β-cyclodextrin studied by capillary electrophoresis, J. Chromatogr. 636 (1993) 149–152.
[35] M. Benes, I. Zuskova, J. Svobodova, B. Gas, Determination of stability constants of complexes of neutral analytes with charged cyclodextrins by affinity capillary electrophoresis, Electrophoresis 33 (2012) 1032–1039.
[36] M. Riesova, J. Svobodova, Z. Tosner, M. Benes, E. Tesarova, B. Gas, Complexation of buffer constituents with neutral complexation agents. Part I. Impact on common buffer properties, Anal. Chem. 85 (2013) 8518–8525.
[37] M. Benes, M. Riesova, J. Svobodova, E. Tesarova, P. Dubsky, B. Gas, Complexation of buffer constituents with neutral complexation agents. Part II. Practical impact in capillary zone electrophoresis, Anal. Chem. 18 (2013) 8526–8534.

Publikace IV

Generalized model of electromigration with 1:1 (analyte:selector) complexation stoichiometry: Part II. Application to dual systems and experimental verification

L. Müllerová, P. Dubský, B. Gaš

Journal of Chromatography A 2015, *1384*, 147-154.

Journal of Chromatography A, 1384 (2015) 147–154

Contents lists available at ScienceDirect

Journal of Chromatography A

journal homepage: www.elsevier.com/locate/chroma

Generalized model of electromigration with 1:1 (analyte:selector) complexation stoichiometry: Part II. Application to dual systems and experimental verification

Ludmila Müllerová, Pavel Dubský*, Bohuslav Gaš

Charles University in Prague, Faculty of Science, Department of Physical and Macromolecular Chemistry, Prague, Czech Republic

ARTICLE INFO

Article history:
Received 31 October 2014
Received in revised form 16 January 2015
Accepted 18 January 2015
Available online 23 January 2015

Keywords:
Dual-selector system
Model of electromigration
Partly dissociated analyte

ABSTRACT

Interactions among analyte forms that undergo simultaneous dissociation/protonation and complexation with multiple selectors take the shape of a highly interconnected multi-equilibrium scheme. This makes it difficult to express the effective mobility of the analyte in these systems, which are often encountered in electrophoretical separations, unless a generalized model is introduced. In the first part of this series, we presented the theory of electromigration of a multivalent weakly acidic/basic/amphoteric analyte undergoing complexation with a mixture of an arbitrary number of selectors. In this work we demonstrate the validity of this concept experimentally. The theory leads to three useful perspectives, each of which is closely related to the one originally formulated for simpler systems. If pH, IS and the selector mixture composition are all kept constant, the system is treated as if only a single analyte form interacted with a single selector. If the pH changes at constant IS and mixture composition, the already well-established models of a weakly acidic/basic analyte interacting with a single selector can be employed. Varying the mixture composition at constant IS and pH leads to a situation where virtually a single analyte form interacts with a mixture of selectors. We show how to switch between the three perspectives in practice and confirm that they can be employed interchangeably according to the specific needs by measurements performed in single- and dual-selector systems at a pH where the analyte is fully dissociated, partly dissociated or fully protonated. Weak monoprotic analyte (R-flurbiprofen) and two selectors (native β-cyclodextrin and monovalent positively charged 6-monodeoxy-6-monoamino-β-cyclodextrin) serve as a model system.

1. Introduction

Selectors are widely used in capillary electrophoresis (CE). A variety of them are available for CE; however, cyclodextrins (CDs) are the most popular, especially when used as chiral selectors [1–9]. Along with their increasing applications in analytical chemistry, theoretical models have been developed describing the electromigration of fully dissociated, neutral, or partly dissociated analytes interacting with one selector [10–23]. Several models dealing with dual- and multi-selector systems have also been published [24–40] (we recently summarized them in a review [41]). However none of these models takes into account the possible protonation equilibria of the analyte along with its simultaneous interaction with multiple selectors.

In Part I of this series, we presented the complete theory of the electromigration of multivalent weak acidic/basic analytes undergoing complexation with a mixture of selectors. The theory results in a generalized model of selector-assisted CE with 1:1 (analyte:selector) complexation stoichiometry (the overall multi-free-analyte-form multi-selector model, $M_A M_S$ model) [42]. In this model, L protonated/deprotonated states of the free (uncomplexed) analyte A_{i0} ($i = \{1, \ldots, L\}$) are considered to be present in a mixture of N selectors. Each of the free analyte forms interacts with each of the selectors S_j ($j = \{1, \ldots, N\}$). The interaction between the ith free analyte form and the jth selector is characterized by a complexation constant K'_{ij} and results in the formation of a complex with mobility μ_{ij}. The free analyte forms have individual mobilities μ_{i0}. Consequently, the effective mobility of the analyte μ_{eff} is:

$$\mu_{\mathrm{eff}} = \frac{\sum_{i=1}^{L} \chi_{i0}\mu_{i0} + \sum_{i=1}^{L}(\chi_{i0}\sum_{j=1}^{N} K'_{ij}\mu_{ij}\chi_{Sj}) \cdot c_{\mathrm{tot}}}{1 + \sum_{i=1}^{L}(\chi_{i0}\sum_{j=1}^{N} K'_{ij}\chi_{Sj}) \cdot c_{\mathrm{tot}}} \quad (1)$$

* Corresponding author at: Charles University in Prague, Faculty of Science, Albertov 2030, CZ-128 40 Prague 2, Czech Republic. Tel.: +420 221951296.
E-mail address: pavel.dubsky@natur.cuni.cz (P. Dubský).

http://dx.doi.org/10.1016/j.chroma.2015.01.055
0021-9673/

where χ_{i0} are the molar fractions of the free analyte forms (related to the total amount of the free analyte), χ_{Sj} are the molar fractions of the selectors in the selector mixture and c_{tot} is the total concentration of the selector mixture. The complexation controls only the total amount of free analyte, but not its distribution into its various forms, A_{i0}. Thus the molar fractions χ_{i0} are determined entirely by the dissociation constants of the free analyte. The M_AM_S model (1) is valid under the following conditions: (i) only 1:1 complexation (analyte:selector) takes place; (ii) the kinetics of the complexation are much faster than those of the electrophoretic movement; (iii) the ionic strength (IS) of the BGE is constant (the complexation constants K'_{ij} are defined by the equilibrium concentrations, not the activities, and therefore depend on the ionic strength of the solution). The detailed derivation and validity conditions of the model are discussed in detail in Part I of this series [42]. Though not given explicitly in Eq. (1), the pH-dependence of the effective mobility of the analyte is implicitly present in the model through the molar fractions χ_{i0}. Notice, however, that the entire model works with the concentration-defined complexation and dissociation constants and thus the actual concentration of hydroxonium ions should be considered rather than the pH, which is dependent on the activity.

The M_AM_S model (1) is generally applicable to any system that fulfills the required conditions mentioned above. In simpler systems, the M_AM_S model reduces to one of the previously published models of electromigration. The model of Wren and Rowe [10] results when a single free analyte form interacts with a single selector (here further referred to as S_AS_S systems). When a single analyte form interacts with multiple selectors, the dual-selector model [40] and the multi-selector model [38,39] published by our group are obtained from the M_AM_S model (1). Finally, when there is only one selector but a monoacidic/monobasic analyte (and the dependence of χ_{i0} on $[H_3O^+]$ is expressed explicitly), the M_AM_S model results in the model of Williams and Vigh [18].

It has already been demonstrated that (i) an analyte which is a weak monovalent [15] or divalent [22] acid and interacts with one selector can be treated as if only one free analyte form were present; (ii) a mixture of selectors can analogically be regarded as a single selector [38–40]. A constant H_3O^+ concentration in the BGE is a prerequisite in the former case and a constant mixture composition is required in the latter case. The M_AM_S model investigated here indicates that the two approaches, (i) and (ii), remain valid even if a weak acidic/basic analyte interacts with multiple selectors. Any M_AM_S system can be viewed as (i) a single-selector system with multiple analyte forms, (ii) a single-analyte-form system with multiple selectors, or simply as a single-analyte-form/single-selector system; depending on whether $[H_3O^+]$ (and consequently also χ_{i0}), the composition of the selector mixture (represented by χ_{Sj}), or both are kept constant.

This work was carried out to demonstrate the validity of the M_AM_S model (1) experimentally. We chose the simplest possible (yet practically highly relevant) M_AM_S system: a weak monoacidic analyte interacting with a mixture of two cyclodextrins. First, we will simplify Eq. (1) by adapting it for two forms of the analyte and two selectors. Second, we will show how the system can be treated from the perspective of (i) multiple analyte forms and a single selector at a constant mixture composition; (ii) a single analyte form and multiple selectors at constant $[H_3O^+]$; and finally the simplest single-analyte-form/single-selector system at both constant mixture composition and constant $[H_3O^+]$. Finally, we will demonstrate the equivalence of the three approaches, which allows the analyst to choose the best one according to the requirements of the particular separation.

2. Materials and methods

2.1. Chemicals

All the chemicals were of analytical-grade purity. R-flurbiprofen, native β-cyclodextrin (β-CD), formic acid, cacodylic acid, lithium hydroxide monohydrate and nitromethane were purchased from Sigma–Aldrich (Prague, Czech Republic). 6-Monodeoxy-6-monoamino-β-cyclodextrin hydrochloride (A-β-CD) was purchased from CycloLab (Budapest, Hungary). Ortho-phosphoric acid was purchased from Lachema (Brno, Czech Republic). NaOH solutions used for rinsing the capillary were purchased from Agilent Technologies (Waldbronn, Germany). IUPAC buffers, pH 1.679, 4.005, and 7.000 (Radiometer, Copenhagen, Denmark), were used for calibration of the pH meter. The water used for preparation of all the solutions was purified by the Rowapur and Ultrapur water purification system (Watrex, San Francisco, USA).

2.2. Instrumentation

All the CE experiments were performed using an Agilent ^{3D}CE capillary electrophoresis instrument operated by ChemStation software (Agilent Technologies, Waldbronn, Germany). The instrument was equipped with a built-in photometric diode array detector (UV detector). The 50 μm id and 375 μm od fused-silica capillary was obtained from Polymicro Technologies (Phoenix, AZ, USA). The total length of the capillary and distance from the inlet to the UV detector were 50.3 cm and 41.8 cm, respectively. A pH meter (PHM 240 pH/ION Meter, Radiometer analytical) was employed to measure the pH of the BGEs.

2.3. Experimental conditions

The pH 2.02 stock buffer contained 96.0 mM ortho-phosphoric acid and 38.1 mM LiOH; the pH 4.01 stock buffer contained 70.0 mM formic acid and 48.0 mM LiOH; the pH 6.28 stock buffer contained 86.0 mM cacodylic acid and 48.0 mM LiOH. Stock solutions containing β-CD were prepared by dissolving the selector directly in the particular buffer. A-β-CD is a monovalent positively charged selector and was purchased as a salt. Therefore, in stock solutions of this selector, the concentrations of LiOH and of the relevant buffering constituent had to be decreased in order to keep the IS of the solution constant so that all the BGEs used in this work had IS of 48 mM according to the calculation by the PeakMaster software [43]. All the stock solutions of A-β-CD contained 10 mM of this selector. The concentrations of the buffer constituents were 76.0 mM ortho-phosphoric acid and 28.1 mM LiOH for the 2.02 pH buffer, 55.4 mM formic acid and 48.0 mM LiOH for the 4.01 pH buffer, and 68.1 mM cacodylic acid and 38.1 mM LiOH for the 6.28 pH buffer. The BGEs containing lower concentrations of the single selectors were prepared by diluting the stock solution of the particular selector and the particular pH with stock buffer of the same pH. The stock solutions of the dual-selector mixtures were prepared by mixing stock solutions of the single selectors (of the particular pH) in the required ratio to obtain the desired mixture composition. Consequently, the stock solution was diluted with pure buffer of the particular pH to obtain BGEs containing a lower concentration of the dual-selector mixture. See Table 1 for the concentration ranges used. All the solutions at the given pH level exhibited the same experimental pH regardless of the presence and amount of selector(s). This indicated that no significant interaction occurred between the selectors and the buffer constituents [44]. Because of the low solubility of R-flurbiprofen at low pH values, the stock solution of 4 mM R-flurbiprofen was prepared by dissolving the appropriate amount of the compound in a 4 mM solution of LiOH. The samples were

Table 1
Concentration ranges of single selectors and of dual-selector mixtures in BGEs used for the determination of the complexation parameters. χ_{S1} represents the molar fraction of A-β-CD in the dual selector mixture.

pH	Selectors	System[a]	χ_{S1}	Range of concentrations (mM)[b]	Number of concentration levels
6.28	A-β-CD	S_AS_S	–	0.1–7.0	8
	A-β-CD + β-CD	M-overall	0.8	0.1–7.0	8
	A-β-CD + β-CD	M-overall	0.6	0.1–7.0	8
4.01	A-β-CD	pH-overall	–	0.05–8.0	9
	β-CD	pH-overall	–	0.1–5.0	8
	A-β-CD + β-CD	M_AM_S-overall	0.8	0.05–10.0	12
	A-β-CD + β-CD	M_AM_S-overall	0.6	0.05–0.8	7
	A-β-CD + β-CD	M_AM_S-overall	0.4	0.1–2.5	7
	A-β-CD + β-CD	M_AM_S-overall	0.2	0.1–5.0	8
2.02	A-β-CD	S_AS_S	–	0.1–7.0	9
	A-β-CD + β-CD	M-overall	0.8	0.2–7.0	9
	A-β-CD + β-CD	M-overall	0.6	0.2–7.0	9

[a] S_AS_S: a single free analyte form interacts with a single selector; M-overall: a single free analyte form interacts with a dual selector mixture; pH-overall: a partly dissociated analyte interacts with a single selector; M_AM_S-overall: a partly dissociated analyte interacts with a dual selector mixture.
[b] A total concentration of the mixture c_{tot} is reported for dual selector mixtures.

prepared by mixing 60 μL of the stock solution of R-flurbiprofen, 30 μL of 1% (v/v) aqueous solution of nitromethane (EOF marker) and 410 μL of the respective pure buffer (the samples did not contain any selector). All the solutions were filtered using syringe filters, pore size 0.45 μm (Sigma–Aldrich, Prague, Czech Republic).

The capillary was thermostated at 25 °C (at least 85% of the migration path is efficiently thermostated, because of the physical limitation of the instrument). Prior to use, a new capillary was flushed with water for 5 min, then with 1 M NaOH for 5 min and twice with water for 5 min. When a BGE containing a lower selector concentration compared to the previous measurement was used, the capillary was flushed with water for 3 min, with 0.1 M NaOH for 3 min and with water for 3 min. Prior to each run, the capillary was flushed for at least 3 min with the relevant BGE. The samples were injected hydrodynamically at 150 mbar s. A voltage of 15 kV was applied (anode on the injection side). Due to the low EOF, a pressure of 35 mbar was applied during all the electrophoretic measurements. The electric current and power in the capillary did not exceed 45 μA and 0.65 W, respectively. Each experiment was repeated at least four times. The software ChemStation (Agilent Technologies) was used for data collection and acquisition. The mathematical software Origin 8.1 (OriginLab Corporation, Northampton, USA) was used for fitting analyte peaks to the Haarhoff van der Linde (HVL) function [45,46], marker peaks to the Gaussian function and effective mobilities and M_AM_S-complexation parameters to the theoretical equations (see Section 3.2 for details). Other calculations were performed using Microsoft Office Excel 2010.

3. Results and discussion

3.1. Theory

The simplest M_AM_S system consists of a weak monoacidic analyte and two selectors. In this system, six forms of the analyte are generally present in the solution: the free deprotonated analyte A^- (mobility μ_{A^-}); the free protonated analyte HA (μ_{HA}, $\mu_{HA} = 0$, for a weak monoacid); the complex of the deprotonated analyte with the first selector A^-S_1 (μ_{A^-S1}; complexation constant K'_{A^-S1}); the complex of the deprotonated analyte with the second selector A^-S_2 (μ_{A^-S2}; K'_{A^-S2}); the complex of the protonated analyte with the first selector HAS_1 (μ_{HAS1}, K'_{HAS1}); and finally the complex of the protonated analyte with the second selector HAS_2 (μ_{HAS2}, K'_{HAS2}). The effective mobility of the analyte can be expressed in a straightforward way (as the sum of the mobilities of the individual analyte forms weighted by their respective molar fractions):

$$\mu_{\text{eff}} = \frac{\mu_{A^-} + K'_{A^-S1}\mu_{A^-S1}c_{S1} + K'_{A^-S2}\mu_{A^-S2}c_{S2} + ([H_3O^+]/K'_{a,HA})(\mu_{HA} + K'_{HAS1}\mu_{HAS1}c_{S1} + K'_{HAS2}\mu_{HAS2}c_{S2})}{1 + K'_{A^-S1}c_{S1} + K'_{A^-S2}c_{S2} + ([H_3O^+]/K'_{a,HA})(1 + K'_{HAS1}c_{S1} + K'_{HAS2}c_{S2})} \quad (2)$$

where $K'_{a,HA}$ is the apparent (concentration-defined) dissociation constant of the free analyte and c_{S1} and c_{S2} are concentrations of the first and the second selector, respectively. Formulated using the M_AM_S model (1) the effective analyte mobility results in the relationship:

$$\mu_{\text{eff}} = \frac{\chi_{A^-}\mu_{A^-} + \chi_{HA}\mu_{HA} + (\chi_{A^-}(K'_{A^-S1}\mu_{A^-S1}\chi_{S1} + K'_{A^-S2}\mu_{A^-S2}\chi_{S2}) + \chi_{HA}(K'_{HAS1}\mu_{HAS1}\chi_{S1} + K'_{HAS2}\mu_{HAS2}\chi_{S2}))c_{\text{tot}}}{1 + (\chi_{A^-}(K'_{A^-S1}\chi_{S1} + K'_{A^-S2}\chi_{S2}) + \chi_{HA}(K'_{HAS1}\chi_{S1} + K'_{HAS2}\chi_{S2}))c_{\text{tot}}} \quad (3)$$

where χ_{S1} and $\chi_{S2} = (1 - \chi_{S1})$ are the molar fractions of the respective selectors in the dual-selector mixture and χ_{A^-} and $\chi_{HA} = (1 - \chi_{A^-})$ are the molar fractions of the dissociated and protonated analyte (related to the total concentration of the free analyte):

$$\chi_{A^-} = \frac{K'_{a,HA}}{K'_{a,HA} + [H_3O^+]} \quad (4)$$

$$\chi_{HA} = \frac{[H_3O^+]}{K'_{a,HA} + [H_3O^+]} \quad (5)$$

Both Eqs. (2) and (3) are rather complicated and introduction of the M_AM_S model does not seem to simplify the situation to any extent. However, Eq. (3) enables closer inspection of the behavior of the system and simplification of the problem, as we will demonstrate later. (We assume constant IS, 1:1 complexation stoichiometry and fast complexation kinetics in the following text.)

First, if $[H_3O^+]$ (and therefore also the molar fractions of the free analyte forms χ_{A^-} and χ_{HA}) and the composition of the selector

mixture (represented by the molar fraction of the first selector $\chi_{S1} = 1 - \chi_{S2}$) are both kept constant, Eq. (3) takes the form:

$$\mu_{\text{eff}} = \frac{\mu_0^{M_AM_S} + \mu_{AS}^{M_AM_S} K'^{M_AM_S}_{AS} c_{\text{tot}}}{1 + K'^{M_AM_S}_{AS} c_{\text{tot}}} \quad (6)$$

where $\mu_0^{M_AM_S}$, $K'^{M_AM_S}_{AS}$ and $\mu_{AS}^{M_AM_S}$ are the M_AM_S-overall mobility of the free analyte, the M_AM_S-overall complexation constant and the M_AM_S-overall mobility of the complex, respectively. The M_AM_S-overall parameters are characteristic for the system at a particular IS, pH and mixture composition. Their explicit expressions can be obtained by comparing Eqs. (3) and (6) (*cf.* also Part I of this paper) and are given in Supplementary information S1 to this paper. Formula (6) has exactly the same form as that obtained by Wren and Rowe for systems with a single analyte form and a single selector (which we will refer to as the "S_AS_S model") [10]. At constant mixture composition and H_3O^+ concentration, the dependence of the effective mobility of the analyte on the total mixture concentration is thus expected to follow the familiar hyperbolic pattern. Therefore, the system can be treated as if only one analyte form and only one selector were present and parameters $\mu_0^{M_AM_S}$, $K'^{M_AM_S}_{AS}$ and $\mu_{AS}^{M_AM_S}$ can be measured experimentally (*e.g.* by affinity capillary electrophoresis – ACE). In addition, some (but not all) optimization strategies developed for S_AS_S systems can be adopted. The "but not all" statement refers to the approximation sometimes assumed in chiral separations that complexes of the two enantiomers with a single selector have the same mobilities. This simplification cannot be employed in the M_AM_S systems as we have already pointed out elsewhere for multi-selector systems [39].

Secondly, when the requirement on constant H_3O^+ concentration is removed, so that the analyte may change its degree of dissociation at a constant composition of the selector mixture, Eq. (3) takes the form:

$$\mu_{\text{eff}} = \frac{\chi_{A^-}\mu_{A^-} + \chi_{HA}\mu_{HA} + (\chi_{A^-}K'^{M}_{A^-S}\mu^{M}_{A^-S} + \chi_{HA}K'^{M}_{HAS}\mu^{M}_{HAS})c_{\text{tot}}}{1 + (\chi_{A^-}K'^{M}_{A^-S} + \chi_{HA}K'^{M}_{HAS})c_{\text{tot}}} \quad (7)$$

where $K'^{M}_{A^-S}$ and K'^{M}_{HAS} are the so-called M-overall constants of complexation of the selector mixture with the dissociated and protonated analyte, respectively, and $\mu^{M}_{A^-S}$ and μ^{M}_{HAS} are the M-overall mobilities of complexes of the two respective analyte forms with the selector mixture. Explicit expressions for the M-overall parameters can be obtained by comparing Eqs. (3) and (7) (*cf.* also Part I of this paper) and are also given in the Supplementary information S2 to this paper. Note that the M-overall parameters (K'^{M} and μ^{M}) do not refer to any complex physically present in the solution, but rather describe the interaction between the individual analyte forms and the mixture as a whole. Specifically, the M-overall mobilities $\mu^{M}_{A^-S}$ or μ^{M}_{HAS}, as appropriate, should be understood to be the mobility the fully dissociated analyte or the fully protonated analyte, respectively, that would be attained at virtually infinite c_{tot}. After substituting Eqs. (4) and (5) into (7), the formula can be rewritten as follows:

$$\mu_{\text{eff}} = \frac{\mu_{A^-} + K'^{M}_{A^-S}\mu^{M}_{A^-S}c_{\text{tot}} + ([H_3O^+]/K'_{a,HA})(\mu_{HA} + K'^{M}_{HAS}\mu^{M}_{HAS}c_{\text{tot}})}{1 + K'^{M}_{A^-S}c_{\text{tot}} + ([H_3O^+]/K'_{a,HA})(1 + K'^{M}_{HAS}c_{\text{tot}})} \quad (8)$$

Eq. (8) has exactly the same form as that published by Williams and Vigh [18] for a weak monoacidic analyte interacting with a single selector (which we will refer to as the "pH-explicit model"). Thus the M_AM_S model shows that any selector mixture of constant composition can be regarded as a single selector and, consequently, the optimization strategies developed for a partly dissociated analyte interacting with one selector can be employed. Determination of the M-overall parameters requires measurements in BGEs with at least two different pH values (keeping IS and mixture composition constant). Consequently, the effective mobility of the analyte can be calculated for BGEs with various pH values (or more precisely $[H_3O^+]$) and various total concentrations of the selector mixture (but constant mixture composition).

Thirdly, if the mixture composition is varied at constant pH, Eq. (3) yields:

$$\mu_{\text{eff}} = \frac{\mu_0^{\text{pH}} + (K'^{\text{pH}}_{AS1}\mu^{\text{pH}}_{AS1}\chi_{S1} + K'^{\text{pH}}_{AS2}\mu^{\text{pH}}_{AS2}\chi_{S2})c_{\text{tot}}}{1 + (K'^{\text{pH}}_{AS1}\chi_{S1} + K'^{\text{pH}}_{AS2}\chi_{S2})c_{\text{tot}}} \quad (9)$$

where μ_0^{pH} is the mobility of the free analyte, K'^{pH}_{AS1} and K'^{pH}_{AS2} are the complexation constants of the analyte with the first and the second selector, respectively, and μ^{pH}_{AS1} and μ^{pH}_{AS2} are the mobilities of the complexes of the analyte with the first and the second selector, respectively, all at the given $[H_3O^+]$. The pH-overall parameters μ_0^{pH}, K'^{pH}_{ASi} and μ^{pH}_{ASi} characterize the electromigration of a partly dissociated analyte in a single selector system at constant pH and were originally introduced for single selector systems by Lelièvre et al. [15]. Explicit expressions can be obtained by comparison of Eqs. (3) and (9) (*cf.* also Part I of this paper) and are given in the Supplementary information S3 to this paper. Analogously to the M-overall mobilities of the complexes, μ^{pH}_{AS1} and μ^{pH}_{AS2} are also the mobilities the analyte would attain at virtually infinite concentration of one or the other selector at the given pH, not the mobilities of any particular complex physically present in the solution. Eq. (9) shows that the M_AM_S system can be treated as if only one analyte form were present. Therefore, the strategy we recently introduced for dual-selector systems interacting with a fully charged analyte [40] (which we will refer to as the "dual-explicit model") can also be applied for partly charged analytes as long as $[H_3O^+]$ (*i.e.*, pH and IS) is held constant. The parameters of complexation with the individual selectors can be determined in the corresponding single selector systems (at the given pH and IS). Consequently, the effective mobility of the analyte in the dual-selector system can be calculated for various compositions and concentrations of the selector mixture.

3.2. Results

We chose R-flurbiprofen as a model weak monoacidic analyte, and the monovalent positively charged A-β-CD and the neutral β-CD as the two selectors in the dual-selector system. We performed measurements of the effective mobility as a function of the total selector concentration at various pH values and mixture compositions as given in Table 1 (IS was constant in all the BGEs used). The dissociation exponent (pK_a) of R-flurbiprofen reported in the literature varies around 4.2 [47–49]. Therefore, the degree of dissociation of the analyte is >99%, ~39% and <1% at pH values of 6.28, 4.01 and 2.02, respectively. In BGEs containing monovalent charged A-β-CD (either as a single selector or as a part of the mixture), the concentration of the buffer constituents was decreased in order to keep IS constant as discussed in Section 2.3. The analyte peaks were fitted to the HVL function [45,46], which yields the migration time of the analyte at its infinite dilution, *i.e.*, unaffected by electromigration dispersion or consumption of the selector by complexation with the analyte [40,50]. According to our experience, viscosity changes do not significantly affect the determined complexation parameters as long as the concentration of the CD does not exceed approximately 10 mM. Therefore, no viscosity correction was employed. The mobilities of the free analyte at each pH were measured separately in selector-free BGEs.

At pH 6.28, the free analyte appears almost exclusively in a single fully deprotonated form. When measured with the single selector, the situation matches the S_AS_S model as originally described by Wren and Rowe [10] and the determined parameters are the "physical" parameters K'_{A^-S}, μ_{A^-S} and μ_{A^-}. When measured at this pH in a selector mixture of constant composition, χ_{S1}, the situation matches the M-overall model [40] and the determined parameters are $K'^{M}_{A^-S}$, $\mu^{M}_{A^-S}$ and $\mu^{M}_{A^-} = \mu_{A^-}$. The same applies to pH 2.02, when the analyte is almost fully protonated and the respective

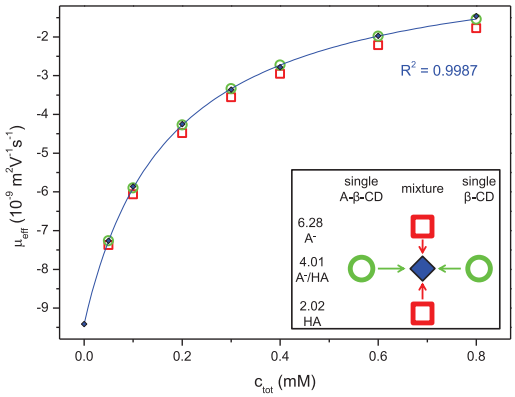

Fig. 1. Dependence of the effective mobility of R-flurbiprofen on the total selector concentration (pH 4.01, mixture of A-β-CD and β-CD, molar fraction of A-β-CD $\chi_{S1} = 0.6$, see Section 2 for experimental details); diamonds: experimental data; line: function (6) fitted to the experimental data, mobility of the free analyte (-9.41×10^{-9} m^2 V^{-1} s^{-1}) fixed during fitting, R^2 of the fit given in the figure; circles: effective mobilities calculated by the dual-explicit model (9) using the pH-overall parameters as input values (Table 2); squares: effective mobilities calculated by the pH-explicit model (8) using the M-overall parameters as input values (Table 2); inset: schematic representation of the two ways by which the effective mobilities can be predicted; A^-: dissociated analyte form, HA: protonated analyte form. (For interpretation of the references to color in text near the figure citation, the reader is referred to the web version of this article.)

parameters are K'_{HAS}, μ_{HAS} and μ_{HA}, K'^{M}_{HAS}, μ^{M}_{HAS} and $\mu^{M}_{HA} = \mu_{HA}$. Both the protonated and deprotonated forms of the analyte coexist in the system at the medium pH of 4.01. When measured with a single selector, the situation matches the pH-overall model [15] and the determined parameters are K'^{pH}_{AS}, μ^{pH}_{AS} and μ^{pH}_{0}. When measured with the dual-selector mixture, the complete M_AM_S-overall model (6) must be employed and the determined parameters are $K'^{M_AM_S}_{AS}$, $\mu^{M_AM_S}_{AS}$ and $\mu^{M_AM_S}_{0} = \mu^{pH}_{0}$. It is worth noting that the M_AM_S model implies that each one of all these dependences follows the same hyperbolical pattern (6). Therefore, S_AS_S as well as pH-overall, M-overall and M_AM_S-overall complexation parameters can be determined by the same kind of ACE experiment [51,52], by fitting the same Eq. (6) to the experimental data.

The resulting data are given in Table 2. The nonlinear curve fit does not indicate any difference between the individual models in terms of the quality of the fit. The coefficients of determination, R^2, as well as the errors of estimates are comparable for all of the S_AS_S, pH-overall, M-overall or M_AM_S-overall data. On one hand, all the parameters are pH-overall since, strictly speaking, the analyte is never fully (de)protonated, as reflected in the very small but nonzero mobility of the free analyte at pH 2.02. On the other hand, the degree of dissociation (protonation) seems negligible at the high (low) pH and the determined complexation parameters can be considered approximately equal to those of the single-analyte forms. The coefficients of determination and the errors of estimate are in perfect agreement with our long-term experience with the ACE measurements [40]. Fig. 1 (blue diamonds and curve) shows a representative data fit for the selected mixture composition, $\chi_{S1} = 0.6$, at the medium pH of 4.01. The figure clearly demonstrates that the experimental data follow the familiar hyperbolical shape even though two free-analyte forms are present and interact with two different selectors. This is in accordance with the M_AM_S-overall model (6).

The M_AM_S model also shows that the effective mobility of the partly dissociated analyte (pH 4.01) in a dual-selector mixture can be predicted either by the pH-explicit (8) or dual-explicit (9) approach. These two approaches might be regarded as "orthogonal" to each other (see the inset in Fig. 1). In the first ("vertical") case, the M-overall parameters are measured in a selected mixture with a constant composition for the individual free analyte forms (dissociated and protonated) and used in the pH-explicit model (8) (red squares in the inset in Fig. 1). In the second ("horizontal") case, the pH-overall parameters are measured at the desired pH with the two single selectors and further used in the dual-explicit model (9) (green circles in the inset in Fig. 1).

We will first investigate the "vertical" approach of obtaining the effective mobility of the analyte in the M_AM_S system. Here we simply treat the mixture of selectors as a single selector and use the measured (M-overall) complexation parameters in Eq. (8). The M-overall parameters were measured in the standard way at low (K'^{M}_{HAS} and μ'^{M}_{HAS}) and high ($K'^{M}_{A^-S}$ and $\mu^{M}_{A^-S}$) pH (red squares in the inset in Fig. 1) and the results are given in Table 2. Because the dual-selector mixture used consists of a charged selector, A-β-CD, combined with a neutral selector, β-CD, the M-overall complexation parameters of the free protonated analyte, K'^{M}_{HAS} and μ'^{M}_{HAS}, could be estimated at low pH provided that the fraction of A-β-CD was high enough to mobilize the neutral form of the analyte. This was true of the model mixtures with $\chi_{S1} = 0.8$ and $\chi_{S1} = 0.6$ (Table 2). In the next step, the measured (M-overall) mobilities of the complexes and the complexation constants were used to predict the effective mobilities of the analyte at pH 4.01 using Eq. (8). The $[H_3O^+]/K'_{a,HA}$ ratio had to be determined for this purpose. This, in principle, could be calculated from the dissociation exponent (pK_a) of the analyte and the desired pH (4.01). Nevertheless, the $[H_3O^+]/K'_{a,HA}$ ratio is IS-specific and therefore the calculation would require the $pK'_{a,HA}$ value determined at the particular IS and conversion of the pH value (activity-defined) to the $[H_3O^+]$ concentration. An alternative and more straightforward strategy is based on taking advantage of the pH-overall mobility of the free analyte, μ^{pH}_0 (see the Supplementary information S1 and S3), which directly yields:

$$\frac{[H_3O^+]}{K'_{a,HA}} = \frac{\mu_{A^-} - \mu^{pH}_0}{\mu^{pH}_0 - \mu_{HA}} \tag{10}$$

where μ_{A^-} and μ^{pH}_0 were measured (without any selector) at pH 6.28 and 4.01, respectively and $\mu_{HA} = 0$. The obtained value $[H_3O^+]/K'_{a,HA} = 1.07$ was used in the calculation. The whole procedure was accomplished at various total mixture concentrations and the predicted effective mobilities were then compared with those measured experimentally. Fig. 1 depicts the experimental data (blue diamonds) and the data obtained by calculation using Eq. (8) (red squares) for the mixture with $\chi_{S1} = 0.6$. The quantitative difference between the measured and the predicted data is summarized in Table 3A. Apart from the calculations for the selector mixtures, $\chi_{S1} = 0.8$ and $\chi_{S1} = 0.6$, the calculation was additionally performed for the single A-β-CD selector system ($\chi_{S1} = 1$). The data suggest that the pH-explicit model with the M-overall parameters yields a slightly biased prediction as the total concentration c_{tot} increases. This observation could be attributed to the biased values of the input parameters (K'^{M}_{HAS}, μ^{M}_{HAS}, $K'^{M}_{A^-S}$, *etc.*) caused by the incomplete (de)protonation of the analyte at the high and low pH values. Nonetheless, and in spite of the fact that the prediction is a little worse compared to the single selector system ($\chi_{S1} = 1$), the experimental results still support the validity of the proposed model quite well.

Secondly, we will investigate the "horizontal" approach for obtaining the effective mobility of the analyte in the M_AM_S system. Now the two ionic forms of the partially dissociated analyte are treated as a single-analyte form and the (pH-overall) complexation parameters are used in Eq. (9). The pH-overall parameters

Table 2
Measured mobilities of the free R-flurbiprofen and its complexation parameters with the single and the dual selector systems at various pH values of the BGE. χ_{S1} refers to the molar fraction of A-β-CD in the dual selector mixture with β-CD (see Section 2 for experimental details), complexation parameters obtained by fit of Eq. (6) to the experimental data (mobility of the free analyte at the particular pH fixed during the fitting).

pH	μ_0[a] (10^{-9} m^2 V^{-1} s^{-1})	Selector	System	K'_{AS} (M^{-1})	μ_{AS} (10^{-9} m^2 V^{-1} s^{-1})	R^2
6.28	−19.53 ± 0.07	A-β-CD	S_AS_S	4100 ± 120	0[a,b]	0.9947
		χ_{S1} = 0.8	M-overall	4550 ± 120	−2.06 ± 0.06	0.9987
		χ_{S1} = 0.6	M-overall	4620 ± 80	−3.80 ± 0.04	0.9992
4.01	−9.41 ± 0.05	A-β-CD	pH-overall	4190 ± 50	3.79 ± 0.02	0.9998
		β-CD	pH-overall	8200 ± 110	−2.63 ± 0.02	0.9996
		χ_{S1} = 0.8	M_AM_S-overall	4980 ± 50	1.76 ± 0.02	0.9997
		χ_{S1} = 0.6	M_AM_S-overall	5800 ± 150	0.17 ± 0.09	0.9987
		χ_{S1} = 0.4	M_AM_S-overall	6900 ± 180	−0.95 ± 0.08	0.9985
		χ_{S1} = 0.2	M_AM_S-overall	7500 ± 120	−1.85 ± 0.03	0.9993
2.02	−0.37 ± 0.05	A-β-CD	S_AS_S	4320 ± 50	7.03 ± 0.01	0.9996
		χ_{S1} = 0.8	M-overall	5460 ± 130	4.18 ± 0.01	0.9975
		χ_{S1} = 0.6	M-overall	6470 ± 170	2.42 ± 0.01	0.9972

[a] Value fixed during the fitting.
[b] Zero mobility of the complex formed of unitary negatively charged analyte and unitary positively charged selector.

were measured in the standard way with the first and the second selector separately at the desired pH of 4.01 (green circles in the inset in Fig. 1). The results are given in Table 2. In the next step, the measured (pH-overall) mobilities of the complexes and complexation constants were used to predict the effective mobilities of the analyte in the mixture of selectors. Eq. (9) applies in this case. The whole procedure was accomplished for four different mixture compositions (χ_{S1} = 0.2, 0.4, 0.6, 0.8) and at various total mixture concentrations. The predicted effective mobilities were then compared with those measured experimentally. Fig. 1 depicts the experimental data (blue diamonds) and the calculation using Eq. (9) (green circles) for the mixture with χ_{S1} = 0.6. The quantitative difference between the measured and the predicted data is summarized in Table 3B. The prediction matches the experimental data almost perfectly.

Finally, the dependences of the M_AM_S-overall complexation parameters $K'^{M_AM_S}_{AS}$ and $\mu^{M_AM_S}_{AS}$ on the mixture composition at constant pH (4.01) can be expressed to further validate the M_AM_S model. At constant pH, the M-overall (specifically dual-explicit) perspective applies. Therefore, the dependences of $K'^{M_AM_S}_{AS}$ and $\mu^{M_AM_S}_{AS}$ on the mixture composition are formally identical to those

Table 3
Median and maximum absolute differences between the measured and the calculated effective mobilities of R-flurbiprofen at pH 4.01 in the dual selector mixtures of A-β-CD and β-CD of various compositions. (χ_{S1} refers to the molar fraction of A-β-CD); (A) calculation by the pH-explicit model (8) using the M-overall parameters of the individual R-flurbiprofen ionic forms determined at low and high pH in the dual-selector mixtures of the specified composition (Table 2); (B) calculation by the dual-explicit model (9) using the pH-overall complexation parameters measured at pH 4.01 with the first and the second selector separately (Table 2); see text for details.

χ_1	$\lvert\mu_{eff}$ (measured) − μ_{eff} (calculated)$\rvert$ (10^{-9} m^2 V^{-1} s^{-1})		Number of concentration levels
	Median	Maximum	
(A)			
0.6	0.20	0.3	7
0.8	0.19	0.4	10
1	0.05	0.1	9
(B)			
0.2	0.06	0.2	8
0.4	0.06	0.3	7
0.6	0.02	0.1	7
0.8	0.07	0.2	10

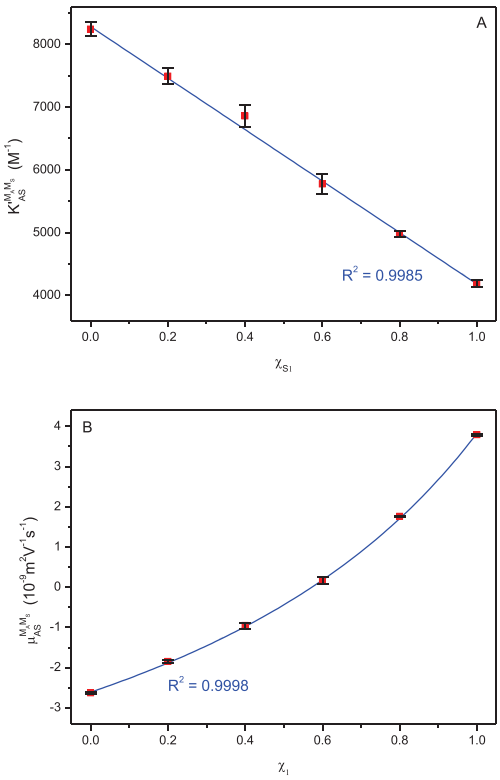

Fig. 2. M_AM_S-overall complexation parameters of R-flurbiprofen with dual-selector mixtures of A-β-CD and β-CD at pH 4.01. *x*-axis: molar fraction of A-β-CD in mixture χ_{S1}. (A) M_AM_S-overall complexation constant, $K'^{M_AM_S}_{AS}$; points: measured values; line: fit to Eq. (11). (B) M_AM_S-overall mobility of the complex, $\mu^{M_AM_S}_{AS}$; points: measured values; line: fit to Eq. (12), single selector complexation constants fixed during the fitting (4190 M^{-1} and 8240 M^{-1} for A-β-CD and β-CD, respectively).

given in Ref. [40] (but now the pH-overall parameters stand in place of the single-analyte-form ones):

$$K'^{M_AM_S}_{AS} = K'^{pH}_{AS1}\mu^{pH}_{AS1}\chi_{S1} + K'^{pH}_{AS2}\mu^{pH}_{AS2}(1-\chi_{S1}) \quad (11)$$

$$\mu^{M_AM_S}_{AS} = \frac{K'^{pH}_{AS1}\mu^{pH}_{AS1}\chi_{S1} + K'^{pH}_{AS2}\mu^{pH}_{AS2}(1-\chi_{S1})}{K'^{pH}_{AS1}\chi_{S1} + K'^{pH}_{AS2}(1-\chi_{S1})} \quad (12)$$

The dependence of the M_AM_S-overall complexation constant, $K'^{M_AM_S}_{AS}$, on the mixture composition, χ_{S1}, is depicted in Fig. 2A. The values vary linearly from the K'^{pH}_{ASi} of the second selector at $\chi_{S1} = 0$ to that of the first selector at $\chi_{S1} = 1$. The linear dependence is in agreement with the model (11). An analogous dependence is depicted for the M_AM_S-overall mobility of complex, $\mu^{M_AM_S}_{AS}$, in Fig. 2B. The data again perfectly match the expected hyperbolic pattern of Eq. (12) bounded with the single selector μ^{pH}_{ASi} values at $\chi_{S1} = 0$ and $\chi_{S1} = 1$, respectively. (The model (12) has four parameters: the pH-overall complexation constants and mobilities of complexes of the two single selector systems. Therefore, the single-selector pH-overall complexation constants K'^{pH}_{AS1} and K'^{pH}_{AS2} were fixed to prevent overfitting.)

This dual-explicit perspective (9) can be advantageously used for optimization of the composition of the dual-selector mixture, as we have shown elsewhere [40]. This allows analysts to find the optimal separation conditions regarding the selectivity, separation time and electromigration order of the analytes. On the other hand, the pH-explicit approach (8) is well established for single selector systems [17–19] and enables separation optimization with respect to the pH of the BGE. The M_AM_S model and the experimental results presented here show that both these approaches are applicable in an M_AM_S system according to the requirements of a particular analysis.

4. Concluding remarks

The M_AM_S model considerably simplifies the model of electromigration of partly dissociated analytes separated by a dual- or multi-selector mixture. First, when the IS, pH and mixture composition are kept constant, the system can be described by the simple S_AS_S-like model of electromigration of a fully dissociated analyte interacting with a single selector. The same precision of the S_AS_S-like model was shown for both a fully and a partly dissociated analyte interacting with either a single-selector or with a dual-selector mixture.

Second, the dual-explicit model (9) originally describing the interaction of a single analyte form with two selectors is useful at constant pH and IS regardless of the degree of dissociation of the free analyte. When the pH-overall parameters are measured for the single selectors, the dual-explicit model has excellent accuracy in calculating the final M_AM_S-overall complexation constant and mobility of the complex along with predicting the resulting effective mobility of the analyte.

Third, the pH-explicit (8) model as derived for the single weak monovalent acidic/basic analyte and single selector can be employed to the constant mixture composition and IS. The M-overall complexation parameters are used as input parameters of the pH-explicit model. This approach was somewhat less accurate than the other two but is still undeniably good enough for practical purposes.

Combination of the mentioned approaches opens the way to optimizing the pH value, mixture composition and its total concentration in the analytical practice of separation of monovalent weak acidic/basic analytes in dual- or multi-selector mixtures in capillary zone electrophoresis.

Conflicts of interest

All the authors declare that there are no conflicts of interest.

Acknowledgements

The authors acknowledge the financial support for this work from Grant No. P206/12/P630 of the Grant Agency of the Czech Republic, and Grant No.669412 of the Grant Agency of Charles University, and also financial support from the Charles University UNCE204025/2012.

Appendix A. Supplementary data

Supplementary data associated with this article can be found, in the online version, at http://dx.doi.org/10.1016/j.chroma.2015.01.055.

References

[1] A. Rizzi, Fundamental aspects of chiral separations by capillary electrophoresis, Electrophoresis 22 (2001) 3079–3106.
[2] B. Chankvetadze, Enantioseparations by using capillary electrophoretic techniques. The story of 20 and a few more years, J. Chromatogr. A 1168 (2007) 45–70.
[3] G. Guebitz, M.G. Schmid, Chiral separation by capillary electromigration techniques, J. Chromatogr. A 1204 (2008) 140–156.
[4] S. Fanali, Chiral separations by CE employing CDs, Electrophoresis 30 (2009) S203–S210.
[5] B. Chankvetadze, Separation of enantiomers with charged chiral selectors in CE, Electrophoresis 30 (2009) S211–S221.
[6] H. Lu, G. Chen, Recent advances of enantioseparations in capillary electrophoresis and capillary electrochromatography, Anal. Methods 3 (2011) 488–508.
[7] P. Jac, G.K.E. Scriba, Recent advances in electrodriven enantioseparations, J. Sep. Sci. 36 (2013) 52–74.
[8] P. Rezanka, K. Navratilova, M. Rezanka, V. Kral, D. Sykora, Application of cyclodextrins in chiral capillary electrophoresis, Electrophoresis 35 (2014) 2701–2721.
[9] L. Escuder-Gilabert, Y. Martin-Biosca, M.J. Medina-Hernandez, S. Sagrado, Cyclodextrins in capillary electrophoresis: recent developments and new trends, J. Chromatogr. A 1357 (2014) 2–23.
[10] S.A.C. Wren, R.C. Rowe, Theoretical aspects of chiral separation in capillary electrophoresis. I. Initial evaluation of a model, J. Chromatogr. 603 (1992) 235–241.
[11] S.A.C. Wren, Chiral separation in capillary electrophoresis, Electrophoresis 16 (1995) 2127–2131.
[12] S.G. Penn, D.M. Goodall, J.S. Loran, Differential binding of tioconazole enantiomers to hydroxypropyl-β-cyclodextrin studied by capillary electrophoresis, J. Chromatogr. 636 (1993) 149–152.
[13] M.M. Rogan, K.D. Altria, D.M. Goodall, Enantiomeric separation of salbutamol and related impurities using capillary electrophoresis, Electrophoresis 15 (1994) 808–817.
[14] P. Britz-McKibbin, D.D.Y. Chen, Prediction of the migration behavior of analytes in capillary electrophoresis based on three fundamental parameters, J. Chromatogr. A 781 (1997) 23–34.
[15] F. Lelievre, P. Gareil, A. Jardy, Selectivity in capillary electrophoresis: application to chiral separations with cyclodextrins, Anal. Chem. 69 (1997) 385–392.
[16] A.M. Rizzi, L. Kremser, pKa shift-associated effects in enantioseparations by cyclodextrin-mediated capillary zone electrophoresis, Electrophoresis 20 (1999) 2715–2722.
[17] Y.Y. Rawjee, D.U. Staerk, G. Vigh, Capillary electrophoretic chiral separations with cyclodextrin additives I. Acids: chiral selectivity as a function of pH and the concentration of β-cyclodextrin for fenoprofen and ibuprofen, J. Chromatogr. 635 (1993) 291–306.
[18] B.A. Williams, G. Vigh, Dry look at the CHARM (charged resolving agent migration) model of enantiomer separations by capillary electrophoresis, J. Chromatogr. A 777 (1997) 295–309.
[19] W. Zhu, G. Vigh, Experimental verification of a predicted, hitherto unseen separation selectivity pattern in the nonaqueous capillary electrophoretic separation of weak base enantiomers by octakis (2,3-diacetyl-6-sulfato)-γ-cyclodextrin, Electrophoresis 21 (2000) 2016–2024.
[20] T.H. Seals, C. Sheng, J.M. Davis, Influence of neutral cyclodextrin concentration on plate numbers in capillary electrophoresis, Electrophoresis 22 (2001) 1957–1973.
[21] W.-C. Yang, A.-M. Yu, X.-D. Yu, H.-Y. Chen, Modeling and optimization of the chiral selectivity of basic analytes in chiral capillary electrophoresis with negatively charged cyclodextrins using electrochemical detection, Electrophoresis 22 (2001) 2025–2031.
[22] N. Mofaddel, H. Krajian, D. Villemin, P.L. Desbene, Enantioseparation of binaphthol and its monoderivatives by cyclodextrin-modified capillary zone electrophoresis: a mathematical approach, Talanta 78 (2009) 631–637.

[23] M. Hammitzsch-Wiedemann, G.K.E. Scriba, Mathematical approach by a selectivity model for rationalization of pH- and selector concentration-dependent reversal of the enantiomer migration order in capillary electrophoresis, Anal. Chem. 81 (2009) 8765–8773.
[24] I.S. Lurie, R.F.X. Klein, T.A. Dal Cason, M.J. LeBelle, R. Brenneisen, R.E. Weinberger, Chiral resolution of cationic drugs of forensic interest by capillary electrophoresis with mixtures of neutral and anionic cyclodextrins, Anal. Chem. 66 (1994) 4019–4026.
[25] O.H.J. Szolar, R.S. Brown, J.H.T. Luong, Separation of PAHs by capillary electrophoresis with laser-induced fluorescence detection using mixtures of neutral and anionic β-cyclodextrins, Anal. Chem. 67 (1995) 3004–3010.
[26] K.W. Whitaker, C.L. Copper, M.J. Sepaniak, Separations of alkyl-substituted anthracenes using cyclodextrin distribution capillary electrochromatography, J. Microcolumn Sep. 8 (1996) 461–468.
[27] X. Peng, M.T. Bowser, P. Britz-McKibbin, G.M. Bebault, J.R. Morris, D.D.Y. Chen, Quantitative description of analyte migration behavior based on dynamic complexation in capillary electrophoresis with one or more additives, Electrophoresis 18 (1997) 706–716.
[28] A.R. Kranack, M.T. Bowser, P. Britz-McKibbin, D.D.Y. Chen, The effects of a mixture of charged and neutral additives on analyte migration behavior in capillary electrophoresis, Electrophoresis 19 (1998) 388–396.
[29] F. Lelievre, P. Gareil, Y. Bahaddi, H. Galons, Intrinsic selectivity in capillary electrophoresis for chiral separations with dual cyclodextrin systems, Anal. Chem. 69 (1997) 393–401.
[30] S. Surapaneni, K. Ruterbories, T. Lindstrom, Chiral separation of neutral species by capillary electrophoresis. Evaluation of a theoretical model, J. Chromatogr. A 761 (1997) 249–257.
[31] M. Fillet, B. Chankvetadze, J. Crommen, G. Blaschke, Designed combination of chiral selectors for adjustment of enantioseparation selectivity in capillary electrophoresis, Electrophoresis 20 (1999) 2691–2697.
[32] A.M. Abushoffa, M. Fillet, P. Hubert, J. Crommen, Prediction of selectivity for enantiomeric separations of uncharged compounds by capillary electrophoresis involving dual cyclodextrin systems, J. Chromatogr. A 948 (2002) 321–329.
[33] A.M. Abushoffa, M. Fillet, R.D. Marini, P. Hubert, J. Crommen, Enantiomeric separation of aminoglutethimide by capillary electrophoresis using native cyclodextrins in single and dual systems, J. Sep. Sci. 26 (2003) 536–542.
[34] X. Zhu, Y. Ding, B. Lin, A. Jakob, B. Koppenhoefer, Transient state of chiral recognition in a binary mixture of cyclodextrins in capillary electrophoresis, J. Chromatogr. A 888 (2000) 241–250.
[35] J.P. Schaeper, S.B. Fox, M.J. Sepaniak, Optimization strategies and modeling of separations of dansyl-amino acids by cyclodextrin-modified capillary electrophoresis, J. Chromatogr. Sci. 39 (2001) 411–419.
[36] N. Matthijs, S. Van Hemelryck, M. Maftouh, D. Luc Massart, Y. Vander Heyden, Electrophoretic separation strategy for chiral pharmaceuticals using highly-sulfated and neutral cyclodextrins based dual selector systems, Anal. Chim. Acta 525 (2004) 247–263.
[37] T. Nhujak, C. Sastravaha, C. Palanuvej, A. Petsom, Chiral separation in capillary electrophoresis using dual neutral cyclodextrins: theoretical models of electrophoretic mobility difference and separation selectivity, Electrophoresis 26 (2005) 3814–3823.
[38] P. Dubsky, J. Svobodova, B. Gas, Model of CE enantioseparation systems with a mixture of chiral selectors Part I. Theory of migration and interconversion, J. Chromatogr. B 875 (2008) 30–34.
[39] P. Dubsky, J. Svobodova, E. Tesarova, B. Gas, Enhanced selectivity in CZE multichiral selector enantioseparation systems: proposed separation mechanism, Electrophoresis 31 (2010) 1435–1441.
[40] L. Mullerova, P. Dubsky, B. Gas, Separation efficiency of dual-selector systems in capillary electrophoresis, J. Chromatogr. A 1330 (2014) 82–88.
[41] L. Mullerova, P. Dubsky, B. Gas, Twenty years of development of dual and multi-selector models in capillary electrophoresis: a review, Electrophoresis 35 (2014) 2688–2700.
[42] P. Dubsky, L. Mullerova, M. Dvorak, B. Gas, Generalized model of electromigration with 1:1 (analyte:selector) complexation stoichiometry: Part I. Theory, J. Chromatogr. A 1384 (2015) 142–146.
[43] M. Jaros, V. Hruska, M. Stedry, I. Zuskova, B. Gas, Eigenmobilities in background electrolytes for capillary zone electrophoresis: IV. Computer program PeakMaster, Electrophoresis 25 (2004) 3080–3085.
[44] M. Riesova, J. Svobodova, Z. Tosner, M. Benes, E. Tesarova, B. Gas, Complexation of buffer constituents with neutral complexation agents: Part I. Impact on common buffer properties, Anal. Chem. 85 (2013) 8518–8525.
[45] P.C. Haarhoff, H.J. van der Linde, Concentration dependence of elution curves in nonideal gas chromatography, Anal. Chem. 38 (1966) 573–582.
[46] G.L. Erny, E.T. Bergstroem, D.M. Goodall, S. Grieb, Predicting peak shape in capillary zone electrophoresis: a generic approach to parametrizing peaks using the Haarhoff-Van der Linde (HVL) function, Anal. Chem. 73 (2001) 4862–4872.
[47] B.D. Anderson, R.A. Conradi, Predictive relationships in the water solubility of salts of a nonsteroidal antiinflammatory drug, J. Pharm. Sci. 74 (1985) 815–820.
[48] G. Bouchard, P.-A. Carrupt, B. Testa, V. Gobry, H.H. Girault, Lipophilicity and solvation of anionic drugs, Chem. – Eur. J. 8 (2002) 3478–3484.
[49] M. Meloun, S. Bordovska, L. Galla, The thermodynamic dissociation constants of four non-steroidal anti-inflammatory drugs by the least-squares nonlinear regression of multiwavelength spectrophotometric pH-titration data, J. Pharm. Biomed. Anal. 45 (2007) 552–564.
[50] M. Benes, I. Zuskova, J. Svobodova, B. Gas, Determination of stability constants of complexes of neutral analytes with charged cyclodextrins by affinity capillary electrophoresis, Electrophoresis 33 (2012) 1032–1039.
[51] K. Uselova-Vcelakova, I. Zuskova, B. Gas, Stability constants of amino acids, peptides, proteins, and other biomolecules determined by CE and related methods: recapitulation of published data, Electrophoresis 28 (2007) 2145–2152.
[52] C. Jiang, D.W. Armstrong, Use of CE for the determination of binding constants, Electrophoresis 31 (2010) 17–27.

4.3 Efektivní mobilita EOF markerů v BGE obsahujícím sulfatovaný β-CD stanovená dvoudetektorovou metodou

Pro stanovení komplexačních parametrů, které jsou vstupními parametry elektromigračních modelů probíraných v kapitolách 4.1 a 4.2, metodou ACE je třeba změřit efektivní mobility analytu v BGE o několika různých koncentracích selektorů. V případě, že selektor je nabitý, může být stanovení efektivní mobility analytu komplikováno interakcí EOF markeru se selektorem.

Jak bylo řečeno v úvodní kapitole 1.2, vhodná metoda pro stanovení efektivní mobility analytů v základních elektrolytech, jejichž některá nabitá složka (typicky selektor) může interagovat s markerem elektroosmotického toku, byla vyvinuta ve skupině profesora Vigha už v roce 1997 [71]. Nicméně pro fungování této metody je nezbytné umístění UV absorpčního detektoru přibližně uprostřed kapiláry, zatímco v komerčních přístrojích je vzdálenost mezi tímto detektorem a výstupním koncem kapiláry konstrukčně pevně daná a poměrně krátká (8,5 cm v případě instrumentace Agilent Technologies používané v této práci).

Proto byla v *Publikaci V* navržena nová metoda založená na stejném principu, ale proveditelná v komerční instrumentaci. I námi navržená metoda je založena na stanovení vzdálenosti mezi zónou markeru umístěnou v neinteragujícím BGE a zónou vzorku nacházející se v BGE obsahujícím interagující složku. Metoda využívá dva detektory: UV absorpční detektor s diodovým polem umístěný u výstupního konce kapiláry a bezkontaktní vodivostní detektor původně vyvinutý v naší skupině [76], který je ovšem nyní běžně komerčně dostupný u výrobce přístroje, firmy Agilent Technologies. Konstrukce kazety, do které se umísťuje kapilára, umožňuje situovat mezi oba detektory další smyčku kapiláry, takže vzdálenost mezi oběma detektory je přibližně stejná, jako mezi vstupem do kapiláry a prvním (vodivostním) detektorem, jak je ukázáno na Obrázku 6.

Průběh měření dvoudetektorovou metodou je schematicky znázorněn v *Publikaci V* (Figure 1), podrobný popis jednotlivých fází metody i způsob vyhodnocení výsledků je uveden v sekci 3.1 této publikace.

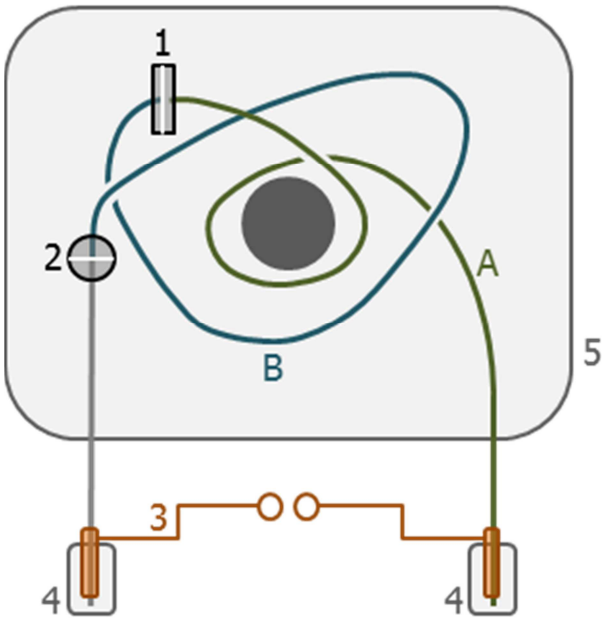

Obrázek 6: Navinutí kapiláry pro měření dvoudetektorovou metodou; 1 – vodivostní detektor; 2 – UV absorpční detektor; 3 – elektrody připojené ke zvroji vysokého napětí; 4 – vialky s BGE; 5 – kazeta pro umístění kapiláry; A – úsek kapiláry od vstupu k vodivostnímu detektoru; B – úsek kapiláry od vodivostního detektoru k UV absorpčnímu detektoru.

Dvoudetektorová metoda byla v *Publikaci V* využita ke stanovení efektivní mobility čtyř často používaných EOF markerů – dimethyl sulfoxidu, mesityl oxidu, nitromethanu a thiomočoviny – v BGE obsahujícím nedefinovaně sulfatovaný β-CD (S-β-CD) v koncentraci 60 g/l (odpovídá přibližně 30 mM). Stanovené mobility jsou uvedené v *Publikaci V* (Table 2).

Nejvyšší efektivní mobilita způsobená interakcí se S-β-CD byla pozorována u thiomočoviny ($-3{,}0\cdot10^{-9}$ m^{2}V^{-1}s^{-1}), což ukazuje, že tato látka není vhodným markerem pro BGE se sulfatovaným cyklodextrinem. Nejnižší (v absolutní hodnotě), ale dvoudetektorovou metodou stále měřitelné, efektivní mobility byly zjištěny pro dimethyl sulfoxid a nitromethan ($-1{,}5\cdot10^{-9}$ m^{2}V^{-1}s^{-1}). Lze tedy konstatovat, že tyto látky jsou ze zvoleného setu nejméně nevhodné jako EOF markery, nicméně i ty se S-β-CD slabě interagují.

Získané výsledky byly dále ověřeny měřeními pomocí CE v klasickém uspořádání. Tak samozřejmě nebylo možné změřit absolutní hodnotu efektivní mobility daného EOF markeru. Nicméně když byly ve vzorku nadávkovány markery dva, bylo možné stanovit rozdíl jejich efektivních mobilit (rozdíl není ovlivněn mobilitou elektroosmotického toku). Tento rozdíl pak byl porovnán s rozdílem efektivních mobilit stanovených dvoudetektorovou metodou a výsledky byly v rámci experimentální chyby shodné (*Publikace V*, Table 3), což potvrzuje spolehlivost výsledků dvoudetektorové metody.

Publikace V

Determination of effective mobilities of EOF markers in BGE containing sulfated β-cyclodextrin by a two-detector method

L. Müllerová, P. Dubský, J. Svobodová, B. Gaš

Electrophoresis 2013, *34*, 768-776.

Electrophoresis 2013, *34*, 768–776

Ludmila Müllerová
Pavel Dubský
Jana Svobodová
Bohuslav Gaš

Faculty of Science, Department of Physical and Macromolecular Chemistry, Charles University in Prague, Prague, Czech Republic

Received September 5, 2012
Revised October 10, 2012
Accepted October 14, 2012

Research Article

Determination of effective mobilities of EOF markers in BGE containing sulfated β-cyclodextrin by a two-detector method

A neutral marker of the EOF can gain a nonzero effective mobility because of its possible interaction with a charged complexing agent, such as a chiral selector in CE. We determined effective mobilities of four compounds often used as EOF markers (dimethyl sulfoxide, mesityl oxide, nitromethane, and thiourea) in the BGE-containing sulfated β-CD (60 g/L). All the compounds studied were measurably mobilized by their interaction with the selector. The highest effective mobility ($-3.0\cdot10^{-9}m^2s^{-1}V^{-1}$) was observed for thiourea and the lowest ($-1.5\cdot10^{-9}m^2s^{-1}V^{-1}$) for dimethyl sulfoxide and nitromethane. The mobilities were determined by a new two-detector pressure mobilization method (2d method), which we propose, and the results were confirmed by standard CE measurements. In the 2d method, one marker zone is situated in the BGE containing the charged selector, while the second marker zone is surrounded with a selector-free BGE, which prevents its complexation. The initial distance between the two marker zones equals the capillary length from the inlet to the first detector. After a brief voltage application, the final distance between the marker zones is determined based on known capillary length from the first to the second detector. The difference between these two distances determines the effective mobility.

Keywords:
Capillary zone electrophoresis / Complexation / EOF determination / EOF markers / Sulfated cyclodextrin
DOI 10.1002/elps.201200490

Additional supporting information may be found in the online version of this article at the publisher's web-site

1 Introduction

CE is a widely used technique for separation of charged analytes. Applicability of CE can be significantly extended by addition of an interacting agent into the BGE. If the BGE contains a chiral selector, then the CE can be used for chiral separations. A wide range of chiral selectors is available so they can be easily altered [1–3] which makes CE a versatile chiral separation method.

Correspondence: Pavel Dubský, Faculty of Science, Department of Physical and Macromolecular Chemistry, Charles University in Prague, Albertov 2030, CZ-128 40 Prague 2, Czech Republic
E-mail: pavel.dubsky@natur.cuni.cz
Fax: +420-2-2491-9752

Abbreviations: CCD detector, contactless conductivity detector; **2d method**, two-detector method; **free-BGE**, interacting agent-free BGE; **M1**, first marker zone; **M2**, second marker zone; **M3**, third marker zone; **MO**, mesityl oxide; **NM**, nitromethane; **SCD**, sulfated β-CD; **SCD-BGE**, BGE-containing sulfated CD; **TU**, thiourea; **UV detector**, UV/Vis absorption detector

The most popular chiral selectors in CE are CDs [1–11]. Among these, charged CDs are the only choice for separation of neutral analytes. The charged CDs are reported to also show better chiral recognition ability for charged analytes compared to neutral CDs [1, 3, 5, 11–13]. Two reasons can be given for this phenomenon. One reason lies in electrostatic forces playing role in the host–guest interaction along with a possible countercurrent flux of a free analyte and an oppositely charged complex of the analyte with the selector [1, 3, 5]. The second reason is connected with the fact, that the charged CDs are often produced as a mixture of compounds differing in degree of substitution and position of substituents. To such a multiselector separation system, a mixed effect of thermodynamic/electrophoretic enantioselective mechanisms is inherent that can significantly increase the separation capability of the system [14, 15]. Especially sulfated and highly sulfated CDs are known as versatile and very effective chiral selectors [6, 9, 16–21].

Colour Online: See the article online to view Figs. 1–4 in colour.

CE is also utilized for determination of physicochemical constants, such as acidity constants, limiting ionic mobilities, ionic radii, critical micelle concentration. Interaction of a complexing agent with an analyte in CE can be described by the complexation constant and the mobility of the complex. Both these parameters are essential for theoretical models of electromigration behavior of such systems and consequently, for both theoretical considerations and practical applications [14, 22, 23]. Methods for determination of complexation constants by CE are summarized in several reviews [24–27]. The most commonly used method is ACE. In this method, the determination is based on measurements of effective mobility which in turn requires precise determination of the mobility of the EOF. Therefore, accurate measurement of the EOF mobility is needed if the interaction of a complexing agent with an analyte is to be studied.

Several methods of EOF mobility determination are summarized in a review by Wang et al. [28], e.g. measurement of mass of liquid transmitted by the EOF, calculation of the EOF based on measurement of streaming potential, monitoring of the electric current during experiments. Much simpler, and thus, by far the most popular is, however, the neutral marker method [29]. In this method, a neutral compound is injected together with the sample. Having no charge, the neutral compound moves in the electric field with the EOF and its "migration time" can be used for the determination of the EOF. There is, however, a danger: when a charged interacting agent is present in the BGE, it can interact not only with analytes as desired, but also with the EOF marker, and thus, impart to the marker a nonzero effective mobility. Consequently, the compound cannot serve any longer as a suitable marker of the EOF. A possible complexation of the EOF marker is unfortunately often omitted in practice.

In 1997, Williams and Vigh [30] published a method for the accurate determination of the analyte mobility in the presence of a charged interacting agent. This method also uses a neutral EOF marker, but its interaction with the interacting agent is prevented by surrounding the marker zone with the BGE free of the interacting agent while the analyte zone is situated in the BGE containing interacting agent. Pressure mobilization of the capillary content is used to measure the distance between the marker and the analyte zone before and after a brief application of driving voltage. In the group of Vigh, this method was successfully used for choosing a suitable marker for particular BGEs containing a charged interacting agent [31, 32] or for indirect determination of the EOF. In the latter case the accurate effective mobility of the charged analyte in a particular interacting BGE is measured by the pressure mobilization method. Then in the standard CE run, the EOF mobility can be determined as the difference between this accurate effective mobility and the apparent mobility of this analyte [33]. However, the method requires placing the UV/Vis absorption detector (UV detector) approximately in the middle of the capillary, which is either difficult or even impossible in common commercial instruments.

Among articles dealing with the determination of interaction constants of various analytes with charged CDs, methanol seems to be the most popular EOF marker [34–43]. The other often used neutral markers are: mesityl oxide (MO) [37, 44–47], DMSO [48–52], thiourea (TU) [53], nitromethane (NM) [54], ethanol [55], and acetone [56]. Muzikar et al. [57] used water-gap next to MO to determine EOF mobility and Cai and Vigh [58] used the method of Williams and Vigh [30] mentioned above. Evans and Stalcup [20] recommended NM as a suitable EOF marker for systems with sulfated CDs. In 2002, Fuguet et al. [59] investigated suitability of various EOF markers (DMSO, TU, formamide, DMF, methanol, acetone, ACN, propan-1-ol, tetrahydrofuran) for several micellar systems: SDS, lithium dodecyl sulfate, lithium perfluorooctane sulfonate, sodium cholate, sodium deoxycholate, tetradecyltrimethylammonium bromide, and hexadecyltrimethylammonium bromide. They stated that interactions of the EOF marker with the micelles are different in each system depending on the nature of the surfactant used. Methanol, ACN, and formamide were the best EOF markers for the systems they studied. To our best knowledge, none such a study has been published for charged CDs, which are one of the most commonly used charged agents in CZE.

In this work, we compare the applicability of four popular EOF markers, which were used for determination of interaction constants of various analytes with charged CDs, namely: DMSO, MO, NM, and TU. For accurate measurement of the effective mobility of these compounds in the interacting BGE (here containing randomly sulfated β-CD (SCD)), we have developed a two-detector method (2d method). This method utilizes two detectors located on the capillary. A UV detector can be placed near the outlet of the capillary, as usual. This makes this method applicable for commercial instruments. A setup using two detectors has been already utilized in CE [60–62] mostly to avoid inaccuracy connected with the Joule heating. Conversely, the 2d method setup and procedure including pressure mobilization of the capillary content enables us to measure effective mobility without the need to evaluate the EOF mobility.

2 Materials and methods

2.1 Chemicals

All chemicals were of analytical grade purity. DMSO, MO, NM, TU, and lithium hydroxide monohydrate were purchased from Sigma Aldrich (Prague, Czech Republic). Succinic acid and NaCl were purchased from Lachema (Brno, Czech Republic). β-CD, sulfated sodium salt (Sigma Aldrich, Prague, Czech Republic), a random mixture of SCDs, was used as an interacting BGE constituent. Water used for preparation of all solutions was purified by Rowapur and Ultrapure water purification system (Watrex, San Francisco, USA).

2.2 Instrumentation

All experiments were performed using an Agilent ^{3D}CE capillary electrophoresis operated by ChemStation software (Agilent Technologies, Waldbronn, Germany). The instrument was equipped with a built-in photometric diode array detector (UV detector) and a contactless conductivity detector of our construction (CCD detector) [63]. Fused-silica capillary of 25 μm id and 375 μm od was provided by Polymicro Technologies (Phoenix, AZ, USA). The total length of the capillary was 60.8 cm, distance from inlet to CCD detector and from inlet to UV detector was 26.6 and 52.3 cm, respectively. Distance between CCD and UV detector was elongated by a capillary loop. PHM 240 pH/ION Meter (Radiometer analytical, Lyon, France) was used for pH measurements.

2.3 Experimental conditions

The running buffer without interacting agent was composed of 20 mM succinic acid and 30 mM lithium hydroxide, pH 5.5 (the choice of this buffer composition is discussed in Section 3.2). The BGE containing an interacting agent was prepared by dissolving CD directly in the running buffer solution to obtain concentration of CD of 60 g/L. Marker compounds (DMSO, MO, NM, TU) were dissolved in water and then mixed with buffer solution to prepare samples (first marker zone (M1) and third marker zone (M3) in the 2d method, samples for standard CE experiments), the markers dissolved in water were used directly as second marker zone (M2) in 2d method. Concentrations of the markers in the samples were 0.5% v/v, 0.1% v/v, 0.3% v/v, and 10 mM, for DMSO, MO, NM, and TU, respectively. All solutions were filtered using syringe filters, pore size 0.45 μm (Supelco, Bellefonte, USA). The capillary was thermostated at 25°C. Prior to use, the new capillary was flushed with water for 20 min, then with 1 M NaOH for 20 min, and then twice with water for 10 min. Prior to each run, the capillary was flushed for 12 min with buffer solution.

Distance from the capillary inlet to the CCD detector was measured by a pressure mobilization method described by Vcelakova et al. [62]. The capillary was filled with water during these measurements, the sample contained TU and NaCl dissolved in water and was injected hydrodynamically (600 mbar s), pressure used for the pressure mobilization was 45 mbar. In measurements of the conductivity of the BGE containing the CD, voltage 15 kV was applied for 3 min. The 2d procedure requires a certain distance between the two detectors (here the UV and the CCD detector). This was obtained by inserting one capillary loop in the cassette between the detectors so their distance was 25.7 cm. The distance between the capillary inlet and the CCD detector must be longer, in our case, it was 26.6 cm. Particular steps of the procedure are listed in Table 1 (exact way how to set up the 2d method is described in the Supporting Information). In standard CE experiments, samples were injected hydrodynamically, 600 mbar s. Applied voltage was 15 kV (anode at injection side). Each experiment was repeated at least four times. The computer program ChemStation (Agilent Technologies) was used for data collection and acquisition. The mathematical computer program Origin 8.1 (OriginLab Corporation, Northampton, USA) was used for fitting marker peaks with the Gaussian function. Calculations were performed by means of Microsoft Office Excel 2003 (Microsoft). Calculations needed for a choice of the BGE constituents were performed by PeakMaster 5.2 software developed in our laboratory [64].

Table 1. Particular steps of the 2d method procedure

Injection of marker zone M1	600 mbar s
Partial filling of the capillary with SCD-BGE	45 mbar · 6.0 min
Partial filling of the capillary with free-BGE	45 mbar · 24.9 min
Injection of marker zone M2	600 mbar s
Partial filling of the capillary with free-BGE	45 mbar · 5.0 min
Partial filling of the capillary with SCD-BGE	45 mbar · 2.0 min
Voltage application	15 kV, 1 min, anode at injection side
Injection of marker zone M3	600 mbar s
Pressure mobilization	45 mbar until recording zone M3 by UV detector

3 Results and discussion

3.1 2d method

The 2d method enables a precise measurement of low electrophoretic mobilities that originally neutral markers gain because of their interaction with a charged selector. In the 2d method, two detectors are utilized to measure distances between two marker zones in the capillary. The first zone of the marker is situated in the BGE containing the interacting agent, in our case SCD, and therefore, this zone can be electrophoretically mobilized by interaction with the agent. The second zone of the marker is surrounded with the BGE without the interacting agent, and thus, the interaction and consequent electrophoretic mobilization is prevented. In the 2d method procedure, a distance between the two marker zones is measured before and after a short application of voltage. The length that the first marker zone (M1) has traveled through the solution due to its interaction with the agent during the voltage application is obtained as a difference between the initial and the final distance between the two marker zones.

Two detectors must be placed on the capillary in order to measure the two above-mentioned distances (see Fig. 1). In our case, the first detector was a CCD detector and the second was a UV detector. If the effective mobility imparted to originally neutral compound by interaction with a negatively charged agent is to be measured, the distances between

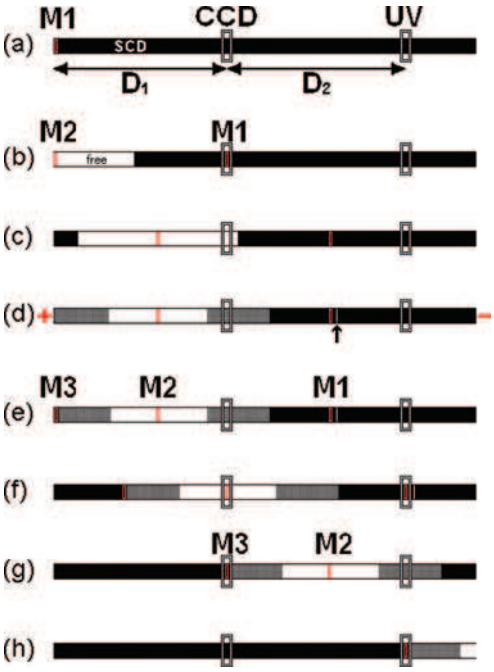

Figure 1. 2d method procedure. CCD: contactless conductivity detector, UV: UV/VIS absorption detector. Black: BGE-containing sulfated CD, white: BGE without CD, gray: area around borders between two BGEs where solution composition is changed due to the voltage application, red: marker zones, arrow: original position of the zone M1 in the solution.

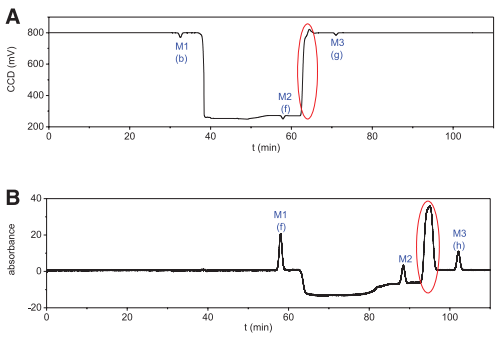

Figure 2. Signal of CCD detector and UV detector in 2d method experiment. Procedure of the method is shown in Fig. 1. (A) CCD, (B) UV detector. Letters in brackets refer to stages of the procedure, red ellipse: effect on the border of two electrolyte zones during voltage application, sample: DMSO in BGE. Detailed experimental conditions are given in Section 2.3.

the detectors should be set as follows: the distance from the capillary inlet to the first detector (D_1) should be similar, but a little longer than the distance from the first to the second detector (D_2).

The 2d method procedure is illustrated in Fig. 1. At the beginning of the measurement, the capillary is filled uniformly with the BGE-containing SCD (SCD-BGE). The M1 is injected (a), then a vial containing SCD-BGE is placed again on the inlet and pressure is applied, so the capillary is hydrodynamically partially filled with the SCD-BGE. Then, the inlet vial is changed and the capillary is filled with the interacting agent-free BGE (free-BGE). While the respective electrolytes are pushed hydrodynamically into the capillary, the M1 zone moves toward the outlet. When the zone M1 is passing the CCD detector, the second marker zone (M2) is injected (b). Finally, after the zone M2, the free-BGE is pushed again into the capillary and the entire trail of zones is completed with some additional SCD-BGE (c). After that, voltage is applied for a short time (d), while both the inlet and outlet are placed in vials containing SCD-BGE (anode at inlet side in our case of the neutral analyte and the negatively charged selector). The negatively charged SCD moves electrophoretically toward the inlet during application of the voltage. The zone M1 can also move a little in the same direction due to its interaction with the SCD, so the distance between M1 and M2 can become shorter. Simultaneously, all the capillary content moves toward the outlet with the EOF which, however, does not affect the distance between the marker zones. The voltage is switched off before either of the zones reaches any detector. When the voltage is switched off, the M3 is injected (e) by pressure (the zone M3 will serve for determining the velocity of the pressure mobilization, which is utilized for the correction terms described later). Then the capillary content is moved toward the outlet by pressure mobilization, while capillary is filled with the SCD-BGE. In an ideal case, the zone M2 passes the CCD detector and the zone M1 passes the UV detector in the same moment. In a real experiment, these two events happen almost simultaneously (f). Finally, the zone M3 is recorded by the CCD detector (g) and then by the UV detector (h).

Figure 2 shows typical CCD and UV detector records from a typical 2d method experiment. In the ideal case, M2 is injected at the very same moment when the M1 peak passes the CCD detector in step (b) of the 2d method procedure. Then the initial distance between the two marker zones M1 and M2 (L_i) is exactly equal the distance between the inlet and CCD detector, D_1. However, in a real measurement, those two events do not happen simultaneously and the distance between the two zones is:

$$L_i = D_1 + \Delta_{fil} \tag{1}$$

where Δ_{fil} is a small correction distance (either positive, negative, or zero) that must be evaluated for every particular experiment as follows:

$$\Delta_{fil} = v_{p1} \cdot \left(\int_{t(M1,CCD)}^{t(M2,treshold)} p(t) \cdot dt + q \cdot \frac{1}{2} \cdot \int_{t(M2,start)}^{t(M2,stop)} p(t) \cdot dt \right)$$

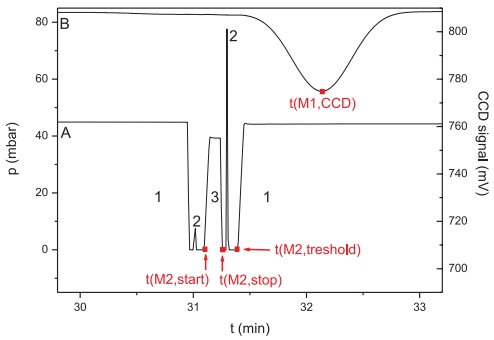

Figure 3. Detail of step (b) of 2d method procedure in real experiment. (A) applied pressure, (B) signal of the CCD detector, 1: partial filling of the capillary with free BGE, 2: artifacts connected with changing of the inlet vial, 3: hydrodynamic injection of the zone M2. Times used in calculation of Δ_{fil} are highlighted.

$$q = \mathrm{sgn}\left(\frac{t\,(M2, start) + t\,(M2, stop)}{2} - t\,(M1, CCD)\right) \tag{2}$$

where p is the applied pressure; v_{p1} is the pressure mobilization velocity; t (*M1,CCD*) is the time, when the zone M1 passes the CCD detector; t (*M2,treshold*) is the time when either filling the capillary with the free-BGE is finished before injection of the zone M2 or the time when filling the capillary with the free-BGE starts again after the zone M2 has been injected (depending on whether the zone M1 passes the CCD detector before or after injection of the zone M2, respectively); t (*M2,start*) is the time when the injection of the zone M2 begins; t (*M2,stop*) is the time when the injection of the zone M2 is ended.

A detail of step (b) in a real experiment is shown in Fig. 3 that depicts the record of the applied pressure and the signal of the first (CCD) detector, where the passage of the zone M1 appears as a negative peak. The times used in calculation of the Δ_{fil}, t (*M2,start*), t (*M2,stop*), t (*M2,treshold*), and t (*M1,CCD*), are highlighted in the picture.

The final distance between the two zones M1 and M2 (L_f) is measured in the step (f) of the procedure. In the ideal case, during the voltage application, the zone M1 migrates the distance D_1–D_2. Therefore, the final distance between the marker zones exactly equals the distance between the two detectors, D_2. Thus, the M1 peak passes the UV detector at the very same moment when the M2 peak passes the CCD detector. However, in a real measurement, those two events do not happen simultaneously, so the real final distance between the two zones is, therefore:

$$L_f = D_2 + \Delta_{det} \tag{3}$$

$$\Delta_{det} = v_{p2} \cdot \int_{t(M1,UV)}^{t(M2,CCD)} p\,(t) \cdot dt \tag{4}$$

where Δ_{det} is a small correction distance (either positive, negative, or zero) that must be evaluated for every particular experiment; v_{p2} is the pressure mobilization velocity (difference between v_{p1} and v_{p2} will be specified later); t (*M1,UV*) is the time when the zone M1 passes the UV detector; t (*M2,CCD*) is the time when the zone M2 passes the CCD detector.

Finally, the distance L_{mig} that the marker M1 passes in the solution due to its interaction with the SCD is:

$$L_{mig} = L_f - L_i = D_2 + \Delta_{det} - \left(D_1 + \Delta_{fil}\right) \tag{5}$$

The effective mobility of the marker u_{eff} is calculated according to the method published by Vigh [30]:

$$u_{eff} = \frac{L_{mig} \cdot S \cdot \kappa_{SCD}}{\int_{t_{U1}}^{t_{U2}} I\,(t) \cdot dt} \tag{6}$$

where S is the cross-section of the capillary; κ_{SCD} is conductivity of the SCD-BGE; t_{U1} and t_{U2} are the times when the voltage was switched on and off, respectively; and I is the electric current during the application of the voltage.

Two aspects should be considered as regards the reliability of the method, both closely connected with the inhomogeneous filling of the capillary. First, the magnitude of the EOF is influenced, among others, by the ionic strength of the BGE [65]. Therefore, the EOF in the capillary filled with SCD-BGE will differ from the EOF in the capillary filled with the free-BGE due to different ζ-potential of the capillary wall. Therefore, in a capillary where the ζ-potential axially varies (which is the case of a heterogenously filled capillary in 2d method), the EOF can be different in different parts of the capillary, as discussed in the study by Williams and Vigh [30]. Nevertheless, these differences in the EOF along the capillary cause a balancing viscous flow and consequently, combination of this viscous flow and the EOF results in an axially invariant bulk flow satisfying the mass conservation. Therefore, the bulk flow is constant along the capillary during the voltage application (step (d) of the 2d method). The axially homogenous bulk flow can also vary in time, during the voltage application. Yet, as this has no effect on the distance between the zones M1 and M2, it cannot influence the performance of the 2d method. Second, addition of CD increases viscosity of solution and therefore, the viscosities of SCD-BGE and free-BGE differ. As ratio of volumes of these two electrolytes in the capillary changes, the velocity of the movement due to pressure mobilization also slightly varies. Therefore, the pressure mobilization velocities v_{p1} and v_{p2} are given by:

$$v_{p1} = \frac{D_2}{\int_{t(M3,CCD)}^{t(M3,UV)} p\,(t) \cdot dt} \tag{7}$$

$$v_{p2} = \frac{D_1}{\int_{t(M3,inj)}^{t(M3,CCD)} p\,(t) \cdot dt} \tag{8}$$

where $t(M3,inj)$, $t(M3,CCD)$, and $t(M3,UV)$ are the times, when the zone M3 is injected, passes the CCD detector and passes the UV detector, respectively.

As can be seen in Fig. 1b, during the injection of the zone M2, a smaller part of the capillary is filled with free-BGE compared to the rest of the procedure. That is why the time interval between $t(M3,CCD)$ (Fig. 1g) and $t(M3,UV)$ (Fig. 1h) is used for calculation of the mobilization velocity v_{p1}. However, the ratio of SCD-BGE and free-BGE in the capillary does not change at all during the interval between $t(M3,inj)$ (Fig. 1e) and $t(M3,CCD)$ (Fig. 1g) and is exactly the same as at $t(M2,CCD)$ and $t(M1,UV)$ (Fig. 1g). Therefore, this time interval is used for the calculation of v_{p2}. The reason that justifies using two detectors in our experimental setup is that it is technically convenient to place the CCD detector somewhere around the half of the capillary (especially with the Agilent ^{3D}CE equipment) while the UV detector is usually fixed at the end of the capillary. The CCD, on the other hand, is not capable to detect a neutral analyte. Therefore, it cannot detect the marker zone in SCD-BGE after the voltage application. In our method, the marker zone M1 (having lower conductivity than the SCD-BGE surrounding it) is detected by the CCD detector before the voltage application (step (b) of the procedure) before any electrophoretic migration occurs. When the marker zone M2 is recorded by the CCD detector in step (f) of the procedure, it is actually the water gap (a zero-system mobility peak) that is detected. The zero mobility of the detected system peak can be easily secured by a proper selection of the free-BGE constituents and verified, e.g. by means of PeakMaster calculation [64] (therefore, no analyte is even needed in the M2 zone in principle). On the other hand, this is not possible for the M1 zone where the presence of the complexing agent may introduce unpredictable system peaks, especially in the case of selectors such are highly charged CDs with unknown mobilities and even with unknown exact composition [66, 67].

The uncertainty in distance D_1 is the source of an error of the 2d method. In our case, this distance can be determined only by a pressure mobilization method [62]. Since the measured distance D_1 is a sum of a real distance D_1^* and an error of its measurement e, then the finally determined migration distance L_{mig} is affected two times by this error:

$$\begin{aligned} D_1 &= D_1^* + e \\ D_2 &= D_{UV} - D_1^* - e \\ L_{mig} &= D_2 + \Delta_{det} - \left(D_1 + \Delta_{fil}\right) \\ &= D_{UV} - D_1^* - e + \Delta_{det} - \left(D_1^* + e + \Delta_{fil}\right) \\ &= D_{UV} - 2D_1^* + \Delta_{det} - \Delta_{fil} - 2e \end{aligned} \tag{9}$$

where D_{UV} is the distance from the capillary inlet to the UV detector. SD of D_1 as measured in our experiments was 0.15 mm, which implies the precision of L_{mig} was 0.3 mm. This length corresponds to the error in effective mobility of $0.6{\cdot}10^{-9}\mathrm{m^2V^{-1}s^{-1}}$.

3.2 Effective mobilities of markers

The 2d method was used to determine effective mobilities of four compounds commonly used as EOF markers. These were DMSO, MO, NM, and TU. On usual terms, these compounds are neutral and therefore do not have any effective mobility so they can serve for determining the mobility of the EOF. However, in a BGE containing a charged interacting agent, the neutral marker can be potentially mobilized by interaction with the agent. Therefore, we verified by the 2d method whether these traditional neutral markers have some effective mobility in the presence of negatively charged SCD (concentration 60g/L).

Distance between the capillary inlet and UV detector D_{UV} as well as the total capillary length was measured directly (by a ruler). However, exact distance D_1 could not be measured in this way because of the construction of the CCD detector. This distance was, therefore, determined by pressure mobilization method described in [62]. The free-BGE had to be chosen carefully to meet the following criteria: (i) at least one of the system mobilities had to be close enough to zero (this is often the case), (ii) all other nonzero system mobilities had to be high enough to move far from the zero position in order not to interfere with the zero peak. Additionally, because the free-BGE was also used for preparation of the SCD-BGE, it should be composed of small molecules in order not to provide concurrent interactions with the selector. Therefore our choice was the BGE consisting of 20 mM succinic acid and 30 mM lithium hydroxide (both are small molecules) which exhibits two system mobilities of $0.008{\cdot}10^{-9}$SCD and $-26.4{\cdot}10^{-9}$ $\mathrm{m^2V^{-1}s^{-1}}$ (calculated by PeakMaster 5.2 [64]).

For evaluation of the effective mobility, the conductivity of the SCD-BGE, κ_{SCD}, must be known (see Eq. (6)). It was measured in separate experiments: the voltage was applied on the capillary homogenously filled with the SCD-BGE and the current I_{hom} was recorded. The conductivity is then:

$$\kappa_{SCD} = \frac{I_{hom} \cdot D_T}{S \cdot U} \tag{10}$$

where D_T is a total length of the capillary and U is the voltage applied.

The L_{mig} and u_{eff} measured by the 2d method are given in Table 2. Absolute values of L_{mig} are significantly higher than the error of the measurement (0.3 mm) which implies

Table 2. Length L_{mig} and corresponding effective mobility u_{eff} resulting from 2d method

	Control measurements (without SCD)	In the BGE-containing SCD	
Marker	L_{mig} (mm)	L_{mig} (mm)	u_{eff} ($10^{-9}\mathrm{m^2V^{-1}s^{-1}}$)
DMSO	0.17 ± 0.07	-0.8 ± 0.1	-1.5 ± 0.2
MO	0.08 ± 0.05	-0.9 ± 0.1	-1.8 ± 0.2
NM	0.22 ± 0.03	-0.8 ± 0.1	-1.5 ± 0.2
TU	0.02 ± 0.05	-1.4 ± 0.1	-3.0 ± 0.2

Table 3. Differences between apparent mobilities in standard CE run and differences between effective mobilities determined by 2d method

Markers		Classical method $u_{app}(1) - u_{app}(2)$ [a)]	2d method $u_{eff}(1) - u_{eff}(2)$
(1)	(2)	($10^{-9}m^2V^{-1}s^{-1}$)	($10^{-9}m^2V^{-1}s^{-1}$)
DMSO	TU	1.3	1.4 ± 0.3
MO	TU	1.1	1.2 ± 0.2
NM	TU	1.3	1.4 ± 0.2
DMSO	MO	0.3	0.3 ± 0.3

a) RSD did not exceed 4%.

that all these markers undertake observable interaction with the sulfated CD. The resulting negative L_{mig} was observed, which should be expected due to the negative mobility of the selector. Control measurements were carried out in order to confirm the 2d method reliability. In these measurements, exactly the same procedure was applied as in experiments with SCD, but the free-BGE was used. Therefore, zero L_{mig} values should result from the control measurements. As can be seen from Table 2, all the L_{mig} lengths measured in the control experiments were less than the precision of the method (0.3 mm).

To verify this surprising finding, we performed standard CE experiments where the neutral markers were used as analytes. In these experiments, SCD-BGE was used as a BGE and two different EOF markers were present in the sample (the pairs of markers are listed in Table 3). Detection at two wavelengths (238 nm and 214 nm) allowed discriminating the two markers according to their specific ratio of peak heights at the two wavelengths. All pairs containing TU were baseline separated (Fig. 4A). Apparently, the separation, though not baseline, was observed between DMSO and MO (Fig. 4B). A mobility difference between each two markers was evaluated from each standard CE experiment. These differences were compared to those determined by the 2d method (Table 3). Remarkably good agreement was observed, which further confirms the results of the 2d method. The results clearly confirm that there is interaction of the generally used EOF markers with the SCD used as a selector.

The standard CE method cannot measure absolute value of the effective mobility. In the standard CE separation, there is no "zero" for comparing the apparent mobility of the studied marker. Even a water-gap cannot mark the zero position correctly, as the water-gap is in fact a system zone and behavior of system zones in BGEs containing an interacting agent is not yet sufficiently described. Therefore, the only way how to determine absolute value of the effective mobility of a weakly interacting compound is to use a more sophisticated method like the 2d method we proposed.

The results of the 2d method measurements have shown that all the markers studied undertake interaction. The weakest interaction was observed for DMSO and NM and therefore these are the most suitable EOF markers for the BGE containing SCD. However, even these compounds are slightly mobilized by the interacting agent and this must be taken into account, especially when low mobilities of analytes are being determined. On the other hand, the determined effective mobility of TU was rather high, and therefore, TU appeared to be definitely an inappropriate EOF marker for this system.

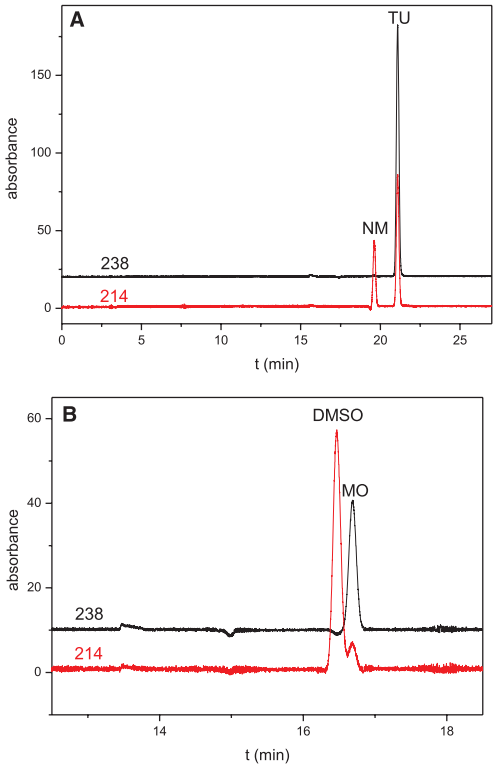

Figure 4. UV detector signal from standard CE experiments. BGE: 20 mM succinic acid, 30 mM LiOH, 60 g/L randomly SCD sodium salt, sample (A): NM and TU dissolved in BGE, sample (B): DMSO and MO dissolved in BGE.

4 Concluding remarks

The proposed 2d method is capable of measurement of accurate effective mobilities in BGEs containing charged interacting agents, for example, a low effective mobility that an originally neutral EOF marker gained from interaction with the agent. The method is based on the pressure mobilization as well as the method published by Williams and Vigh [30]. However, the 2d method is more easily applicable in commercial instrumentation. By this method, we have

determined effective mobilities of DMSO, MO, NM, and TU (compounds often used as EOF markers) in BGE containing SCD, an often used chiral selector. Differences between these effective mobilities were compared with results of standard CE experiments with good agreement. All the compounds studied were mobilized by interaction with the selector. TU had the highest effective mobility (in absolute value), and therefore, appeared to be an inappropriate EOF marker for this system. NM and DMSO appeared to be suitable EOF markers, however, even they were slightly mobilized by the week interaction with the selector. It should be taken into account when they are used as EOF markers.

The authors acknowledge the financial support of this work from Grant No. 203/08/1428 and Grant No. P206/12/P630 of the Grant Agency of the Czech Republic, from the Grant No. 669412 of the Grant Agency of Charles University and from the long-term research plan of the Ministry of Education of the Czech Republic, MSM 0021620857.

The authors have declared no conflict of interest.

5 References

[1] Van Eeckhaut, A., Michotte, Y., *Electrophoresis* 2006, *27*, 2880–2895.

[2] Guebitz, G., Schmid, M. G., *J. Chromatogr. A* 2008, *1204*, 140–156.

[3] Lu, H. A., Chen, G. N., *Anal. Methods* 2011, *3*, 488–508.

[4] Schmitt, U., Branch, S. K., Holzgrabe, U., *J. Sep. Sci.* 2002, *25*, 959–974.

[5] Scriba, G. K. E., *Electrophoresis* 2003, *24*, 4063–4077.

[6] Juvancz, Z., Kendrovics, R. B., Ivanyi, R., Szente, L., *Electrophoresis* 2008, *29*, 1701–1712.

[7] Scriba, G. K. E., *J. Sep. Sci.* 2008, *31*, 1991–2011.

[8] Cucinotta, V., Contino, A., Giuffrida, A., Maccarrone, G., Messina, M., *J. Chromatogr. A* 2010, *1217*, 953–967.

[9] Kitagawa, F., Otsuka, K., *J. Chromatogr., B: Anal. Technol. Biomed. Life Sci.* 2011, *879*, 3078–3095.

[10] Fanali, S., *Electrophoresis* 2009, *30*, S203–S210.

[11] Chankvetadze, B., *Electrophoresis* 2009, *30*, S211–S221.

[12] Kwaterczak, A., Duszczyk, K., Bielejewska, A., *Anal. Chim. Acta* 2009, *645*, 98–104.

[13] Morin, P., Bellessort, D., Dreux, M., Troin, Y., Gelas, J., *J. Chromatogr. A* 1998, *796*, 375–383.

[14] Dubsky, P., Svobodova, J., Gas, B., *J. Chromatogr., B: Anal. Technol. Biomed. Life Sci.* 2008, *875*, 30–34.

[15] Dubsky, P., Svobodova, J., Tesarova, E., Gas, B., *Electrophoresis* 2010, *31*, 1435–1441.

[16] Verleysen, K., Van den Bosch, T., Sandra, P., *Electrophoresis* 1999, *20*, 2650–2655.

[17] Perrin, C., Vander Heyden, Y., Maftouh, M., Massart, D. L., *Electrophoresis* 2001, *22*, 3203–3215.

[18] Matthijs, N., Perrin, C., Maftouh, M., Massart, D. L., Vander Heyden, Y., *J. Pharm. Biomed. Anal.* 2002, *27*, 515–529.

[19] Vescina, M. C., Fermier, A. M., Guo, Y., *J. Chromatogr. A* 2002, *973*, 187–196.

[20] Evans, C. E., Stalcup, A. M., *Chirality* 2003, *15*, 709–723.

[21] Gomez-Gomar, A., Ortega, E., Calvet, C., Andaluz, B., Merce, R., Frigola, J., *J. Chromatogr. A* 2003, *990*, 91–98.

[22] Wren, S. A. C., Rowe, R. C., *J. Chromatogr.* 1992, *603*, 235–241.

[23] Williams, B. A., Vigh, G., *J. Chromatogr. A* 1997, *777*, 295–309.

[24] Busch, M. H. A., Carels, L. B., Boelens, H. F. M., Kraak, J. C., Poppe, H., *J. Chromatogr. A* 1997, *777*, 311–328.

[25] Rundlett, K. L., Armstrong, D. W., *Electrophoresis* 2001, *22*, 1419–1427.

[26] Tanaka, Y., Terabe, S., *J. Chromatogr., B: Anal. Technol. Biomed. Life Sci.* 2002, *768*, 81–92.

[27] Jiang, C. X., Armstrong, D. W., *Electrophoresis* 2010, *31*, 17–27.

[28] Wang, W., Zhou, F., Zhao, L., Zhang, J. R., Zhu, J. J., *J. Chromatogr. A* 2007, *1170*, 1–8.

[29] Lukacs, K. D., Jorgenson, J. W., *HRC & CC, J. High Resolut. Chromatogr. Chromatogr. Commun.* 1985, *8*, 407–411.

[30] Williams, B. A., Vigh, G., *Anal. Chem.* 1997, *69*, 4445–4451.

[31] Li, S. L., Vigh, G., *Electrophoresis* 2003, *24*, 2487–2498.

[32] Tutu, E., Vigh, G., *Electrophoresis* 2011, *32*, 2655–2662.

[33] Cai, H., Nguyen, T. V., Vigh, G., *Anal. Chem.* 1998, *70*, 580–589.

[34] Martin-Biosca, Y., Garcia-Ruiz, C., Marina, M. L., *Electrophoresis* 2000, *21*, 3240–3248.

[35] Mori, M., Naraoka, H., Tsue, H., Morozumi, T., Kaneta, T., Tanaka, S., *Anal. Sci.* 2001, *17*, 763–768.

[36] Bo, T., Yang, X. D., Gao, F., Liu, H. W., Li, K. A., Xiu, L. Z., *Chromatographia* 2002, *55*, 217–223.

[37] Suss, F., Sanger-Van de Griend, C., Scriba, G. K. E., *Electrophoresis* 2003, *24*, 1069–1076.

[38] Ivanyi, R., Jicsinszky, L., Juvancz, Z., Roos, N., Otta, K., Szejtli, J., *Electrophoresis* 2004, *25*, 2675–2686.

[39] Lin, C. E., Lin, S. L., Cheng, H. T., Fang, I. J., Kuo, C. M., Liu, Y. C., *Electrophoresis* 2005, *26*, 4187–4196.

[40] Lucangioli, S. E., Tripodi, V., Masrian, E., Scioscia, S. L., Carducci, C. N., Kenndler, E., *J. Chromatogr. A* 2005, *1081*, 31–35.

[41] Tang, W. H., Muderawan, I. W., Ng, S. C., Chan, H. S. O., *Anal. Chim. Acta* 2005, *554*, 156–162.

[42] Wu, S. H., Ding, W. H., *Electrophoresis* 2005, *26*, 3528–3537.

[43] Al Azzam, K. M., Saad, B., Aboul-Enein, H. Y., *Electrophoresis* 2010, *31*, 2957–2963.

[44] Rodriguez, M. A., Liu, Y., McCulla, R., Jenks, W. S., Armstrong, D. W., *Electrophoresis* 2002, *23*, 1561–1570.

[45] Ha, P. T. T., Van Schepdael, A., Van Vaeck, L., Augustijns, P., Hoogmartens, J., *J. Chromatogr. A* 2004, *1049*, 195–203.

[46] Lin, C. E., Lin, S. L., Fang, I. J., Liao, W. S., Chen, C. C., *Electrophoresis* 2004, *25*, 2786–2794.

[47] Lantz, A. W., Rodriguez, M. A., Wetterer, S. M., Armstrong, D. W., *Anal. Chim. Acta* 2006, *557*, 184–190.

[48] Marziali, E., Raggi, M. A., Komarova, N., Kenndler, E., *Electrophoresis* 2002, *23*, 3020–3026.

[49] Stettler, A. R., Schwarz, M. A., *J. Chromatogr. A* 2005, *1063*, 217–225.

[50] Vaccher, M. P., Lipka, E., Bonte, J. P., Foulon, C., Goossens, J. F., Vaccher, C., *Electrophoresis* 2005, *26*, 2974–2983.

[51] Kwaterczak, A., Duszczyk, K., Bielejewska, A., *Anal. Chim. Acta* 2009, *645*, 98–104.

[52] Sohajda, T., Beni, S., Varga, E., Ivanyi, R., Racz, A., Szente, L., Noszal, B., *J. Pharm. Biomed. Anal.* 2009, *50*, 737–745.

[53] Karakasyan, C., Taverna, M., Millot, M. C., *J. Chromatogr. A* 2004, *1032*, 159–164.

[54] Gratz, S. R., Stalcup, A. M., *Anal. Chem.* 1998, *70*, 5166–5171.

[55] Danel, C., Duval, C., Azaroual, N., Vaccher, C., Bonte, J. P., Bailly, C., Landy, D., Goossens, J. F., *J. Chromatogr. A* 2011, *1218*, 8708–8714.

[56] Zakaria, P., Macka, M., Haddad, P. R., *Electrophoresis* 2004, *25*, 270–276.

[57] Muzikar, M., Havel, J., Macka, M., *Electrophoresis* 2002, *23*, 1796–1802.

[58] Cai, H., Vigh, G., *J. Microcolumn Sep.* 1998, *10*, 293–299.

[59] Fuguet, E., Rafols, C., Bosch, E., Roses, M., *Electrophoresis* 2002, *23*, 56–66.

[60] Beckers, J. L., Verheggen, T. P. E. M., Everaerts, F. M., *J. Chromatogr.* 1988, *452*, 591–600.

[61] Kasicka, V., Prusik, Z., Mudra, P., Stepanek, J., *J. Chromatogr. A* 1995, *709*, 31–38.

[62] Vcelakova, K., Zuskova, I., Kenndler, E., Gas, B., *Electrophoresis* 2004, *25*, 309–317.

[63] Gas, B., Zuska, J., Coufal, P., van de Goor, T., *Electrophoresis* 2002, *23*, 3520–3527.

[64] Jaros, M., Hruska, V., Stedry, M., Zuskova, I., Gas, B., *Electrophoresis* 2004, *25*, 3080–3085.

[65] VanOrman, B. B., Liversidge, G. G., McIntire, G. L., Olefirowicz, T. M., Ewing, A. G., *J. Microcolumn Sep.* 1990, *2*, 176–180.

[66] Chen, F. T. A., Shen, G., Evangelista, R. A., *J. Chromatogr. A* 2001, *924*, 523–532.

[67] Amini, A., Rundlof, T., Rydberg, M. B. G., Arvidsson, T., *J. Sep. Sci.* 2004, *27*, 1102–1108.

4.4 Určení parametrů HVL funkce z geometrických charakteristik píku

HVL funkce (21) je vhodným popisem tvaru píku deformovaného elektromigrační disperzí. V kontextu této dizertační práce je významný především její parametr a_1, který má význam migračního času odpovídajícího efektivní mobilitě analytu při jeho nekonečném zředění. Hodnotu tohoto parametru je tedy třeba určit pro daný EMD deformovaný pík analytu, aby bylo možné z daného elektroforetického experimentu správně vyhodnotit efektivní mobilitu analytu – která pak slouží například ke stanovení komplexačních parametrů metodou ACE.

Tvar EMD deformovaného píku lze také popsat pomocí určitých geometrických charakteristik, které může například automaticky odečítat software pro sběr elektroforetických dat. Těmito charakteristikami jsou:

(i) čas odpovídající maximu píku, t_M;

(ii) šířka píku v určité frakci jeho maximální výšky w_α, $\alpha \in (0; 1)$ (například $w_{0,5}$ – šířka v polovině výšky);

(iii) asymetrie píku q. Ta může být definována například jako poměr šířek píku ve dvou různých frakcích jeho maximální výšky w_β / w_α, či jako poměr pravé a levé položířky v určité frakci maximální výšky píku $w_{P\alpha}/w_{L\alpha}$. ChemStation software dodávaný spolu s CE přístroji firmy Agilent Technologies používá faktor chvostování píku podle Amerického lékopisu (*U. S. Pharmacopeia tailing factor*), $T_{USP} = w_{0,05}/\left(2 \cdot w_{L0,05}\right)$, poměr šířky píku v 5 % výšky ku dvounásobku levé položířky v 5 % výšky.

Nicméně vztah mezi těmito „viditelnými“ geometrickými charakteristikami píku na jedné straně a na straně druhé parametry odpovídající HVL funkce (21), které mají fyzikální význam, není přímočarý. Proto bylo dosud nutné určit parametry HVL funkce nelineární regresí, což vyžadovalo export experimentálního elektroferogramu do vhodného softwaru (například Origin).

Jak je detailně odvozeno v *Publikaci VI*, asymetrie píku q závisí z parametrů HVL funkce pouze na parametru a_3, $q = f_q(a_3)$. Lze tedy definovat závislost parametru a_3 na geometrické charakteristice asymetrie píku q:

$$a_3 = f_q^{-1}(q) \tag{38}$$

Dále lze odvodit vztah mezi parametry a_1 (migrační čas odpovídající efektivní mobilitě) a a_2 (symetrické rozšíření píku) a geometrickými charakteristikami t_M a w_α:

$$a_1 = t_M - w_\alpha \cdot K_\alpha(a_3) \equiv t_M - w_\alpha \cdot K_\alpha(q) \tag{39}$$

$$a_2 = w_\alpha \cdot L_\alpha(a_3) \equiv w_\alpha \cdot L_\alpha(q) \tag{40}$$

Hodnoty převodních parametrů K_α a L_α pro zvolené α závisí opět pouze na parametru a_3 a tedy skrze rovnici (38) na geometrické charakteristice asymetrie píku q.

Bohužel, závislost žádného z parametrů a_3, K_α a L_α na geometrické charakteristice q nelze vyjádřit analytickým výrazem. Nicméně pro zvolenou hodnotu α a daný způsob vyjádření asymetrie píku q lze závislost těchto parametrů na hodnotě q určit numericky. To bylo v *Publikaci VI* provedeno pro $\alpha = 0{,}5$ a $q = T_{USP}$, protože $w_{0,5}$ a T_{USP} jsou geometrické charakteristiky píku odečítané automaticky softwarem ChemStation. Získané závislosti jsou uvedeny v *Publikaci VI* (Figure 1). Tyto závislosti byly zaneseny do souboru MS Excel (lze stáhnout ze stránek naší výzkumné skupiny [77]), který na jejich základě přepočítá geometrické charakteristiky t_M, $w_{0,5}$ a T_{USP} poskytnuté softwarem ChemStation na parametry příslušné HVL funkce a_1, a_2 a a_3.

Správnost takto určených parametrů byla v *Publikaci VI* ověřena jejich porovnáním s výsledky fitování píků pomocí programu Origin 8.1 a to jednak pro píky simulované v programu Simul 5 Complex [78], jednak pro reálný elektroferogram (*Publikace VI*, Table 1, Table 2, Figure 3). Shoda byla velmi dobrá. V případě reálného elektroferogramu byla chyba srovnatelná s frekvencí, s jakou jsou experimentální data přístrojem zaznamenávána.

Parametry HVL funkce spočtené výše uvedeným způsobem lze použít přímo – například parametr a_1 pro výpočet efektivní mobility analytu při jeho nekonečném zředění, nebo mohou sloužit jako velmi přesný počáteční odhad pro nelineární regresi.

Publikace VI

Determination of the correct migration time and other parameters of the Haarhoff–van der Linde function from the peak geometry characteristics

P. Dubský, M. Dvořák, **L. Müllerová**, B. Gaš

Electrophoresis 2015, *36*, 655-661.

Pavel Dubský
Martin Dvořák
Ludmila Műllerová
Bohuslav Gaš

Department of Physical and Macromolecular Chemistry, Faculty of Science, Charles University in Prague, Prague, Czech Republic

Received October 1, 2014
Revised November 14, 2014
Accepted November 14, 2014

Research Article

Determination of the correct migration time and other parameters of the Haarhoff–van der Linde function from the peak geometry characteristics

For Gaussian peaks, the migration time of the analyte results as the position of the top of the peak and the zone variance is proportional to the peak width. Similar relations have not yet been derived for the Haarhoff–van der Linde (HVL) function, which appears as a fundamental peak-shape function in electrophoresis. We derive the relations between the geometrical measures of the HVL-shaped peak, that is the position of its maximum, its width and a measure of its asymmetry, and the respective parameters a_1, a_2, and a_3, of the corresponding HVL function. Under the condition of the HVL-shaped peak, the a_1 parameter reflects the true migration time of the analyte, which may differ from the peak top position significantly. Our procedure allows us to express the parameters without the need of any external data processing (nonlinear regression). We demonstrate our approach on simulated peaks and on experimental data integrated by the ChemStation software (delivered with the CE instrumentation by Agilent Technologies). A significant improvement is achieved reading the migration time of the experimental and simulated peaks, which draws the error of the HVL-shaped peak migration time evaluation down to the resolution of the data sampling rate.

Keywords:
Electromigration dispersion / Haarhoff–van der Linde / Migration time
DOI 10.1002/elps.201400463

1 Introduction

In CZE measurements, asymmetrical peaks are often observed due to electromigration dispersion (EMD). EMD is caused by local changes in electrophoretic mobility of a substance/analyte in the zone of the corresponding peak. These changes in electrophoretic mobility may be related to changes in pH or conductivity in the zone of the particular peak or to the presence of complex-forming constituents in BGE [1–3]. Erny et al. [4, 5] showed that the Haarhoff–van der Linde (HVL) function [6] often correctly describes peak shapes observed in CZE and is very suitable for fitting CZE peaks. The HVL function was also found to be the solution of the linearized model of electromigration with a small nonlinear disturbance [7].

Other peak-shape functions have been proposed. While the HVL function is exactly valid only for an infinitely narrow injection zone, the so-called HVLR function additionally results as the solution of the linearized model of electromigration as the injection zone grows in width [7]. The situation further complicates if the conditions of the linearized model are not satisfied. In such cases some semiempirical approaches succeeded in finding a suitable peak-shape function [8, 9].

In this we focus on the HVL peak function, mainly for the following two reasons. First, we intend to provide a fundamental mathematical analysis of the HVL function that results in formulas that relate the geometrical properties of the function to its parameterization given in the theoretical section. This practice is similar to that applied on the Gaussian-shaped peaks, where the peak variance is estimated, for example from its FWHM. Second, the linearized theory of electromigration shows that as far as the peak of the analyte obeys the HVL shape, the a_1 parameter of the HVL function gives the correct migration time of the analyte (as expected from its electrophoretical mobility). The herein-introduced relations will provide a correction term that allows the analysts to find the (unobservable) a_1 position of the peak from its directly observable properties, such as the peak top position, width, and asymmetry. Unfortunately though, the relations cannot be found in the closed form. Instead, a lookup table of a set of coefficients is introduced. This procedure is still generally more convenient compared to the otherwise needed

Correspondence: Dr. Pavel Dubský, Department of Physical and Macromolecular Chemistry, Faculty of Science, Charles University in Prague, Albertov 2030, CZ-128 40 Prague 2, Czech Republic
E-mail: pavel.dubsky@natur.cuni.cz

Abbreviations: EMD, electromigration dispersion; **HVL**, Haarhoff–van der Linde

Colour Online: See the article online to view Figs. 1–3 in colour.

data export and nonlinear curve fitting. It allows us to utilize the output of the standard data integration software and a simple tool such as MS Excel for a_1 calculation as we will demonstrate in the experimental section.

It should be pointed out that there are two different parameterizations of the HVL function in the literature. The older type of parameterization, which was first used in the software PeakFit® (www.sigmaplot.com) and thereafter adopted by Erny et al. [4] and many other authors, is defined by the following formula:

$$HVL(t; a_0, a_1, a_2, a_3) = \frac{\frac{a_0 a_2}{a_1 a_3 \sqrt{2\pi}} \exp\left[\frac{-1}{2}\left(\frac{t-a_1}{a_2}\right)^2\right]}{\frac{1}{\exp\left(\frac{a_1 a_3}{a_2^2}\right)-1} + \frac{1}{2}\left[1+\mathrm{erf}\left(\frac{t-a_1}{\sqrt{2}a_2}\right)\right]}, \tag{1}$$

where a_0 is the area of the peak. Although not explicitly stated in Eq. (1), parameters a_1 and a_2 are dependent on time, namely $a_1 = v_0 t$ and $a_2 = \sqrt{2\delta t}$, where v_0 is the linear velocity and δ the diffusion coefficient of the electromigration zone corresponding to the particular peak. These two terms, v_0 and δ, are explained in [7] in more detail. The parameter a_2 describes diffusional (symmetrical) broadening of the peak and as we shall see later, it is directly proportional to the peak width. The parameter a_3 is usually said to be a measure of the peak distortion and is defined as the ratio $-v_{\mathrm{EMD}}/v_0$, where v_{EMD} is the difference in the electromigration velocity at the base and at the top of the peak. It can be indeed shown that the HVL function becomes a symmetrical Gaussian function if $a_3 = 0$ regardless of the choice of the remaining parameters and it becomes asymmetric as $a_3 \neq 0$. The parameter a_3 enters the definition of the HVL function in two ways. First, it appears in the numerator of the HVL function where it plays only a role of a multiplicative factor having no influence on the asymmetry of the HVL function. Hence, the asymmetry of the HVL function must be governed by the term $\exp(\frac{a_1 a_3}{a_2^2})$ in the denominator. However, the value of this asymmetry-determining term depends not only on a_3 but also on a_1 and a_2. Therefore, the value of a_3 itself is not deterministic for the peak distortion (asymmetry). From the physical perspective, the parameter a_3, although closely related to the EMD, does not take into account the effect of the diffusion. Yet, it is the counterbalance of the EMD and diffusion that determines the final peak shape. At this point, the second type of parameterization of the HVL function naturally follows from the linear model of electromigration and was introduced in the aforementioned paper by Hruška et al. [7]. The related formula is:

$$HVL_\delta(t; a_0, a_1, a_2, a_{3\delta}) = \frac{\frac{a_0}{a_2 a_{3\delta}\sqrt{2\pi}} \exp\left[-\frac{1}{2}\left(\frac{t-a_1}{a_2}\right)^2\right]}{\frac{1}{\exp(a_{3\delta})-1} + \frac{1}{2}\left[1+\mathrm{erf}\left(\frac{t-a_1}{\sqrt{2}a_2}\right)\right]}. \tag{2}$$

The definition of the parameters a_0, a_1, and a_2 remains unchanged. The only difference lies in the definition of the parameter $a_{3\delta}$, which now equals $-v_{\mathrm{EMD}}/2\delta$ and includes both effects of the EMD and the diffusion (therefore the δ subscript). After this redefinition of the a_3 parameter, the asymmetry-determining term depends only on $a_{3\delta}$ (see Eq. (2)), so the geometrical distortion (asymmetry) of the peak is given solely by the $a_{3\delta}$ value. Later in this article, we will use this latter parameterization (Eq. (2)). Notice, however, that both the parameterizations describe exactly the same HVLi peak shape and result in the same a_0, a_1 , and a_2 parameters. The $a_{3\delta}$ is given by substitution $a_{3\delta} = \frac{a_1 a_3}{a_2^2}$. Therefore we will further omit the δ subscript in HVL_δ (Eq. (2)) and stay on the general term "HVL function."

If the peaks are significantly distorted due to the EMD, a question arises what is the "true" migration time as expected from the effective electrophoretic mobility of the analyte. The analyte migration time is usually measured at the top of the electrophoretic peak. Nevertheless, Le Saux et al. [10] have proven that the peak apex position, t_M, shifts with increasing the analyte concentration leading to over- or underestimation of the analyte effective mobility. Instead, the parameter a_1 of the HVL function fitted to the peak is proposed as the accurate migration time, which does not depend on the analyte concentration. This is later substantiated by the linear theory of electromigration [7], which stays that the a_1 parameter of the HVL function be the expected migration time of the analyte. Based on this justification we will use the a_1 parameter in the meaning of the parameter of the HVL function as well as the correct migration time of the analyte interchangeably throughout this article. For the sake of clarity, we will further refer to the migration time of the top of the peak, t_{M}, as to the "experimental" migration time, while the expected migration time of the analyte, a_1, will be denoted as the "theoretical" migration time. Notice that if there is no EMD, $a_3 \to 0$, the peak has a Gaussian shape, and the parameter a_1 coincides with t_{M}. Finally, we should mention that the HVL function accounts only for the EMD-related shift of the peak apex out of the expected migration time, a_1. Namely in the case of highly overloaded samples, higher order nonlinear (de)stacking effects may arise in an electrophoretic system that affect both the peak shape and observed velocity (migration time) of the analyte [11, 12].

2 Theory

2.1 General

In order to investigate the geometrical properties of the HVL function in more detail, it is useful to introduce its normalized form $hvl(\tau; a_{3\delta}) \equiv HVL(\tau; a_0 = 1, a_1 = 0, a_2 = 1, a_{3\delta})$ of one independent variable, τ, and the single parameter, $a_{3\delta}$:

$$hvl(\tau; a_{3\delta}) = \frac{\frac{1}{a_{3\delta}\sqrt{2\pi}} \exp\left(\frac{-\tau^2}{2}\right)}{\frac{1}{\exp(a_{3\delta})-1} + \frac{1}{2}\left\{1+\mathrm{erf}\left(\frac{\tau}{\sqrt{2}}\right)\right\}}. \tag{3}$$

Using this new auxiliary function we can simplify the HVL function to the form of

$$HVL(t; a_0, a_1, a_2, a_{3\delta}) = F hvl(\tau; a_{3\delta}) \quad (4)$$

where the constant F is defined as a_0/a_2 and the substitution:

$$\tau = \frac{t - a_1}{a_2} \quad (5)$$

applies. In the rest of this section we shall denote the maximum of $hvl(\tau; a_{3\delta})$ by θ and the position of the maximum by τ_Θ. Realize (see Eq. (3)) that both θ and τ_Θ depend only on $a_{3\delta}$. Likewise the hvl function, quantities θ and τ_Θ have only an auxiliary role in this text and their physical meaning, if any, is not significant here. In addition to introducing the hvl function, we need to solve the inverse problem of finding τ for a specified h such that $hvl(\tau; a_{3\delta}) = h$. Since the hvl has one maximum at τ_Θ, the inverse problem results in two solutions in the domains $(-\infty;\tau_\Theta\rangle$ and $\langle\tau_\Theta;\infty)$. Thus we introduce restrictions of function $hvl(\tau; a_{3\delta})$ to the respective intervals by defining $hvlL(\tau; a_{3\delta}) = hvl(\tau; a_{3\delta})|_{(-\infty;\tau_\Theta\rangle}$ and $hvlR(\tau; a_{3\delta}) = hvl(\tau; a_{3\delta})|_{\langle\tau_\Theta;\infty)}$. This allows us to express the values of $\tau_L = hvl\,L^{-1}(h; a_{3\delta})$ and $\tau_R = hvl\,R^{-1}(h; a_{3\delta})$ for an arbitrary $h \in (0, \Theta\rangle$ so that $hvl(\tau_L; a_{3\delta}) = hvl(\tau_R; a_{3\delta}) = h$. It indeed applies $hvlL^{-1}(\Theta; a_{3\delta}) = hvl\,R^{-1}(\Theta; a_{3\delta}) = \tau_\Theta$.

From Eq. (4) it follows that the maximum, M, of the original HVL function equals to $M = F\Theta$. This maximum is situated at a position of t_M, which can be expressed as:

$$t_M = a_1 + \tau_\Theta a_2. \quad (6)$$

This is a simple consequence of Eqs. (4) and (5) and the fact that τ_Θ is the position of the maximum of $hvl(\tau; a_{3\delta})$. Equation (6) provides the first relationship between the (yet unknown) parameters of the HVL function and the physical characteristics of the peak, that is its experimental migration time, t_M. In order to get further, we will get rid of the parameter a_1 in Eq. (6) and show that the a_2 parameter is proportional to the geometrical width of the HVL peak.

Let α be an arbitrary number from (0, 1) and denote w_α the full width of the HVL peak at α-fraction of its height, αM. It is easy to think over that there exist just one $\tau_{L\alpha} \in (-\infty, \tau_\Theta)$ and one $\tau_{R\alpha} \in (\tau_\Theta, \infty)$ such that:

$$\alpha\Theta = hvl(\tau_{L\alpha}; a_{3\delta}) = hvl(\tau_{R\alpha}; a_{3\delta}). \quad (7)$$

Both $\tau_{L\alpha}$ and $\tau_{R\alpha}$ depend only on $a_{3\delta}$. Using Eqs. (5) and (4) this translates into the physical time domain as:

$$t_{L\alpha} = a_2\tau_{L\alpha} + a_1 \quad (8a)$$

$$t_{R\alpha} = a_2\tau_{R\alpha} + a_1 \quad (8b)$$

$$HVL(t_{L\alpha}; a_0, a_1, a_2, a_{3\delta}) = HVL(t_{R\alpha}; a_0, a_1, a_2, a_{3\delta}) = \alpha M \quad (8c)$$

The difference between $t_{L\alpha}$ and $t_{R\alpha}$ is the width, w_α:

$$w_\alpha \equiv t_{R\alpha} - t_{L\alpha} = a_2(\tau_{R\alpha} - \tau_{L\alpha}). \quad (9)$$

The subtraction (9) gives the a_1 parameter vanished and shows that the HVL peak width is directly proportional to the a_2 parameter, and vice versa.

$$a_2 = w_\alpha\, L_\alpha(a_{3\delta}) \quad (10)$$

The constant of proportionality, L_α, depends only on the $a_{3\delta}$ parameter. This means that HVL functions that may differ in their sizes, heights, widths, and peak top positions share the same set of L_α coefficients as only the function of their distortions (asymmetries) determined by the $a_{3\delta}$ parameter.

The remaining task is thus to find the relation between the $a_{3\delta}$ value and the distortion (asymmetry) of the HVL peak. This can be easily done by realizing that the ratio of the two w_α values is independent of a_2 as follows directly from Eq. (10). In this way we are left with a formula depending solely on $a_{3\delta}$:

$$q_{\alpha\beta} = \frac{w_\alpha}{w_\beta} = \frac{L_\beta}{L_\alpha} = f_q(a_{3\delta}). \quad (11)$$

If the function f_q is continuous and monotonous, the $a_{3\delta}$ parameter is obtained from the measure of the peak widths ratio, $q_{\alpha\beta}$, as:

$$a_{3\delta} = f_q^{-1}(q_{\alpha\beta}). \quad (12)$$

The α and β fractions of the peak height at which the peak distortion (asymmetry) is measured can, in principle, be chosen arbitrarily. Alternatively, t_M (resp. τ_M) can stay for either $t_{R\alpha}$ or $t_{L\alpha}$ (resp. $\tau_{R\alpha}$ or $\tau_{L\alpha}$) in Eq. (9) resulting in the peak half-widths, $w_{L\alpha}$ or $w_{R\alpha}$. In this way, the ratio of the peak half-width to the full-width as well as the ratio of the two (rightward and leftward) half-widths at the same α-fraction of the peak height may serve the purpose.

Finally, let us summarize the entire procedure of finding the individual parameters of the HVL function from its geometrical properties. Apart from the experimental migration time, w_α is used as a measure of the peak width and $q_{\alpha\beta}$ as a measure of its distortion (asymmetry). Parameter $a_{3\delta}$ of the corresponding HVL function then results as the function $f_q^{-1}(q_{\alpha\beta})$(Eq. (12)). Next, the L_α coefficient relates the w_α measure of the peak width to its actual a_2 parameter (Eq. (10)). Since the L_α is only the function of $a_{3\delta}$, which itself is a function of $q_{\alpha\beta}$, the L_α coefficients can be advantageously related to the $q_{\alpha\beta}$ directly rather than through the $a_{3\delta}$ parameter, $L_\alpha \equiv L_\alpha(q_{\alpha\beta})$. As the last step, the a_1 parameter is determined from the peak top position, t_M, and Eq. (6). For the practical purposes, Eq. (6) can be rearranged as:

$$a_1 = t_M - \tau_\Theta a_2 = t_M - \tau_\Theta w_\alpha L_\alpha = t_M - w_\alpha K_\alpha, \quad (13)$$

where K_α forms yet another set of coefficients dependent on $a_{3\delta}$ (τ_Θ is an $a_{3\delta}$-dependent constant that need not to be specified). Similarly to the previous case of the L_α coefficients, K_α can be related to the $q_{\alpha\beta}$ directly, $K_\alpha \equiv K_\alpha(q_{\alpha\beta})$.

Unfortunately, none of the f_q^{-1}, L_α, and K_α functions of $q_{\alpha\beta}$ can be found in the closed form. Instead, they can be easily solved numerically for a chosen $q_{\alpha\beta}$ parameter by modeling the normalized $hvl(\tau; a_{3\delta})$ function for various values of $a_{3\delta}$. Once generated for the normalized function, the

coefficients can serve for any HVL-shaped peak since they are fully determined by the peak distortion (asymmetry), regardless of its actual size, that is height, width, or area. We finally emphasize that although the entire procedure is based on the δ-parameterization of the HVL function (Eq. (2)) this fact only concerns the $a_{3\delta}$ parameter, that is the values derived for the $f_q^{-1}(q_{\alpha\beta})$ function, because parameters a_1 and a_2 are the same in both parameterizations.

Equations (10), (12), and (13) form a unique mapping from the parametric space of the HVL function (a_1, a_2, $a_{3\delta}$) to the physical domain of the HVL peak (t_M, w_α, $q_{\alpha\beta}$) and vice versa. It is evident that one may choose (fix) the a_1, a_2, and $a_{3\delta}$ parameters of the HVL function while the physical characteristics t_M, w_α, and $q_{\alpha\beta}$ will result. Similarly though, one may now fix the experimental time (peak top position), width, and asymmetry (at a certain peak–height ratio) of the HVL peak and the Eqs. (10), (12), and (13), or effectively the coefficients K_α and L_α, secure that the parameters a_1, a_2 and $a_{3\delta}$ adjust themselves so that the resulting HVL function will exhibit the exact top position, width, and asymmetry as desired. This has a practical consequence that may not be apparent at the first sight but will be discussed in the experimental part of this article.

2.2 Application to the ChemStation software output

We will illustrate the above-introduced relations on determining the HVL parameters of the electrophoretic peaks analyzed by the ChemStation software. The ChemStation is a standard software package supplied with the CE equipment by Agilent Technologies, Waldbronn, Germany. As many other data analysis software packages, ChemStation provides an automated peak analysis with detailed report on peak properties, including system performance parameters such as peak width, asymmetry, number of theoretical plates (equivalent to chromatography), etc. Nevertheless, the HVL fit is not available, which primarily affects the reading of the migration time, which is attributed to t_M rather than a_1. This may result in misleading assessments of the electrophoretic mobilities of the analytes if EMD is present. In order to overcome this problem, the data are to be exported into a third-party software tool and then reprocessed manually with the HVL nonlinear regression, including the peak detection, baseline definition and its subtraction. This procedure tends to be laborious and needs a certain level of experience especially in order to supply a reasonable estimate for the initial values of the HVL parameters. Our proposed procedure not only aims to provide such estimates but should enable the analysts to completely avoid the need of the external data processing.

Of the parameters reported by the ChemStation software, t_M denotes here the peak top position, $w_{0.5}$ the full width at the 50% of the peak height, and T_{USP} the U.S. Pharmacopeia (USP) tailing factor: [13]

$$T_{USP} = \frac{w_{0.05}}{2\, w_{L0.05}}, \tag{14}$$

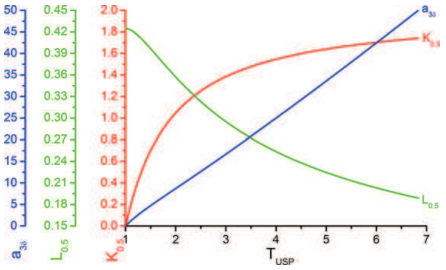

Figure 1. Dependencies of the $a_{3\delta}$ parameter, $K_{0.5}$ coefficient, and $L_{0.5}$ coefficient on the USP tailing factor, T_{USP}. See discussion with Eq. (14). Each dependency has its own *y*-axis.

where $w_{L0.05}$ and $w_{0.05}$ are the left half-width and full-width of the peak measured at 5% of its height, respectively. The USP tailing factor is used as the measure of the peak asymmetry (cf. Eq. (11)). We generated the $f_q^{-1}(T_{USP})$, $L_{0.5}(T_{USP})$, and $K_{0.5}(T_{USP})$ dependencies by means of our software ResolutionAnalyzer (http://echmet.natur.cuni.cz, paper accepted for publication in this special issue). Unambiguous functions have been observed (Fig. 1). Specifically, for $T_{USP} = 1$(symmetrical peak), the $a_{3\delta} = 0$ and the HVL function becomes a Gaussian. Thus also the $K_{0.5}$ coefficient becomes zero as there is not shift of the a_1 parameter out of the peak apex, t_M, regardless of the peak width. Finally, the $L_{0.5}$ coefficient becomes equal to 0.425 ($\frac{1}{2\sqrt{2\ln(2)}}$), the well-known coefficient of proportionality between the peak FWHM measure and the Gaussian $a_2 \equiv \sigma$ parameter. As the peak asymmetry grows, the $a_{3\delta}$ parameter increases (by definition) as well as the $K_{0.5}$ coefficient does. On the other hand, the $L_{0.5}$ coefficient decreases with the increasing asymmetry of the peak. This can be easily understood when realizing that the EMD (asymmetrical peak distortion, reflected by the $a_{3\delta}$ parameter) contributes to the overall peak width apart from the diffusion (symmetrical peak dispersion, reflected by the a_2 parameter). Thus if two peaks have the same overall widths, $w_{0.5}$, while the first is more EMD-distorted than the other, then the first one must be less diffusion-dispersed than the latter. Since $L_{0.5}$ coefficient is the coefficient of proportionality between the diffusional dispersion, a_2, and the peak width, $w_{0.5}$, it naturally decreases with the peak distortion, $a_{3\delta}$ (or equivalently T_{USP}).

The values were generated with the discretization of $a_{3\delta} = 0.01$, in the interval of $a_{3\delta} \in \langle 0; 50\rangle$ (equivalent to $T_{USP} \in \langle 1;$ approx. $6.836\rangle$. The resulting discretization of the L_α and K_α coefficients is $max(\Delta L_{0.5}) = 1.7 \times 10^{-5}$, and $max(\Delta K_{0.5}) = 1.7 \times 10^{-3}$. The HVL function is dissymmetrical with respect to the $a_{3\delta}$ parameter (tailing for $a_{3\delta} > 0$ and fronting for $a_{3\delta} < 0$), so it results:

$$a_{3\delta}(T_{USP}) = -a_{3\delta}\left(\frac{T_{USP}}{2T_{USP} - 1}\right) \tag{15}$$

Equation (15) extends the applicability of the numerical solution to $a_{3\delta} \in \langle -50; 50\rangle$ (T_{USP} approx. $\langle 0.146; 6.836\rangle$).

We implemented the calculation into a simple excel sheet that can be downloaded for free at our website (http://echmet.natur.cuni.cz). t_M, $w_{0.5}$, and T_{USP} serve as the input parameters based on which the a_1, a_2, and $a_{3\delta}$ parameters of the HVL peak are obtained as an output. The ResolutionAnalyzer software can be used in order to generate the f_q^{-1}, L_α, and K_α dependencies for other than $w_{0.5}$ and T_{USP} geometrical measures of the peak width and asymmetry.

3 Materials and methods

Experimental conditions of the real experiment were as follows. The experiment was performed using an Agilent ^{3D}CE equipment operated under the ChemStation software (Agilent Technologies, Waldbronn, Germany) control. Fused-silica capillaries (50 μm id, 375 μm od) were provided by Polymicro Technologies (Phoenix, AZ, USA). The total length of the capillary and the effective length to the detector were 52.0 and 43.5 cm, respectively. The PHM 220 instrument (Radiometer, Copenhagen, Denmark) calibrated with the standard IUPAC buffers, pH 7.000 and pH 10.012, (Radiometer, Lyon, France) was used for the pH measurements. The BGE contained 50 mM Tris and 50 mM Tricine, experimental pH 8.13. The ionic strength of the BGE was 25.76 mM according to the PeakMaster calculation. The complexation agent β-CD was dissolved directly in the running buffer at a concentration of 0.1 mM. The injected sample was 0.3 mM analyte ((*R*)-(–)-2-fluoro-α-methyl-4-biphenylacetic acid) and 0.07% v/v DMSO, which served as the EOF marker, both dissolved directly in the running buffer. Detection was performed with the DAD at the wavelength of 214 nm. The samples were injected hydrodynamically for 30 mbar·s. The applied voltage was 20 kV (cathode at the detector side). The operating temperature was 25°C.

Simulations were performed for the β-CD concentration of 1.0 mM in the running buffer and three different concentrations of the analyte ((*R*)-(–)-2-fluoro-α-methyl-4-biphenylacetic acid) in the injected sample: 0.01, 0.3, and 1.5 mM. In this way we were able to model systems with no, medium, and high EMD of the analyte peak. Other experimental conditions used in the simulations were similar to those in the experiment but it was not our intention to mimic the experiment with simulation exactly (as we are only interested in generating various shapes of the resulting peaks). Our SIMUL Complex software [14] was used for the simulations. The number of nodes in the *x*-axis was 50 000. The simulations were performed by means of the Intel® Core™ i7–960 processor, 3.40 GHz. The simulation time was in the range of hours.

4 Results and discussion

In order to verify the accuracy and applicability of the proposed method for determining the parameters of the HVL function, we tested this method on several peaks generated using our simulation program Simul 5 Complex [14] and on a real experiment. As a model system we chose a system with complexing constituents where the EMD of the analyte peak occurs due to the complexation [15, 16]. The ChemStation software allows the user to gain values of FWHM, $w_{0.5}$, and the USP tailing factor, T_{USP}. The calculation procedure is described in detail in Section 2.2 above. For the simulated peaks, the t_M, $w_{0.5}$, and T_{USP} were determined manually by means of the Origin 8.1 software. For the experimental peak, the integration was performed in the ChemStation software and the resulting values of t_M, $w_{0.5}$, and T_{USP} were used. The Origin 8.1 software was also utilized for the HVL nonlinear regression.

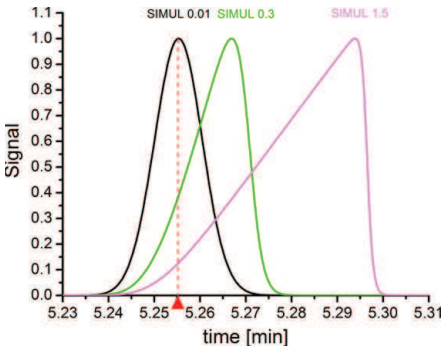

Figure 2. Simulated electropherograms of *R*-flurbiprofen in concentrations of 0.01, 0.3, and 1.5 mM with β-CD in the BGE. BGE consists of 50 mM Tris, 50 mM Tricine buffer, and 1 mM β-CD. See Section 3 for other simulation details. Theoretical migration time is depicted by the vertical line and the arrow at the *x*-axis. *y*-Axis is depicted on a normalized scale. See Table 1 for peak asymmetries and other characteristics.

Simulated electropherograms are shown in Fig. 2. If a low concentration of the analyte is injected (SIMUL 0.01) almost completely symmetrical Gaussian peak is observed. At the midrange concentration (SIMUL 0.3), the peak becomes medium distorted. A highly distorted peak is observed at the highest concentration of the analyte (SIMUL 1.5). The experimental migration times, t_M, and the parameters a_1 of the HVL fits of the peaks are given in Table 1. As expected, the experimental migration times, t_M, differ significantly for the individual peaks, while the a_1 parameter stays at the original position of the symmetrical (undistorted) peak (SIMUL 0.01). The estimate, denoted as $\tilde{a}_1$ in Table 1, results as the corrected experimental migration time, t_M, by Eq. (13). It is evident that the correction (13) significantly reduces the difference between the migration time read and the theoretical migration time of the peak, a_1. For all the EMD-dispersed peaks the estimated values, $\tilde{a}_1$, are much closer to the theoretical migration time, a_1, than is the experimental migration time, t_M. The correction factor to the migration time $w_\alpha K_\alpha$ in Eq. (13) is in the order of several percent. For the highly symmetrical peak (SIMUL 0.01) however, the correction

Table 1. Simulated data of *R*-flurbiprofen in concentrations of 0.01, 0.3, and 1.5 mM with 1 mM β-CD in the BGE

Name	Peak characteristics			HVL fit				HVL estimate			
	t_M (min)	$w_{0.5}$ (min)	T_{USP}	a_1 (min)	a_2 (min)	$a_{3\delta}$	R^2	$\tilde{a}_1$ (min)	$\tilde{a}_2$ (min)	$\tilde{a}_{3\delta}$	R^2
SIMUL 0.01	5.255	0.0123	0.9894	5.2552	0.00522	–0.032	0.99996	5.2547	0.00522	–0.135	0.99637
SIMUL 0.3	5.267	0.0139	0.6928	5.2542	0.00521	–6.905	0.99997	5.2541	0.00518	–7.115	0.99948
SIMUL 1.5	5.294	0.0244	0.5520	5.2538	0.00542	–33.95	0.99976	5.2534	0.00531	–36.25	0.99905

Experimental migration time, t_M; FWHM, $w_{0.5}$; and USP tailing factor, T_{USP} of peaks of *R*-flurbiprofen in various concentrations. a_1, a_2, and $a_{3\delta}$ parameters of the HVL fit of the individual peaks with Eq. (2). $\tilde{a}_1$, $\tilde{a}_2$, and $\tilde{a}_{3\delta}$ estimates of the respective HVL parameters by Eqs. (13), (10), and (12).

factor is so small (less than 0.006%) that it does not have any real impact.

The $\tilde{a}_2$ and $\tilde{a}_{3\delta}$ estimates are also summarized in Table 1. Although the $\tilde{a}_{3\delta}$ estimate differs from the actual $a_{3\delta}$ parameter of the HVL fit by an error as low as 5%, this error is significantly higher than the discretization with which the $a_{3\delta} = f_q^{-1}(T_{USP})$ dependence was generated. We attribute this discrepancy to either the data sampling rate, which affects the precision of the T_{USP} reading, or the fact that the HVL shape does not match the simulated peaks exactly. It seems (data not shown) that the former applies mostly to the symmetrical peaks with low $a_{3\delta}$ values while the latter becomes marginally significant for the highly distorted peaks with high $a_{3\delta}$ values. With the real data, the data noise would moreover most probably overweight both these effects. Fortunately though, the L_α and K_α coefficients are not too much sensitive to the exact T_{USP} value so that the $\tilde{a}_2$ and namely $\tilde{a}_1$ estimates are made precisely enough.

Additionally, the R^2 (coefficient of determination) is reported in Table 1 that quantifies how well the fitted/estimated function reflects the simulated data. The coefficients of determination are nearly 1 for the HVL fits indicating that the HVL function really evolves under the ideal conditions of the simulation (narrow injection zone, EMD, and diffusion effects only). Only negligibly lower coefficients of determination are observed when the HVL function is constructed using the $\tilde{a}_1$, $\tilde{a}_2$, and $\tilde{a}_{3\delta}$estimates. At high EMD peak distortion, the quality of the estimate is just as good as the actual fit, since the $K_{0.5}$ and $L_{0.5}$ coefficients become less sensitive to the peak asymmetry and neither the HVL function fits the peak absolutely perfectly. At low EMD peak distortion, the difference in the quality of the HVL fit and the estimate is the most significant, since even the smallest change in the $\tilde{a}_{3\delta}$estimate results in a slightly different HVL function shape. This, however, does not significantly affect the $\tilde{a}_1$ and $\tilde{a}_2$ estimates as discussed above.

The experimental electropherogram is shown in Fig. 3. The fitted and estimated a_1, a_2, and $a_{3\delta}$ parameters of the corresponding HVL functions are also given in Table 2. Figure 3 reveals a tiny shift of the estimated HVL function (green dashed line) from the fitted HVL function (red line) to the lower times. This is also reflected in the R^2 value of the estimate, which is 0.9779 compared to the 0.9992 by the fitting procedure. A deeper analysis reveals that this is primarily caused by the data sampling rate and the noise. The

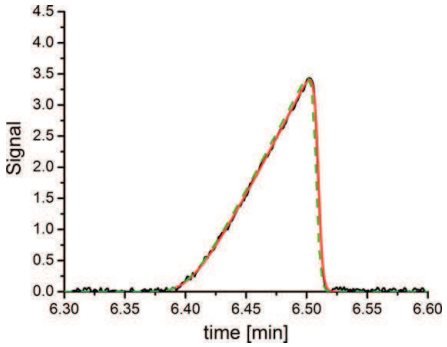

Figure 3. Peak of *R*-flurbiprofen in a concentration of 0.3 mM with 0.1 mM β-CD in the BGE. Black trace: experimental record; red solid line: HVL fit; green dashed line: HVL constructed from the $\tilde{a}_1$, $\tilde{a}_2$, and $\tilde{a}_{3\delta}$ estimates. BGE consists of 50 mM Tris, 50 mM Tricine buffer, and 0.1 mM β-CD. See Section 3 for other experimental details. See Table 1 for the characteristics of the experimental peak and the HVL functions.

ChemStation software reads the experimental peak top position, t_M, at the highest point of the measured peak, which is influenced both by the sampling rate and the noise. The HVL fit is primarily driven by the data points at the inclination and the declination edges of the peak, while the very few data points at the top of the peak does not have any significant influence. In our case, the apex of the HVL fit is shifted rightward from the experimental top position, t_M. The difference is $+1.5 \times 10^{-3}$ min, which is equivalent to approximately two data points with the sampling rate of 8.4×10^{-4}min. The fitting procedure makes the HVL fit robust against the data sampling rate and noise, so that the HVL peak overlaps the experimental peak well on the expense of (or possibly with the benefit of) adjusting its apex as needed. To the contrary, the apex of the HVL function resulting from the $\tilde{a}_1$, $\tilde{a}_2$, and $\tilde{a}_{3\delta}$ estimates must be located exactly at the predefined position of t_M as discussed at the very end of Section 2.1. Simultaneously, width, $w_{0.5}$, and asymmetry, T_{USP}, of the HVL peak are also kept by the estimating procedure. This may result in the shift of the entire HVL function towards the experimental peak top position compared to the HVL fit. Hence, the difference of the $\tilde{a}_1$ estimate from the actual a_1 parameter of the HVL fit equals -1.6×10^{-3}min (two data points), which is in

Table 2. Experimental data of *R*-flurbiprofen in a concentration of 0.3 mM with 0.1 mM β-CD in the BGE

Name	Peak characteristics			HVL fit				HVL estimate			
	t_M (min)	$w_{0.5}$ (min)	T_{USP}	a_1 (min)	a_2 (min)	$a_{3\delta}$	R^2	$\tilde{a}_1$ (min)	$\tilde{a}_2$ (min)	$\tilde{a}_{3\delta}$	R^2
Experiment	6.501	0.0554	0.5574	6.4123	0.0132	−30.10	0.9992	6.4107	0.01265	−32.325	0.9779

BGE consists of 50 mM Tris, 50 mM Tricine buffer and 0.1 mM β-CD. See Section 3 for other experimental details. Experimental migration time, t_M; FWHM, $w_{0.5}$; and USP tailing factor, T_{USP} of the peak of *R*-flurbiprofen. a_1, a_2, and $a_{3\delta}$ parameters of the HVL fit of the peak with Eq. (2). $\tilde{a}_1$, $\tilde{a}_2$, and $\tilde{a}_{3\delta}$ estimates of the respective HVL parameters by Eqs. (13), (10), and (12).

accordance with the $+1.5 \times 10^{-3}$ min shift of the fitted HVL apex out of the t_M position. When the tops of the estimated and fitted HVL functions are synchronized, no observable difference between the two is present and the R^2 value of the estimate grows up to 0.9983. It is important to note that such a bias has a negligible effect when compared to the error introduced if the uncorrected migration time were read from its experimental value, t_M. In our case the difference of $(t_M - a_1)$ is as large as 8.9×10^{-2} min (106 data points), which is over 50 times larger than that of $(\tilde{a}_1 - a_1)$. In conclusion, the correction of the experimental migration time, t_M, introduced by Eq. (13) is reasonably significant and made within the actual precision of the data sampling rate.

As a final point, let us underscore the fact that the migration time correction, that is the shift of the peak maximum, t_M, out of its theoretical position, a_1, does not only depend on the K_α parameter, that is the distortion (asymmetry) of the peak, but is directly proportional to its actual width, w_α (Eq. (13)). Thus although the experimental peak has its distortion comparable to, or even slightly less than, that of the simulated peak SIMUL 1.5 (cf. the respective coefficients $a_{3\delta}$ in Tables 1 and 2), the migration time shift is twice as significant for the experimental peak as for the simulated one since the former is twice as wide (Tables 1 and 2, parameter $w_{0.5}$).

5 Concluding remarks

We derived relations between the geometrical characteristics of the HVL function and its a_1, a_2, and $a_{3\delta}$ parameters. The relations require a set of coefficients that cannot be expressed analytically but were generated numerically for the FWHM, $w_{0.5}$, as a measure of the peak width, and the USP tailing factor, T_{USP}, as a measure of the peak distortion (asymmetry). The relations were successfully applied on simulated electropherograms of various peak distortions and an experimental electropherogram. The theoretical migration time of the peak was estimated as a corrected experimental migration time that would be otherwise falsely assigned to the position of the top of the peak. It was demonstrated that the procedure is directly applicable to the output of automated data integration software, such as ChemStation (CE instrumentation by Agilent Technologies). The correction of the migration time provided the accurate value comparable to that obtained by the HVL fit within the precision of the data sampling rate. Thus, the herein-introduced procedure may serve as a quick and easy alternative to the HVL fitting of the data that requires external data processing. Alternatively, it can provide a very precise estimate of the initial values of the HVL fit in an automated manner.

The authors acknowledge the financial support for this work from the grant agency of the Charles University, grants 669412 and 570213, and the grant agency of the Czech Republic, grant number P206/12/P630.

The authors have declared no conflict of interest.

6 References

[1] Xu, X., Kok, W. T., Poppe, H., *J. Chromatogr. A* 1996, *742*, 211–227.

[2] Horká, M., Šlajs, K., *Electrophoresis* 2000, *21*, 2814–2827.

[3] Hruška, V., Svobodová, J., Beneš, M., Gaš, B., *J. Chromatogr. A* 2012, *1267*, 102–108.

[4] Erny, G. L., Bergström, E. T., Goodall, D. M., *Anal. Chem.* 2001, *73*, 4862–4872.

[5] Erny, G. L., Bergström, E. T., Goodall, D. M., *J. Chromatogr. A* 2002, *959*, 229–239.

[6] Haarhoff, P. C., van der Linde, H. J., *Anal. Chem.* 1966, *38*, 573–582.

[7] Hruška, V., Riesová, M., Gaš, B., *Electrophoresis* 2012, *33*, 923–930.

[8] García-Alvarez-Coque, M. C., Simó-Alfonso, E. F., Sanchis-Mallols, J. M., Baeza-Baeza, J. J., *Electrophoresis* 2005, *26*, 2076–2085.

[9] Zhang, J., Huang, Q., Jin, J., Chang, J., Li, S., Fan, L., *Cao, C., Talanta* 2013, *105*, 278–286.

[10] Le Saux, T., Varenne, A., Gareil, P., *Electrophoresis* 2005, *26*, 3094–3104.

[11] Gebauer, P., Thormann, W., Boček, P., *Electrophoresis* 1995, *16*, 2039–2050.

[12] Gebauer, P., Boček, P., *Electrophoresis* 2009, *30*, S27–S33.

[13] Chapter <621> in United States Pharmacopeia 34, 2011, United States Pharmacopeia Convention, ISBN 37-692-5390-6.

[14] Hruška, V., Beneš, M., Svobodová, J., Zusková, I., Gaš, B., *Electrophoresis* 2012, *38*, 938–947.

[15] Hruska, V., Svobodova, J., Benes, M., Gas, B., *J. Chromatogr. A* 2012, *1267*, 102–108.

[16] Benes, M., Svobodova, J., Hruska, V., Dvorak, M., Zuskova, I., Gas, B., *J. Chromatogr. A* 2012, *1267*, 109–115.

5 Závěr

Předkládaná dizertační práce byla zaměřena na matematický popis komplexujících systémů kapilární elektroforézy, ve kterých analyt interaguje se dvěma či více selektory, případně se vedle komplexací účastní ještě acidobazických rovnovah. Dále se práce zabývala stanovením správné efektivní mobility analytu v komplexujících systémech.

Pro popis systémů, kde plně nabité analyty interagují se záměrně připravenou směsí dvou selektorů, byl použit souhrnně-komplexační model. Tento model ukazuje, že pokud se nemění složení směsi (reprezentované molární frakcí prvního selektoru ve směsi), lze se směsí zacházet jako s jedním selektorem. Parametry komplexace analytu s tímto „souhrnným“ selektorem lze pro dané složení směsi pomocí tohoto modelu spočítat z parametrů charakterizujících komplexaci analytu s každým čistým selektorem zvlášť. Ze souhrnných komplexačních parametrů lze následně předpovědět závislost efektivní mobility analytu na celkové koncentraci směsi selektorů. Tento model poskytuje užitečný vhled do mechanizmu separace díky tomu, že molární frakce prvního selektoru ve směsi může nabývat pouze hodnot od nuly do jedné, zatímco závislost efektivní mobility analytu, případně vhodného parametru charakterizujícího úspěšnost separace, jako je rozdíl nebo poměr mobilit separovaných analytů, sleduje tvar odpovídající komplexaci s jediným selektorem. Experimentálně byl tento koncept ověřen na modelovém systému dvou plně nabitých analytů a dvou různých dvojic neutrálních selektorů. Byla pozorována velmi dobrá shoda mezi předpovězenými a změřenými souhrnnými komplexačními parametry pro jednotlivé směsi a potvrdila se i schopnost modelu předpovídat závislost poměru mobilit analytů (selektivity) na celkové koncentraci směsi selektorů.

Analyty, kterými jsou často slabé kyseliny, báze nebo amfolyty, se mohou v systému vyskytovat ve více volných formách, mezi kterými se ustavují acidobazické rovnováhy. Každá z těchto forem pak může vytvářet komplexy s přítomnými selektory. Zahrnutím těchto rovnovah do souhrnně-komplexačního modelu byl vytvořen generalizovaný model elektromigrace v komplexujících systémech se stechiometrií komplexace 1:1. Tento model vůbec poprvé popisuje systémy, ve kterých více volných forem analytu interaguje s více selektory. Důležitou vlastností tohoto modelu je, že umožňuje nahlížet na tyto velmi složité systémy různými způsoby, ukazuje za jakých podmínek a jakým způsobem lze vzájemně provázané acidobazické a komplexační rovnováhy od sebe oddělit a pracovat s nimi

samostatně. Platnost modelu byla experimentálně ověřena na nejjednodušším možném, nicméně z praktického hlediska velmi významném, systému s více volnými formami analytu a s více selektory: slabou jednosytnou kyselinou jako analytem a dvěma cyklodextriny, z nichž jeden byl neutrální a jeden kladně nabitý. Pro dva různé způsoby předpovědi efektivní mobility analytu v takovém systému, které generalizovaný model umožňuje, byla pozorována shoda mezi predikcí a experimentem. Výsledky dále potvrdily, že v souladu s generalizovaným modelem je závislost elektivní mobility analytu na celkové koncentraci selektoru, původně odvozená pro jedinou formu volného analytu interagující s jediným selektorem, univerzálně použitelná pro systémy se stechiometrií komplexace 1:1 bez ohledu na to, zda jedna nebo více volných forem analytu interaguje s jedním nebo více selektory.

Ve druhé části této práce byla představena dvoudetektorová metoda umožňující stanovit správnou efektivní mobilitu analytu v systému, kde může nabitá interagující složka základního elektrolytu, například nabitý selektor, interagovat s markerem elektroosmotického toku. Stanovení správné efektivní mobility je klíčové pro určení komplexačních parametrů, se kterými pracují výše zmiňované elektromigrační modely. Pomocí navržené metody byla posouzena vhodnost čtyř populárních EOF markerů pro použití v základním elektrolytu obsahujícím jeden z nejčastěji používaných selektorů, nedefinovaně sulfatovaný β-cyklodextrin. Jako nejméně nevhodné markery se ukázaly dimethyl sulfoxid a nitromethan (nicméně i ty se selektorem slabě interagují).

Dále byl navržen způsob, kterým lze z geometrických charakteristik elektroforetického píku deformovaného elektromigrační disperzí určit parametr odpovídající HVL funkce, který má význam migračního času analytu při jeho nekonečném zředění, a to bez potřeby nelineární regrese. To značně usnadní vyhodnocení správných migračních časů a potažmo i efektivních mobilit a komplexačních parametrů v komplexujících systémech, ve kterých dochází k elektromigrační disperzi zón analytů, například z důvodu významného úbytku selektoru v zóně analytu v důsledku silné komplexace.

Literatura

[1] Van Eeckhaut A., Michotte Y., *Electrophoresis* 2006, *27*, 2880-2895.

[2] Guebitz G., Schmid M. G., *J. Chromatogr. A* 2008, *1204*, 140-156.

[3] Schmitt U., Branch S. K., Holzgrabe U., *J. Sep. Sci.* 2002, *25*, 959-974.

[4] Juvancz Z., Bodane Kendrovics R., Ivanyi R., Szente L., *Electrophoresis* 2008, *29*, 1701-1712.

[5] Scriba G. K. E., *J. Sep. Sci.* 2008, *31*, 1991-2011.

[6] Cucinotta V., Contino A., Giuffrida A., Maccarrone G., Messina M., *J. Chromatogr. A* 2010, *1217*, 953-967.

[7] Lu H., Chen G., *Anal. Methods* 2011, *3*, 488-508.

[8] Stepanova N. D., Stepanov A. V., *Zh. Prikl. Khim.* 1969, *42*, 1670-1673.

[9] Chankvetadze B., *TrAC, Trends Anal. Chem.* 1999, *18*, 485-498.

[10] Wren S. A. C.; Rowe R. C., *J. Chromatogr.* 1992, 603, 235-241.

[11] Riesova M., Svobodova J., Tosner Z., Benes M., Tesarova E., Gas B., *Anal. Chem.* 2013, *85*, 8518-8525.

[12] Benes M., Zuskova I., Svobodova J., Gas B., *Electrophoresis* 2012, *33*, 1032-1039.

[13] Mullerova L., Dubsky P., Gas B., *J. Chromatogr. A* 2015, *1384*, 147-154.

[14] Hruska V., Svobodova J., Benes M., Gas B., *J. Chromatogr. A* 2012, *1267*, 102-108.

[15] Benes M., Svobodova J., Hruska V., Dvorak M., Zuskova I., Gas B., *J. Chromatogr. A* 2012, *1267*, 109-115.

[16] Haarhoff P. C., van der Linde H. J., *Anal. Chem.* 1966, *38*, 573-582.

[17] Erny G. L., Bergstroem E. T., Goodall D. M., Grieb S., *Anal. Chem.* 2001, *73*, 4862-4872.

[18] Hruska V., Riesova M., Gas B., *Electrophoresis* 2012, 33, 923-930.

[19] Penn S. G., Goodall D. M., Loran J. S., *J. Chromatogr.* 1993, *636*, 149-152.

[20] Uselova-Vcelakova K., Zuskova I., Gas B., *Electrophoresis* 2007, *28*, 2145-2152.

[21] Scriba G. K. E., *J. Pharm. Biomed. Anal.* 2001, *27*, 373-399.

[22] Jac P., Scriba G. K. E., *J. Sep. Sci.* 2013, *36*, 52-74.

[23] Wren S. A. C., *J. Chromatogr.* 1993, *636*, 57-62.

[24] Penn S. G., Bergstrom E. T., Goodall D. M., Loran J. S., *Anal. Chem.* 1994, *66*, 2866-2873.

[25] Wren S. A. C., *Electrophoresis* 1995, *16*, 2127-2131.

[26] Britz-McKibbin P., Chen D. D. Y., *J. Chromatogr. A* 1997, *781*, 23-34.

[27] Seals T. H., Sheng C., Davis J. M., *Electrophoresis* 2001, *22*, 1957-1973.

[28] Chankvetadze B., *J. Chromatogr. A* 1997, *792*, 269-295.

[29] Rogan M. M., Altria K. D., Goodall D. M., *Electrophoresis* 1994, *15*, 808-817.

[30] Rawjee Y. Y., Staerk D. U., Vigh G., *J. Chromatogr.* 1993, *635*, 291-306.

[31] Rawjee Y. Y., Williams R. L., Vigh G., *J. Chromatogr. A* 1993, *652*, 233-245.

[32] Williams B. A., Vigh G., *J. Chromatogr. A* 1997, *777*, 295-309.

[33] Zhu W., Vigh G., *Electrophoresis* 2000, *21*, 2016-2024.

[34] Lelievre F., Gareil P., Jardy A., *Anal. Chem.* 1997, *69*, 385-392.

[35] Rizzi A. M., Kremser L., *Electrophoresis* 1999, *20*, 2715-2722.

[36] Yang W.-C., Yu A.-M., Yu X.-D., Chen H.-Y., *Electrophoresis* 2001, *22*, 2025-2031.

[37] Mofaddel N., Krajian H., Villemin D., Desbene P. L., *Talanta* 2009, *78*, 631-637.

[38] Hammitzsch-Wiedemann M., Scriba G. K. E., *Anal. Chem.* 2009, *81*, 8765-8773.

[39] Chen F.-T. A., Shen G., Evangelista R. A., *J. Chromatogr. A* 2001, *924*, 523-532.

[40] Chankvetadze B., Blaschke G., *J. Chromatogr. A* 2001, *906*, 309-363.

[41] Schmitt U., Ertan M., Holzgrabe U., *Electrophoresis* 2004, *25*, 2801-2807.

[42] Lurie I. S., *J. Chromatogr. A* 1997, *792*, 297-307.

[43] Fillet M., Hubert P., Crommen J., *J. Chromatogr. A* 2000, *875*, 123-134.

[44] Lurie I. S., Klein R. F. X., Dal Cason T. A., LeBelle M. J., Brenneisen R., Weinberger R. E., *Anal. Chem.* 1994, *66*, 4019-4026.

[45] Surapaneni S., Ruterbories K., Lindstrom T., *J. Chromatogr. A* 1997, *761*, 249-257.

[46] Zhu X., Ding Y., Lin B., Jakob A., Koppenhoefer B., *J. Chromatogr. A* 2000, *888*, 241-250.

[47] Abushoffa A. M., Fillet M., Servais A.-C., Hubert P., Crommen J., *Electrophoresis* 2003, *24*, 343-350.

[48] Nhujak T., Sastravaha C., Palanuvej C., Petsom A., *Electrophoresis* 2005, *26*, 3814-3823.

[49] Schaeper J. P., Fox S. B., Sepaniak M. J., *J. Chromatogr. Sci.* 2001, *39*, 411-419.

[50] Abushoffa A. M., Fillet M., Marini R. D., Hubert P., Crommen J., *J. Sep. Sci.* 2003, *26*, 536-542.

[51] Abushoffa A. M., Fillet M., Hubert P., Crommen J., *J. Chromatogr. A* 2002, *948*, 321-329.

[52] Sepaniak M. J., Copper C. L., Whitaker K. W., Anigbogu V. C., *Anal. Chem.* 1995, *67*, 2037-2041.

[53] Szolar O. H. J., Brown R. S., Luong J. H. T., *Anal. Chem.* 1995, *67*, 3004-3010.

[54] Matthijs N., Van Hemelryck S., Maftouh M., Luc Massart D., Vander Heyden Y., *Anal. Chim. Acta* 2004, *525*, 247-263.

[55] Fillet M., Chankvetadze B., Crommen J., Blaschke G., *Electrophoresis* 1999, *20*, 2691-2697.

[56] Chankvetadze B., Burjanadze N., Crommen J., Blaschke G., *Chromatographia* 2001, *53*, S296-S301.

[57] Nemeth K., Varga E., Ivanyi R., Szeman J., Visy J., Jicsinszky L., Szente L., Forro E., Fueloep F., Peter A., Simonyi M., *J. Pharm. Biomed. Anal.* 2010, *53*, 382-388.

[58] Beni S., Sohajda T., Neumajer G., Ivanyi R., Szente L., Noszal B., *J. Pharm. Biomed. Anal.* 2010, *51*, 842-852.

[59] Tabi T., Magyar K., Szoeko E., *Electrophoresis* 2003, *24*, 2665-2673.

[60] Peng X., Bowser M. T., Britz-McKibbin P., Bebault G. M., Morris J. R., Chen D. D. Y., *Electrophoresis* 1997, *18*, 706-716.

[61] Kranack A. R., Bowser M. T., Britz-McKibbin P., Chen D. D. Y., *Electrophoresis* 1998, *19*, 388-396.

[62] Jiang C., Armstrong D. W., *Electrophoresis* 2010, *31*, 17-27.

[63] Dubsky P., Svobodova J., Gas B., *J. Chromatogr. B* 2008, *875*, 30-34.

[64] Dubsky P., Svobodova J., Tesarova E., Gas B., *Electrophoresis* 2010, *31*, 1435-1441.

[65] Riekkola M.-L., Joensson J. A., Smith R. M., *Pure Appl. Chem.* 2004, *76*, 443-451.

[66] Wang W., Zhou F., Zhao L., Zhang J.-R., Zhu J.-J., *J. Chromatogr. A* 2007, *1170*, 1-8.

[67] Fuguet E., Rafols C., Bosch E., Roses M., *Electrophoresis* 2002, *23*, 56-66.

[68] Evans C. E., Stalcup A. M., *Chirality* 2003, *15*, 709-723.

[69] Kitagawa F., Otsuka K., *J. Chromatogr. B* 2011, *879*, 3078-3095.

[70] Matthijs N., Perrin C., Maftouh M., Massart D. L., Vander Heyden Y., *J. Pharm. Biomed. Anal.* 2001, *27*, 515-529.

[71] Williams B. A., Vigh G., *Anal. Chem.* 1997, *69*, 4445-4451.

[72] Cai H., Nguyen T. V., Vigh G., *Anal. Chem.* 1998, *70*, 580-589.

[73] Li S., Vigh G., *Electrophoresis* 2003, *24*, 2487-2498.

[74] Tutu E., Vigh G., *Electrophoresis* 2011, *32*, 2655-2662.

[75] Xu X., Kok W. T., Poppe H., *J. Chromatogr. A* 1996, *742*, 211-227.

[76] Gas B., Zuska J., Coufal P., van de Goor T., *Electrophoresis* 2002, *23*, 3520-3527.

[77] echmet.natur.cuni.cz [staženo 25. 5. 2015].

[78] Svobodova J., Benes M., Dubsky P., Vigh G., Gas B., *Electrophoresis* 2012, *33*, 3012-3020.

Přílohy

A. Seznam publikací

1. Determination of effective mobilities of EOF markers in BGE containing sulfated β-cyclodextrin by a two-detector method
   L. Müllerová, P. Dubský, J. Svobodová, B. Gaš
   Electrophoresis 2013, *34*, 768-776.

2. Separation efficiency of dual-selector systems in capillary electrophoresis
   L. Müllerová, P. Dubský, B. Gaš
   Journal of Chromatography A 2014, *1330*, 82-88.

3. Twenty years of development of dual and multi-selector models in capillary electrophoresis: A review
   L. Müllerová, P. Dubský, B. Gaš
   Electrophoresis 2014, *35*, 2688-2700.

4. Generalized model of electromigration with 1:1 (analyte:selector) complexation stoichiometry: Part I. Theory
   P. Dubský, **L. Müllerová**, Martin Dvořák, B. Gaš
   Journal of Chromatography A 2015, *1384*, 142-146.

5. Generalized model of electromigration with 1:1 (analyte:selector) complexation stoichiometry: Part II. Application to dual systems and experimental verification
   L. Müllerová, P. Dubský, B. Gaš
   Journal of Chromatography A 2015, *1384*, 147-154.

6. Determination of the correct migration time and other parameters of the Haarhoff-van der Linde function from the peak geometry characteristics
   P. Dubský, M. Dvořák, **L. Müllerová**, B. Gaš
   Electrophoresis 2015, *36*, 655-661.

B. Seznam konferenčních příspěvků

Přednášky

1. Effective mobilities of EOF markers in interacting BGE determined by a new two-detector method
   L. Müllerová, P. Dubský, J. Svobodová, B. Gaš
   12th International Symposium and Summer School on Bioanalysis, červenec 2012, Cluj-Napoca, Rumunsko

2. Properties of Dual-Cyclodextrin Separation Systems: Experimental Verification of Proposed Model
   L. Müllerová, P. Dubský, B. Gaš
   13th International Symposium and Summer School on Bioanalysis, červenec 2013, Debrecen, Maďarsko

3. Overall complexation: a useful description of dual-cyclodextrin separation systems in capillary electrophoresis
   L. Müllerová, P. Dubský, B. Gaš
   9th International Students Conference ‘Modern Analytical Chemistry’, září 2013, Praha, Česká republika

4. Interaction of a partly dissociated analyte with a dual selector system
   L. Müllerová, P. Dubský, B. Gaš
   Advances in Chromatography and Electrophoresis & Chiranal 2014, únor 2014, Olomouc, Česká republika

5. Can docking software predict chiral separation selectivity in HPLC?
   L. Müllerová, T. Dzimbova
   14th International Symposium and Summer School on Bioanalysis, červen/červenec 2014, Smolenice, Slovensko

Plakátová sdělení

1. Ion pairing of selected cations with dodecylsulfate micelles in electrophoretic systems
   L. Müllerová, J. Lokajová, M. Riesová, B. Gaš
   Advances in Chromatography and Electrophoresis & Chiranal, únor 2010, Olomouc, Česká republika

2. Interactions of selected cations with dodecylsulfate micelles in electrophoretic systems
   L. Müllerová, J. Lokajová, M. Riesová, B. Gaš
   International Symposium on Microscale BioSeparation MSB, březen 2010, Praha, Česká republika

3. Determination of Alcaline Cation Mobility in Background Electrolytes Containing Micelles
   L. Müllerová, P. Dubský, J. Svobodová, B. Gaš
   HPLC 2011 – 36th International Symposium on High-Performance Liquid Phase Separations and Related Techniques, červen 2011, Budapešť, Maďarsko

4. Determination of effective mobilities of four popular EOF markers in BGE containing highly sulfated β-cyclodextrin
   L. Müllerová, P. Dubský, J. Svobodová, B. Gaš
   Advances in Chromatography and Electrophoresis & Chiranal, červen 2012, Olomouc Česká republika

5. Two Detector Method for Determination of Accurate Effective Mobilities in Interacting BGE
   L. Müllerová, P. Dubský, J. Svobodová, B. Gaš
   ITP 2012 – 19th International Symposium, Exhibit & Workshops on Electro- and Liquid Phase-separation Techniques, září/říjen 2012, Baltimore, MD, USA

6. Separation by a Dual Mixture of Cyclodextrins Described by Overall Complexation Parameters
   L. Müllerová, P. Dubský, B. Gaš
   HPLC 2013 – 39th International Symposium on High Performance Liquid Phase Separations and Related Techniques, červen 2013, Amsterdam, Nizozemsko

7. An Electromigration Model of Partly Dissociated Analyte Interacting with a Dual Selector System – Simpler than Expected
   L. Müllerová, P. Dubský, B. Gaš
   ITP & LACE 2014 – 21st International Symposium on Electro- and Liquid Phase-Separation Techniques & 20th Latin-American Symposium on Biotechnology, Biomedical, Biopharmaceutical, and Industrial Applications of Capillary Electrophoresis and Microchip Technology, říjen 2014, Natal, RN, Brazílie

Jiné

1. PeakMaster for beginners (workshop)
   L. Müllerová, M. Riesová
   10th International Students Conference ‘Modern Analytical Chemistry’, září 2014, Praha, Česká republika

2. Computer Optimization of Electrolytes for Capillary Electrophoresis (Pre-Symposium Course)
   L. Müllerová, M. Riesová, B. Gaš
   ITP & LACE 2014 – 21st International Symposium on Electro- and Liquid Phase-Separation Techniques & 20th Latin-American Symposium on Biotechnology, Biomedical, Biopharmaceutical, and Industrial Applications of Capillary Electrophoresis and Microchip Technology, říjen 2014, Natal, RN, Brazílie